DOKUZ EYLÜL UNIVERSITY

GRADUATE SCHOOL OF NATURAL AND APPLIED SCIENCES

VIBRATION ANALYSIS AND MEASUREMENT OF BEAMS HAVING MULTIPLE CRACKS

by

Kemal MAZANOĞLU

January, 2011

İZMİR

VIBRATION ANALYSIS AND MEASUREMENT OF BEAMS HAVING MULTIPLE CRACKS

A Thesis Submitted to the
Graduate School of Natural and Applied Sciences of Dokuz Eylül University
In Partial Fulfillment of the Requirements for the Degree of Doctor of Philosophy in Mechanical Engineering, Machine Theory and Dynamics Program

by
Kemal MAZANOĞLU

January, 2011
İZMİR

Ph.D. THESIS EXAMINATION RESULT FORM

We have read the thesis entitled **"VIBRATION ANALYSIS AND MEASUREMENT OF BEAMS HAVING MULTIPLE CRACKS"** completed by **KEMAL MAZANOĞLU** under supervision of **PROF. DR. MUSTAFA SABUNCU** and we certify that in our opinion it is fully adequate, in scope and in quality, as a thesis for the degree of Doctor of Philosophy.

Prof. Dr. Mustafa SABUNCU

Supervisor

Prof. Dr. Hira KARAGÜLLE	Assist. Prof. Dr. Gülden KÖKTÜRK
Thesis Committee Member	Thesis Committee Member
Prof. Dr. Eres SÖYLEMEZ	Assoc. Prof. Dr. Zeki KIRAL
Examining Committee Member	Examining Committee Member

Prof. Dr. Mustafa SABUNCU
Director
Graduate School of Natural and Applied Sciences

ACKNOWLEDGMENTS

I would like firstly to thank my supervisor, Prof. Dr. Mustafa SABUNCU, for his guidance throughout the doctorate study. This thesis cannot be completed without his valuable supports and positive criticisms.

I am sincerely grateful to Prof. Dr. Hira KARAGÜLLE and Assist. Prof. Dr. Gülden KÖKTÜRK for their valuable suggestions and discussions in periodical meetings of the thesis.

I would also like to express my appreciation to Scientific Research Projects Council of the Dokuz Eylül University for their support with the project number: 2008.KB.FEN.014.

My thanks also extent to Prof. Dr. İsa YEŞİLYURT and Assist. Prof. Dr. Hasan ÖZTÜRK for their helps and useful advices. I would also like to send my thanks to my other colleagues for their morality supports.

Finally, I wish to send my appreciation to my dear family for their encouragements and patience through this study.

Kemal MAZANOĞLU

VIBRATION ANALYSIS AND MEASUREMENT OF BEAMS HAVING MULTIPLE CRACKS

ABSTRACT

Vibration based methods are widespread through the non-destructive methods for detection and identification of cracks in mechanical and structural systems including beam type elements. The methods are effective since any damage leads to changes in vibration characteristics that are easily measured. However, identification of cracks can be more difficult for general beam elements having several complexities.

This thesis presents continuous methods for flexural vibration analyses of multiple cracked beams and detection methods for single and double cracked beams. Vibration of beams are analysed with different geometric, boundary, and crack properties. Vibration analyses of the beams having multiple transverse cracks, multiple height-edge cracks, and asymmetric double edge cracks are all presented. Both open and breathing crack models are considered. Energy based numerical solution method is used in the analyses by describing the energies consumed caused by each crack. Interactions between the crack effects are also described.

Contour lines representing natural frequency ratios are employed for detecting single crack. As a contribution to current literature addressing the inverse problems, a frequency based algorithm is developed for detection of double cracks. An automated single and double crack detection system is established by using theoretical and measured natural frequencies. In measurement, stable natural frequencies are obtained by means of a statistical approach (RSZF) using an interpolation technique (DASI). Direct and inverse methods presented in this thesis simplify the crack detection, are convenient for different structures, ideal for automation, and require low process time, memory and disc capacity.

Keywords : Multiple cracked beams, flexural vibration, energy used continuous solution, crack detection, natural frequency contour lines, RSZF, DASI.

ÇOK ÇATLAKLI ÇUBUKLARIN TİTREŞİM ANALİZİ VE ÖLÇÜMÜ

ÖZ

Titreşim esaslı metotlar, çubuk tipi elemanlar içeren mekanik ve yapısal sistemlerdeki çatlakların tespit edilmesi ve tanımlanması için kullanılan tahribatsız metotlar arasında yaygındır. Bu metotlar, her hasarın kolaylıkla ölçülen titreşim karakteristiklerinde değişimlere neden olmasından dolayı etkilidirler. Fakat, çeşitli karmaşıklıklara sahip genel çubuk elemanları için çatlakların tanımlanması daha zor olabilir.

Bu tez çok çatlaklı çubukların eğilme titreşim analizleri için sürekli metotlar ile birlikte tek ve çift çatlaklı çubuklar için tespit metotlarını sunmaktadır. Çubukların titreşimi farklı geometri sınır ve çatlak koşulları ile analiz edilmiştir. Çoklu dik çatlaklara, çoklu yan kenar çatlaklarına ve asimetrik çift taraflı çatlaklara sahip çubukların titreşim analizleri gösterilmiştir. Açık ve nefes alan çatlak modellerinin ikisi de incelenmiştir. Analizler içinde her çatlağın sebep olduğu enerji yutumları tanımlanarak enerji esaslı nümerik çözüm metodu kullanılmıştır. Çatlak etkileri arasındaki etkileşimler ayrıca tanımlanmıştır.

Tek çatlağın tespiti için doğal frekans oranlarını gösteren kontur çizgileri kullanılmıştır. Şu anki ters problemleri işaret eden literatüre katkı olarak, iki çatlağın tespiti için frekans esaslı bir algoritma geliştirilmiştir. Teorik ve ölçülen frekansları kullanarak bir otomatik tek ve çift çatlak tespit sistemi kurulmuştur. Ölçümde, değişmeyen doğal frekanslar bir interpolasyon tekniği (DASI) kullanan bir istatistik yaklaşım (RSZF) yardımıyla elde edilmiştir. Bu tezde sunulan direk ve ters metotlar çatlak tespitini basitleştirirler, farklı yapılar için uygundurlar, otomasyon için idealdirler ve düşük işlem zamanı, hafıza ve disk kapasitesi gerektirirler.

Anahtar sözcükler : Çok çatlaklı çubuklar, eğilme titreşimi, enerji kullanan sürekli çözüm, çatlak tespiti, doğal frekans kontur çizgileri, RSZF, DASI.

CONTENTS

Page

CHAPTER ONE
INTRODUCTION

1.1 Introduction

Mechanical systems or their structures frequently employ beam type elements which have to resist physical or chemical loading effects such as impacts, fatigues, corrosions, welds, etc. All these influences can result in flaws that lead to change of the dynamic behaviour of the structures. The most common damage type is the fatigue crack in beam shaped mechanical or structural elements under dynamic loading. Understanding the vibration effects of cracks enables their recognition in practical applications of vibration monitoring. Therefore, the vibration identification of cracked beams has been universally interested by many researchers.

Exact identification of dynamic behaviours is significant for the success of vibration based crack identification methods which are supported by the theoretical vibration models. Crack identification methods on direct use of several practical applications of measurements and vibration monitoring may not need a theoretical vibration model. These methods are generally based on the inspection of mode shape changes and need measurements with very high quality which use expensive data acquisition and monitoring systems having the properties such as multiple sensors, high sensitivity, large hard disc capacity, and fast processing. Ideal system settled for the crack identification should be inexpensive, non-invasive and automated, so that subjective operator differences are avoided.

This doctorate thesis study presents direct and inverse methods for multiple crack identification based on flexural vibrations of the beams. Motivation of the thesis is shaped according to lacks observed by the literature review presented in the following chapter. A global continuous approach valid for the beams having different geometric, boundary and crack properties has not been presented yet. Multiple cracked beams are not frequently considered. In addition, any multiple crack detection method has not been proposed yet by using only the natural frequency

contours. This is significant lack for crack detection since natural frequency is the most effortlessly measured modal parameter and contour lines of natural frequency ratios can be the most simple observation technique.

1.2 Aims and Objectives

This thesis has two general aims to achieve.

First objective is to develop a general vibration analysis method including a crack modelling for multiple cracked beams. Proposed method should be adoptable for different physical and boundary conditions of beams and different crack types. The specifications such as accurate results, short solution time, and convenience for inverse methods are also aimed for achievements of the developed analysis method. Instead of finite element based approaches, function based continuous approaches including analytical and numerical solution methods are investigated due to their advantage of short solution time.

Secondly, it is aimed to develop a crack detection method for multiple cracked beams. The method should be non-invasive, robust, and convenient for automation. It should need minimum numbers of parameters and data samples to use in experiment. Parameters should be easily measured. Therefore, methods based on natural frequency changes are investigated instead of the methods using mode shape control. Flexural vibration frequencies are used due to their easy observation through the low frequency band in measurement. To develop processes resulting in maximum data quality with minimum samples is also aimed for increasing the success of the crack detection method in applications.

1.3 Thesis Organisation

This thesis is divided into eight chapters summarised as follows:

Chapter 1 discusses the importance of using continuous approaches in cracked beams vibration analyses and using crack detection methods which are simple, effective, accurate and automated as much as possible. Aims and objectives are given for determining the scope of the thesis.

Chapter 2 gives comprehensive review of the studies presented in existing literature. So many studies about the cracked beam vibration analysis, crack modelling, and crack detection are mentioned in the separate sections.

Chapter 3 introduces the vibration analysis of the un-cracked beams and presents continuous methods for the beams with multiple cracks and additional masses. Vibration effects of cracks modelled by rotational springs are investigated by the analytical and numerical methods employing local and continuous flexibility models respectively. While additional masses are modelled by lumped masses in the analytical solution, they are considered as solid in the energy used numerical solution.

Chapter 4 presents the vibration analysis of multiple cracked non-uniform Euler–Bernoulli beams using the distributions of the energies consumed caused by the transverse open cracks. A rotational spring model is used for describing the energy consumed that is equal to total strain change distributed along the beam length. In the cases of multiple cracks, the energy consumed caused by one crack varies with the influence of other cracks.

Chapter 5 presents a vibration analysis of non-uniform Euler–Bernoulli beams having multiple height-edge open cracks. Change of the strain energy distribution given for the transverse cracks is modified for height-edge cracks. If the beam has

multiple cracks, it is assumed that the strain disturbance caused by one of the cracks is damped as much as the depth ratio of the other cracks at their locations.

Chapter 6 presents a method for the flexural vibration of non-uniform Rayleigh beams having double-edge transverse cracks which are symmetric or asymmetric around the central layer of the beam's height. The breathing crack models are employed. Distribution of the energy changes along the beam length is determined by taking the effects of tensile and compressive stress fields into account. Effects of neutral axis deviations are also included in the model.

Chapter 7 presents an algorithm for identification of double cracks in beams and the processes minimising the measurement errors in experiment. Theoretical natural frequency prediction tables prepared by using the single cracked beam model are employed in crack detection. Single cracks are identified by plotting frequency contour lines. Double cracks are detected by the algorithm that searches convenient position pairs over the frequency map. Measurement sensitivity of the experimental data is increased by presented process including a statistical approach and an interpolation technique.

Chapter 8 gives general contributions of the thesis, overview of the specific conclusions, and scopes for the future works.

CHAPTER TWO
LITERATURE REVIEW

2.1 Introduction

Comprehensive review of the previous studies is presented here for the vibration analysis of cracked beams and detection of the cracks. Overviews of the methods examining the changes in dynamic behaviours and measured vibration responses to detect, locate, and characterise damage are given by Dimarogonas (1996) and Doebling, Farrar, & Prime (1998). Specifically, effects of structural damages on natural frequencies and crack identification methods based on the frequencies are summarised by Salawu (1997). Sabnavis, Kirk, Kasarda, & Quinn (2004) summarise the studies presented for detection of the cracks. Good overview for vibration based condition monitoring techniques used in time, frequency or modal domains are presented by Carden & Fanning (2004). More recently, Yan, Cheng, Wu, & Yam (2007) review the developments in modern-type crack detection methods such as wavelet, genetic algorithms, and neural networks in addition to the traditional methods. The papers presented for multiple crack effects and identification methods are reviewed by Sekhar (2008). The papers including the crack modelling approaches based on fracture mechanics are reviewed by Papadopoulos (2008).

In literature, presented methods can be considered under main titles as cracked beam vibration analysis, crack modelling, and crack detection.

2.2 Cracked Beam Vibration Analysis

Structures can be damaged by various external or internal influences such as impacts, fatigues, corrosions and welds. All these influences can result in flaws that lead to change of the dynamic behaviour of the structures. The most common damage type for beam shaped mechanical or structural elements under dynamic loading is the fatigue crack. Understanding the vibration effects of cracks is critically significant for recognising cracks in practical applications of vibration monitoring. In

the literature, vibration analyses of the cracked beams are inspected both analytically and numerically.

Bending vibration of an un-cracked uniform beam is simply analysed by well known continuous solution method. In the method, singular values are determined for the matrix including the terms of the equation set obtained by deflection, slope, moment, and shear changes along the beam. Sinusoidal and hyperbolic sinusoidal terms of the equation set satisfying the boundary conditions at the two ends of the beam form the 4×4 matrix. When the cracks exist, terms of the 4 new equations obtained from continuity and compatibility conditions are added into the matrix for each crack location. At result, n cracks cause $4(n+1)$ equations. Matrix size and accordingly solution time undesirably increase as the number of cracks increases. It should also be noted that to construct the linear system by using this method for a general case of n cracks is not a simple task. This should be the main reason for which cases of just one crack (Dado, 1997; Nandwana & Maiti, 1997a; Rizos, Aspragathos, & Dimaragonas, 1990) and two cracks (Douka, Bamnios, & Trochidis, 2004; Ostachowicz & Krawczuk, 1991) are considered in the literature. Consequently, this method is not so convenient for the vibration analyses of the multiple cracked beams. Shifrin & Ruotolo (1999) extend this base method by using $n+2$ equations for analysing the vibration of the beams with *n* cracks.

Solution of the equation set can also be simplified by the analytical transfer matrix method that contributes the analyses of the cracked beams by reducing the size of the matrix. Lin (2004) uses this method for the analyses of the single cracked beams. However, advantage of the analytical transfer matrix method comes into existence when the multiple cracked beams are considered as given in the studies of Khiem & Lien (2001, 2004), Lin, Chang, & Wu (2002), Patil & Maiti (2003), and Tsai & Wang (1997). Fernandez-Saez & Navarro (2002) presents another analytical approach including the eigenvalue problems formulated by closed-form expressions for the successive lower bounds of the fundamental frequency. Matveev & Bovsunovsky (2002) and Mei, Karpenko, Moody, & Allen (2006) present some other analytical approaches for flexural vibration analysis of the beams.

It should be noted that analytical solution is very difficult for the non-uniform beams due to the geometric nonlinearities causing nonlinear equations. Therefore, limited number of studies is presented for the analytical solution of non-uniform beams. Li (2001, 2002) presents an approach that is used for determining natural frequencies and mode shapes of cracked stepped beams having varying cross-section and cracked non-uniform beams having concentrated masses. However, only some specific forms of non-uniformities can be dealt with in these papers. Analytical methods also suffer from the lack of the fact that the stress field induced by the crack is decaying with the distance from the crack.

Some researchers take into account the exponentially decaying effects of strain/stress fields due to cracks. These effects also cause the nonlinearities and require different approaches in solution. The energy used methods, employing exponentially decaying stress/strain functions based on a variational principle, are proposed to develop and solve vibration equations for these continuous models. Chondros, Dimarogonas, & Yao (1998, 2001) and Chondros (2001) use the variational formulation to develop the differential equation and boundary conditions of single-edge and double-edge cracked beams as one dimensional continuum. The differential equation and associated boundary conditions for a nominally uniform Euler–Bernoulli beam containing one or more pairs of symmetric cracks are derived by Christides & Barr (1984). Shen & Pierre (1994) solve the varying energy distribution problem for single cracked beams by using many termed Galerkin's method. Carneiro & Inman (2001) review this paper by modifying the derivation of the equation of motion in order to overcome the lack of self-adjointness. Another approach based on the stiffness definition of cracked beams using strain energy variation around the crack is proposed by Yang, Swamidas, & Seshadri (2001), for single and double cracked beams. The case where two or more cracks lie in close proximity to each other is not analysed in this study. All these approaches suffer from the overlap of exponential functions when the multiple cracks interact with each other. An approach for defining interaction of strain disturbances is presented by Mazanoglu, Yesilyurt, & Sabuncu (2009) on the first three flexural vibration

modes of multiple cracked non-uniform beams. The Rayleigh–Ritz approximation method is used in solution. Interaction of strain disturbances presented for transverse cracks is then modified for cracks on unusual edge of an Euler–Bernoulli beam (Mazanoglu & Sabuncu, 2010a) and for asymmetric double-edge breathing cracks on the Rayleigh beam (Mazanoglu & Sabuncu, 2010b).

Except for the methods based on a variational principle, some other methods are also presented for the vibration analysis of cracked beams. Fernandez-Saez, Rubio, & Navarro (1999) describe the transverse deflection of the cracked beam by adding the polynomial functions to the deflection of the un-cracked beam. With this new admissible function, which satisfies the boundary and kinematic conditions, and by using the Rayleigh method, fundamental frequency is obtained. Chaudhari & Maiti (1999, 2000) propose a method for defining transverse vibrations of tapered beams and geometrically segmented slender beams with a single crack using the Frobenius technique. Even though the beams have a single crack, their results are quite coarse. An approach, which uses modified Fourier series, is developed by Zheng & Fan (2001) for computing natural frequencies of a non-uniform beam with arbitrary number of cracks. A semi-analytical model for nonlinear vibrations based on an extension of the Rayleigh–Ritz method is presented by El Bikri, Benemar, & Bennouna (2006). The results, which are mainly influenced by the choice of the admissible functions, are restricted with a single crack and fundamental frequency.

Many of the other approaches are based upon the finite element methods. Gounaris & Dimarogonas (1988) and Papaeconomou & Dimarogonas (1989) construct the special cracked element for the vibration of the cracked beam. They develop a compliance matrix for the behaviour of the beam in the vicinity of the crack. Mohiuddin & Khulief (1998) develop a finite element model for a tapered rotating cracked shaft. Yokoyama & Chen (1998) present the matrix equation for free vibrations of the cracked beam that is constructed from the basic standard beam elements combined with the modified line–spring model. Zheng & Kessissoglou (2004) describe an overall additional flexibility instead of the local additional flexibility for adding into the flexibility matrix of the corresponding intact beam

element. Kisa & Gurel (2006, 2007) present a numerical model that combines the finite element and component mode synthesis methods for the modal analysis of multi-cracked beams and single cracked stepped beams with circular cross-section. Tabarraei & Sukumar (2008) present the extended finite element method for mesh independent modelling of the discontinuous fields like cracks. Use of the finite element methods to solve the forward problem of crack identification is presented by numerous researches (Dharmaraju, Tiwari, & Talukdar, 2004; Lee, 2009a; Lee, 2009b; Orhan, 2007; Ozturk, Karaagac, & Sabuncu, 2009; Yuen, 1985). Finite element models may be preferable since they can be applicable for any structural members. However, there are so many parameters that can be varied in flexural vibration of structural members with cracks that it would be very difficult to present and compare results for all cases. Parameters may vary mainly with modelling of the crack and meshing properties. Indiscriminate application of the frequencies calculated using the finite element methods, without consideration of the assumptions under which the crack models are derived, might lead to gross errors. On the other hand, careful observation of the behaviour of these damage models can lead to extension of their utility in practical engineering. Behaviour of the damages can be observed by the special element or connection models. If the FEM includes no special models for the cracks, method should be supported by extremely refined meshes near the cracks for an accurate solution even though the computation time increases.

2.3 Crack Modelling

In the literature, researchers use several crack models for describing the effects of crack on dynamic behaviour of the beam. In general, there exist three basic crack models, namely the equivalent reduced section model, the local flexibility model from the fracture mechanics and the continuous crack flexibility model. Most studies include the local flexibility model which use massless rotational spring or locally reduced cross-section. Magnitudes of the flexibility changes are estimated by the theoretical and experimental outputs of fracture mechanics (Sih, 1973; Tada, Paris, & Erwin,1973).

In most papers, parts of the beam separated by the cracks are connected by using rotational springs providing compatibility and continuity conditions at the crack locations. The effect of rotational spring is considered as the effect of hinge causing local flexibility between two parts of the beam. This model can be used in the fundamental solution of the cracked uniform beams, (Dado, 1997; Douka, Bamnios, & Trochidis, 2004; Ostachowicz & Krawczuk, 1991; Nandwana & Maiti, 1997a; Rizos, Aspragathos, & Dimaragonas, 1990; Chang & Chen, 2005) and analytical transfer matrix method (Khiem & Lien, 2001, 2004; Patil & Maiti, 2003). The papers presented by Chaudhari & Maiti (1999, 2000), Fernandez-Saez & Navarro (2002), Khiem & Lien, (2002), Lee (2009b), Morassi & Rollo (2001), Yang, Chen, Xiang, & Jia (2008) can be selected throughout many other studies that use rotational spring model in their solution methods for identifying local flexibility effects of crack on vibration. Similarly, Yokoyama & Chen (1998) present line-spring crack model used especially in the finite element based solutions. In the continuous crack flexibility models, crack caused additional flexibility effects are distributed along the beams with exponentially decaying functions. The energy change or the additional flexibility calculated by fracture mechanics formulations are distributed along the beam based on a variational principle presented by Carneiro & Inman (2001), Chondros, Dimarogonas, & Yao (1998, 2001), Chondros (2001), Christides & Barr (1984), Hu & Liang (1993), Shen & Pierre (1994). Another distribution function is proposed by Yang, Swamidas, & Seshadri (2001) when the beam is under the effect of only additional strain. Mazanoglu, Yesilyurt, & Sabuncu (2009) modify the distribution function for multiple cracked beams. The energy consumed calculated from the fracture mechanics is verified by means of rotational spring located at the crack tip and is modified by additional rotational spring corresponding to the effects of stress fields near the crack tip. The formulations written for the energy consumed and its distribution form are revised for the height-edge cracks (Mazanoglu & Sabuncu, 2010a) and double-edge cracks (Mazanoglu & Sabuncu, 2010b).

In literature, cracks are also considered with two models that assume the cracks always open or breathing in time. The nonlinear effect of a breathing crack on the

flexural vibration of cracked structures is discussed in some papers (Cheng, Wu, Wallace, & Swamidas, 1999; Chondros, Dimarogonas, & Yao, 2001; Friswell & Penny, 2002; Luzzato, 2003; Matveev & Bovsunovsky, 2002; Qian, Gu, & Jiang, 1990). Mazanoglu & Sabuncu (2010b) combine the open and breathing cracks in the same model. The difference of solutions between the open and breathing crack models is quite small when the amplitude is not so large, and the difference becomes large as the amplitude increased. Thus, most researchers assume the crack remains open in their models to simplify the problem by ignoring nonlinear influences. However, it is clear that there exists frequency modulation caused by the strain/stress difference during the breathing of crack. Therefore, some researchers investigate this effect in measured data by means of several crack detection techniques (Douka & Hadjileontiadis, 2005; Loutridis, Douka, & Hadjileontiadis, 2005; Prabhakar, Sekhar, & Mohanty, 2001; Pugno, Surace, & Ruotolo, 2000; Saavedra & Cuitino, 2002; Sekhar, 2003).

Different crack models classified according to the position and propagation characteristics. Most of the researchers present vibration analysis of a beam with transverse edge crack which is the most critical in respect of fracture of the beam. Vibration effects of the transverse double edge cracks with symmetric depths are also investigated (Al-Said, 2007; Al-Said, Naji, & Al-Shukry, 2006; Chondros, Dimaragonas, & Yao, 1998; Christides & Barr, 1984; Lin, 2004; Ostachowicz & Krawczuk, 1991). In addition, Mazanoglu & Sabuncu (2010b) present a model for the symmetric and asymmetric double-edge cracks that is also true for the single-edge cracks. The cracks on the unusual surface of the beam, called height-edge cracks, are also modelled by Mazanoglu & Sabuncu (2010a). Nandwana & Maiti (1997a) investigate the vibration of the beams with inclined edge or internal cracks. Fracture mechanics formulations for many different cases of the cracks are given by Tada, Paris, & Irwin (1973). Different crack cases can also be considered by means of advanced mesh techniques. Extended finite element meshing procedure developed by Tabarraei & Sukumar (2008) is shown on the examples of double-edge crack and inclined central crack.

2.4 Crack Detection

Numerous methods and approaches are presented for detection and identification of cracks. In many cases, exact identification of the changes in dynamic behaviour is significant for the success of vibration based crack identification methods which are supported by the theoretical vibration models. Contrarily, crack identification methods based on direct use of several practical applications of measurements and vibration monitoring sometimes may not need a theoretical vibration model. These methods are generally based on the inspection of mode shape changes and need measurements with very high quality which use expensive data acquisition and monitoring systems having the properties such as multiple sensors, high sensitivity, large hard disc capacity, and fast processing. Ideal system settled for the crack identification should be inexpensive, non-invasive and automated, so that subjective operator differences are avoided.

In the literature, cracks are identified by observing the changes in modal parameters like natural frequencies and mode shapes. These variations can be detected by means of several monitoring systems that use signal processing techniques or algorithms. In very rare cases, previously modelling of the system may not be required for crack detection in non-model based approaches. Crack detection methods proposed in the literature are summarised here by considering them under subtitles of frequency based methods, mode shape based methods, and other methods.

2.4.1 Frequency Based Methods

Natural frequencies and frequency spectra of any system directly represent characteristic vibration behaviour of that system. Changes in frequency parameters can easily be observed in measurements without the requirement of extended measuring systems. Therefore, crack detection methods based on natural frequencies are the most popularly proposed and used by the researchers.

The majority of studies are related with the identification of single transverse crack in a beam using the lowest three natural frequencies represented in the frequency contour graph. Liang, Choy, & Hu (1991) propose that the location and the size of a crack can be identified through finding the intersection point of three frequency contour lines. The scheme is adapted to the crack detection in stepped beams (Nandwana & Maiti, 1997b), geometrically segmented beams (Chaudhari & Maiti, 2000) and truncated wedged beams (Chinchalkar, 2001). Chen, He, & Xiang (2005) present an experimental detection of single crack using frequency contour lines of the first three vibration modes. Measurement errors are minimised by means of the method of zoom fast Fourier transform which improves the frequency resolution. Yang, Swamidas, & Seshadri (2001) also use the frequency contours for crack identification. Owolabi, Swamidas, & Seshadri (2003) report the damage detection schemes depending on the measuring changes in the first three natural frequencies and the corresponding amplitudes of the frequency response functions. It is also suggested that two measurements are sufficient to detect a crack in a beam. Dado (1997) presents a comprehensive algorithm, which uses the lowest two natural frequencies as inputs, for detection of a crack in beams under different end conditions. Kim & Stubbs (2003) and Kim, Ryu, Cho, & Stubbs (2003) present a crack detection algorithm to locate and size cracks in beam type structures using a few natural frequencies. Lin (2004) determines the crack location and its sectional flexibility by measuring any two natural frequencies used in characteristic equation. The crack size is then computed by using the relationship between the sectional flexibility and the crack size. Dharmaraju, Tiwari, & Talukdar (2004) develop a general identification algorithm to estimate crack flexibility coefficients and the crack depth based on the force-response information. The general identification algorithm is extended to overcome practical limitations of measuring with a few degrees of freedom. The static reduction scheme is incorporated into the identification algorithm for reducing the number of response measurements. Al-Said (2007) proposes a crack identification technique, which uses shift of first three natural frequencies, for stepped cantilever beam carrying a rigid disk at its tip. In many cases, the theoretical natural frequencies do not exactly intersect with the frequencies observed in measurement. Therefore, the zero-setting procedure is

recommended and thus results are shown by frequency falling ratios. In experiment, natural frequency shifts are generally obtained by the spectral investigation of the frequency response function.

Another frequency used method, called mechanical impedance, is based upon spatial or spectral investigation of anti-resonance frequencies in experiments. Zeros of frequency response functions, where the output velocities have peak values, are known as anti-resonance frequencies. Prabhakar, Sekhar, & Mohanty (2001) suggest the measurement of mechanical impedance for crack detection and condition monitoring of rotor-bearing systems. Bamnios, Douka, & Trochidis (2002) analytically and experimentally investigate the influence of transverse open crack on the mechanical impedance of cracked beams under various boundary conditions. Dilena & Morassi (2004) deal with the identification of single open crack using the method based on measurements of damage-induced shifts in natural frequencies and anti-resonant frequencies. Dilena & Morassi (2005) also present the same method for identification of a single defect in a discrete beam–like system with lumped masses. However, experiments of Dharmaraju & Sinha (2005) conducted on a free–free beam show that sharp slope change cannot be observed through the change of first anti-resonance frequencies obtained as a function of measuring location.

In consideration of the papers presented for the multiple cracks, although most of studies address the forward problem, some of the papers present also the multiple crack detection methods using the knowledge of dynamic response of the beam. Simultaneous detection of location and size of multiple cracks in a beam is much more involved and complex than the detection of single crack. A frequency measurement based method that combines the vibration modelling through transfer matrix method and the approach given by Hu & Liang (1993) is presented by Patil & Maiti (2003) for detection of multiple open cracks. Khiem & Lien (2004) apply the dynamic stiffness matrix method to detect multiple cracks in beams using natural frequencies. A diagnostic technique, which uses the changes of first three natural frequencies, is presented by Morassi & Rollo (2001) for a simply supported beam with two cracks having equal severity. Douka, Bamnios, & Trochidis (2004) use the

anti-resonance changes, complementary with natural frequency changes, in a prediction scheme for crack identification in double crack beams. Chen, Zi, Li, & He (2006) propose dynamic mesh-refinement method, which sets the relationship between the natural frequency ratios and crack parameters, for identification of multiple cracks. Lee (2009a) presents a simple method for detecting *n* cracks using 2*n* natural frequencies by means of the finite element and the Newton–Raphson methods. Detailed review of the studies presented for solving forward and inverse problem of the vibration based identification of multiple cracks are given by Sekhar (2008). The use of contour graphs for detecting multiple cracks has not been presented yet.

2.4.2 Mode Shape Based Methods

Mode shape is the other significant modal parameter changing with existence of the damages. When technical and procedural requirements in measurements are considered, investigation of the mode shape changes is much more difficult than the frequency based techniques. However, if these requirements are provided, mode shape changes supported by the powerful signal processing techniques can be successful indicators of the damages.

In literature, many studies are presented for crack detection by using the changes in mode shapes or their derivatives without the use of any advanced processing techniques. West (1984) presents possibly the first systematic use of mode shape information for the location of structural damage without the use of prior finite element model. The mode shapes are partitioned using various schemes, and the change in modal assurance criteria across the different partitioning techniques is used to localise the structural damage. Rizos, Asparagathos, & Dimarogonas (1990) identify the depth and location of a crack by observing the mode shape of the structure from the measured amplitudes. Pandey, Biswas, & Samman (1991) demonstrate that absolute changes in mode shape curvature can be a good indicator of damage for the finite element beam structures they considered. Farrar & Jauregui (1998) compare the changes in properties such as the flexibility or stiffness matrices

derived from measured modal properties and changes in mode shape curvature for locating structural damage. Ratcliffe (1997) proposes a damage detection method that uses modified Laplacian operator on mode shape data. Narayana & Jeberaj (1999) present a new technique for locating crack using a few vibration mode shapes of a beam and one of the modal parameters that changes globally. Matveev & Bovsunowsky (2002) develop the algorithm of consecutive calculation of cracked beam mode shapes amplitudes, to investigate the regularities of mode shapes and to study the non-linear distortion level of displacement. Kim et al. (2003) formulate a damage index algorithm to identify damage from monitoring changes in modal strain energy.

In recent years, spatial investigation of mode shape changes is considered together with the advanced processing techniques. Many of them are based on the spatial wavelet analyses. Initial studies for crack identification with the application of wavelet theory in spatial domain are presented by Liew & Wang (1998), Quek, Wang, Zhang, & Ang (2001) and Angelo & Arcangelo (2003). In the paper presented by Rucka & Wilde (2006), the theory is applied to the deflected beam whose deflection rate is continuously obtained by the support of image processing. However, crack depth cannot be estimated in these papers. Douka, Loutridis, & Trochidis (2003) analyse the fundamental vibration mode of a cracked cantilever beam using continuous wavelet transform in spatial domain and estimate both location and size of the crack. An intensity factor is defined to relate size of the crack with the coefficients of the wavelet transform. Lam, Lee, Sun, Cheng, & Guo (2005) estimate the location and extend of a crack on the obstruction area where vibration responses are not available. Presented crack detection method for partially obstructed beams is developed from the spatial wavelet transform and the Bayesian approach. Chang & Chen (2005) and Chasalevris & Papadopoulos (2006) present methods that combine the spatial wavelet analysis to find the locations of multiple cracks and natural frequency changes to find the severity of the cracks. Similarly, multiple cracks on stepped beams are located by wavelet analysis in the paper of Zhang, Wang, & Ma (2009). Based on the identified crack locations, a simple transform

matrix method requiring only the first two tested natural frequencies is used to identify the crack depths.

Hadjileontiadis, Douka, & Trochidis (2005a) estimate the location and size of the crack by analysing the fundamental vibration mode with fractal dimension measure. They also analyse the modal changes by using kurtosis values obtained from the vibration data taken along the beam (Hadjileontiadis, Douka, & Trochidis, 2005b).

2.4.3 Other Methods

Investigation of the changes in damping parameter due to cracks does not pay attention among the researchers. In early years, a few studies are presented to test the variation characteristics of damping parameter as a result of crack propagation. Morgan & Osterle (1985) propose probably first damping based method which employs an abnormal increase in damping coefficients, suggesting more energy dissipation, can indicate damage in the structure as observed experimentally in most cases.

Time–frequency analyses are also presented for identifying the presence of a crack. In the paper of Sekhar (2003), wavelet is applied to the time data taken from selected position of a rotor. A model based wavelet approach is proposed for online identification of a crack in a rotor while it is passing through its flexural critical speed. Douka & Hadjileontiadis (2005) reveal the nonlinear behaviour of the system by using time–frequency methods as an alternative to Fourier analysis methodology. They utilise from empirical mode decomposition, Hilbert transform and instantaneous frequency methods in crack detection. Zhu & Law (2006) estimate the locations and depths of the cracks by wavelet analysis of the data taken from single measuring point. However, spatial changes of the wavelet coefficients are obtained by means of load moving along the beam. Leonard (2007) uses phase and frequency spectrograms to directly obtain the breathing effects of crack causing nonlinear vibration.

In the last two decades, genetic algorithms have been recognised as promising intelligent search techniques for difficult optimization problems. Genetic algorithms are stochastic search techniques based on the mechanism of natural selection and natural evolution. Mares & Surace (1996) employ a genetic algorithm to identify damage in elastic structures. Solution procedures employing genetic algorithms by means of the results obtained by the finite element model are proposed for detecting multiple cracks in beams (Ruotolo & Surace, 1997) and for detecting shaft crack in rotor–bearing system (He, Guo, & Chu, 2001). Krawczuk (2002) uses the wave propagation approach combined with a genetic algorithm for damage detection in beam–like structures. In recent years, Vakil-Baghmisheh, Peimani, Sadeghi, & Ettefagh (2008) present a method employing an analytical model and a genetic algorithm to monitor the possible changes in the natural frequencies of the cantilever beam.

Lee (2009b) presents a simple method to identify multiple cracks in a beam using vibration amplitudes. The inverse problem is solved iteratively for the crack locations and sizes using the Newton–Raphson method and the singular value decomposition method. An iterative neural network technique is proposed by Chang, C.C., Chang, T.Y.P., Xu, & Wang (2000) for structural damage detection. Mahmoud & Kiefa (1999) propose a neural network, which uses six natural frequencies as inputs, for detecting crack size and crack location. Suresh, Omkar, Ganguli, & Mani (2004) use less number of modal frequencies to train a neural network for identifying both the location and depth of a crack. A statistical neural network is proposed by Wang & He (2007) to detect the crack through measuring the reductions of natural frequencies.

CHAPTER THREE
CONTINUOUS APPROACHES FOR FLEXURAL VIBRATION OF THE BEAMS WITH ADDITIONAL MASSES AND MULTIPLE CRACKS

3.1 Introduction

This chapter presents the methods for continuous vibration analyses of multiple cracked beams. Vibration of the beam with additional masses is also considered as a specific case of the beam. First of all, the theories of analytical and energy based numerical solution methods are explained for the flexural vibration of beams without crack. Many components such as discs, gears, etc. can be considered as additional masses on the beams when they have the effect that is not negligible on vibrations. Therefore, the theories are expanded to cover the vibration of beams with additional masses. Lumped and solid mass models are employed in analytical and numerical solution methods respectively. Cracks are modelled by rotational springs describing the flexibility changes locally and continuously. Local and continuous flexibility models are used in the analytical and numerical solution methods respectively. Convenient flexibility changing functions are presented for both models.

Results of the methods are compared with the results of a commercial finite element program. Efficiencies of all methods are discussed on fixed-fixed beam with an additional mass. Vibration effects of the additional mass, one crack, and two cracks are presented on the results of methods considered. Good agreements are observed between the results of the methods employed.

3.2 Flexural Vibration of Un-cracked Beams

Free bending vibration of a uniform beam is identified by following differential equation.

$$EI\frac{\partial^4 w(z,t)}{\partial z^4}+\rho A\frac{\partial^2 w(z,t)}{\partial t^2}=0\,, \tag{3.1}$$

where, E, I, and ρ represent elasticity module, area moment of inertia, and density respectively. Flexural displacement is symbolised by w, and variables z, t are the position along the beam length and time respectively. Exact analytical method or approximate numerical methods can be employed for the solution of Equation (3.1).

3.2.1 Analytical Solution

In analytical solution, Equation (3.1) is separated into independent variables of w and t. Frequency parameter, which depends upon the natural frequency, can be written as:

$$\beta = \sqrt[4]{\frac{\rho A \omega^2}{EI}}, \tag{3.2}$$

which is located into following solution form of uniform beam.

$$W(z) = C_1 \cos \beta z + C_2 \sin \beta z + C_3 \cosh \beta z + C_4 \sinh \beta z . \tag{3.3}$$

C_1, C_2, C_3, and C_4 are the coefficients of harmonic and hyperbolic terms in the mode shape function, $W(z)$. Linear algebraic equation set is formed by using mode shape and its derivatives corresponding to slope, moment, and shear force. Each function should satisfy the boundary conditions such as fixed, free, and pinned. For fixed end, displacement and slope should be zero. Contrarily, moment and shear force are equated to zero for free end. There is no displacement and moment near the pinned joint. Four functions are obtained by using the conditions at two ends. β values causing singularity in 4×4 matrix, which is formed by harmonic and hyperbolic terms of functions, are found.

3.2.2 Numerical Solution

Vibration problem of beams can also be solved approximately by using the energy based approaches such as Rayleigh and Rayleigh–Ritz methods. These methods are based on the principle of energy conservation which dictates the maximum values of potential and kinetic energies should be equal.

$$PE - KE = 0\,, \tag{3.4}$$

where, PE and KE represent maximums of potential and kinetic energies that can be formulated for Euler–Bernoulli beams as follow:

$$PE = \int_{z=0}^{L} \frac{1}{2} EI(z) \left(\frac{d^2 W(z)}{dz^2} \right)^2 dz\,, \tag{3.5}$$

$$KE = \int_{z=0}^{L} \frac{1}{2} \rho A(z) \omega^2 \left(W(z) \right)^2 dz\,. \tag{3.6}$$

Formulation of maximum kinetic energy is modified for the Rayleigh beams, which take into account the effect of rotary inertia around the axis perpendicular to the bending plane, as follows:

$$KE = \int_{z=0}^{L} \frac{1}{2} \rho A(z) \omega^2 \left(W(z) \right)^2 dz + \int_{z=0}^{L} \frac{1}{2} \rho I(z) \omega^2 \left(\frac{dW(z)}{dz} \right)^2 dz\,. \tag{3.7}$$

If κ_j is defined as the coefficient of admissible mode shape function, the derivatives of Equation (3.4) or those of Rayleigh quotient derived from Equation (3.4) should be equal to zero.

$$\partial \left(PE - KE \right) / \partial \kappa_j = 0\,. \tag{3.8}$$

If $\chi_j(z)$ are a series of functions satisfying the end conditions, the mode shape function can be written as:

$$W(z) = \sum_{j=1}^{m} \kappa_j \chi_j(z). \tag{3.9}$$

The functions, $\chi_j(z)$, are given in Table 3.1 for several end conditions. The natural frequencies can be found by minimising the determinant of the matrix, which is formed by the derivatives of function series, obtained from Equation (3.8).

Table 3.1 The functions satisfying several end conditions.

End conditions	$\chi_j(z)$
Fixed-Fixed	$(z/L)^{j+1}(1-z/L)^2$
Pinned-Pinned	$(z/L)^{j}(1-z/L)$
Fixed-Free	$(z/L)^{2}(1-z/L)^{j-1}$
Fixed-Pinned	$(z/L)^{j+1}(1-z/L)$

3.3 Flexural Vibration of the Beams with Additional Masses

3.3.1 Analytical Solution Using Lumped Mass Model

In simplified analytical solution, additional masses can be modelled using lumped masses as shown in Figure 3.1. Effects of additional masses are contributed into beam's vibration by describing compatibility and continuity conditions at their locations. Displacements and slopes are assumed equal at just left and right sides of lumped masses.

$$W_i(z) = W_{i+1}(z),$$
$$W_i'(z) = W_{i+1}'(z) \qquad i = 1,....,n. \tag{3.10}$$

In addition, following compatibility conditions should be satisfied for identifying the vibration of a beam with lumped masses.

$$\mu_i W_i(z) = \left[W_{i+1}'''(z) - W_i'''(z)\right],$$
$$\lambda_i W_i'(z) = \left[W_{i+1}''(z) - W_i''(z)\right] \qquad i = 1,....,n \tag{3.11}$$

where μ_i, λ_i can be defined as follows:

$$\mu_i = \frac{m_i \omega^2}{EI}, \tag{3.12}$$

$$\lambda_i = \frac{J_i \omega^2}{EI}. \tag{3.13}$$

m_i and J_i describe i^{th} lumped mass and polar mass moment of inertia respectively. If a beam with $n+1$ sections separated by n masses is analysed, vibration form of each section can be expressed by a function including harmonic and hyperbolic terms as follows:

$$W_i(z) = C_{4i-3}\cos\beta z + C_{4i-2}\sin\beta z + C_{4i-1}\cosh\beta z + C_{4i}\sinh\beta z, \qquad i = 1,...,n+1 \tag{3.14}$$

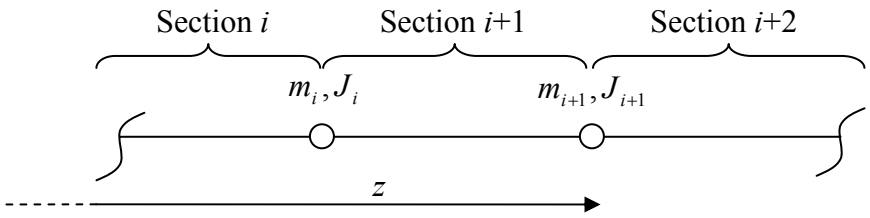

Figure 3.1 Beam model with lumped masses.

As a result, totally four boundaries at two ends, and four boundaries at each mass location give $4n+4$ functions. Zero determinant of the matrix obtained by harmonic and hyperbolic terms of the functions gives the frequency parameter, β.

3.3.2 Numerical Solution Using Solid Mass Model

In more realistic model, the additional masses can be considered with thicknesses as shown in Figure 3.2. In this case, the problem can be solved by one of the energy used numerical methods. In the method, following equation representing the kinetic effects of the additional masses is contributed into the kinetic energy expressions given in Equations (3.6) and (3.7).

$$KE_{m(i)} = \int_{z(m(i))-\frac{t(i)}{2}}^{z(m(i))+\frac{t(i)}{2}} \rho_{m(i)} A_{m(i)}(z)\omega^2 \left(W(z)\right)^2 dz + \int_{z(m(i))-\frac{t(i)}{2}}^{z(m(i))+\frac{t(i)}{2}} \rho_{m(i)} I_{m(i)}(z)\omega^2 \left(\frac{dW(z)}{dz}\right)^2 dz$$

$$i = 1,....,n \qquad (3.15)$$

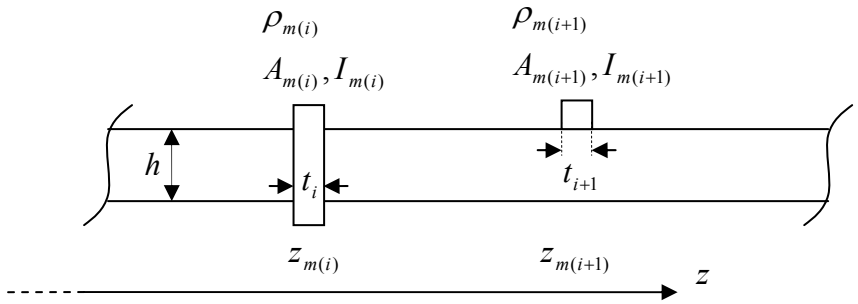

Figure 3.2 Beam model with additional masses having thickness.

If the additional masses are the parts of the beam or joined into the beams by powerful welding, minor changes in potential energy caused by the additional stress fields around the masses can also be considered. These stress fields decaying with the distance from the masses should be described by a function. Unless, this decaying function is described, using a few termed deflection function in the energy methods can result in deficient approximation due to the instantaneous potential energy

change. The issue of stress fields caused by the additional masses, which stays out of the scope of this research, is not investigated. In many cases, the additional stress fields due to the additional masses remain minor. In these cases, potential effects of the additional masses can be neglected for simplicity.

3.4 Flexural Vibration of the Beams with Multiple Cracks

3.4.1 Analytical Solution Using Local Flexibility Model

In general analytical approaches, cracks are modelled by rotational springs, which are joints of the sections separated by the cracks, as shown in Figure 3.3. Existence of n cracks requires the expression of n local flexibility changes for connecting n+1 sections. Vibration form of each section can be expressed by harmonic and hyperbolic terms that are represented by the function written in Equation (3.3). Continuity at the crack location is provided by the continuity conditions come through with negligible effects of crack width. Deflection, bending moment and shear force are assumed to be equal at right hand and left hand sides of the crack as follow:

$$W_i(z) = W_{i+1}(z),$$
$$W_i''(z) = W_{i+1}''(z),$$
$$W_i'''(z) = W_{i+1}'''(z), \qquad i = 1,....,n. \tag{3.16}$$

In addition, compatibility condition relates bending moment with the difference of slopes between both sides of the crack as represented in following equation:

$$W_i''(z) = \alpha_i \left[W_{i+1}'(z) - W_i'(z) \right], \qquad i = 1,....,n. \tag{3.17}$$

α is the parameter related with stiffness that defined as follows:

$$\alpha_i = \frac{k_i}{EI}, \tag{3.18}$$

where k_i represents the local rotational stiffness caused by i^{th} crack, and it is described by the fracture mechanics theory.

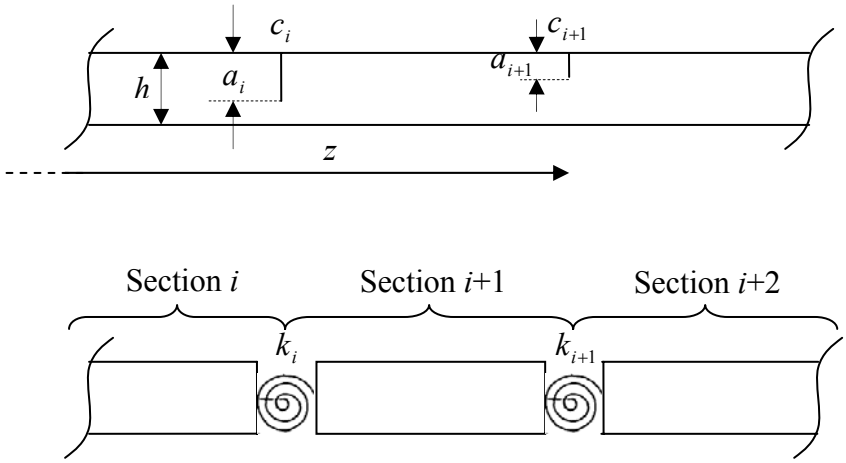

Figure 3.3 Multiple cracked beam with rotational spring crack model.

Local stiffness of the cracked beam has been explained by two common formulations in the literature. One of them is presented in the studies of Dado (1997), Douka, Bamnios, & Trochidis (2004), Li (2001), Rizos, Aspragathos, & Dimaragonas (1990), and Shifrin & Ruotolo (1999). The other formulation possibly presented by Ostachowicz & Krawczuk (1991) at first and employed in the studies of Chaudhari & Maiti (2000), Chen, He, & Xiang (2005), Lin (2004), Nandwana & Maiti (1997a) is given as follows:

$$k_i = \frac{Ebh^2}{72\pi f(a_i)}, \tag{3.19}$$

where, b and h symbolise width and depth of the beam respectively. $f(a_i)$ is called as flexibility compliance function of i^{th} crack that is formulated as follows:

$$f(a_i) = 0.6384\left(\frac{a_i}{h}\right)^2 - 1.035\left(\frac{a_i}{h}\right)^3 + 3.7201\left(\frac{a_i}{h}\right)^4 - 5.1773\left(\frac{a_i}{h}\right)^5 + 7.553\left(\frac{a_i}{h}\right)^6 - 7.3324\left(\frac{a_i}{h}\right)^7 + 2.4909\left(\frac{a_i}{h}\right)^8 \quad (3.20)$$

As a result, the equation set having size, $4n+4$, is formed by $4n$ equations of continuity and compatibility conditions and 4 equations of the end conditions. Matrix shaped by harmonic and hyperbolic terms of the equation set must be singular for determining natural frequencies.

3.4.2 Numerical Solution Using Continuous Flexibility Model

In continuous flexibility model, flexibility change caused by the crack is described as exponentially decaying strain change distributed along the beam. Energy correspond of this strain change is used in solution. The energy change due to crack opening can be balanced as the energy stored by a rotational spring located at the crack tip or a linear spring located at the crack mouth as shown in Figure 3.4. Since there is no spring in reality, the energy stored by the spring model is lost somewhere and is called 'the energy consumed'. Fracture mechanics theory describes the change of structural strain/stress energies with crack growth (Sih, 1973). The strain stored due to a crack is determined by means of the stress intensity factor for the Mode I crack and thus strain energy release rate. Clapeyron's Theorem states that only half of the work done by the external moment is stored as strain/stress energy when a crack exists on a beam. The remaining half is the energy consumed by the crack that can be formulated as follows:

$$\Delta U = CE = D(a)M(z_c)^2, \quad (3.21)$$

where, $M(z_c)$ is the bending moment at the crack location of beam that is formulated as:

$$M(z_c) = E' I(z_c) \frac{d^2 W(z_c)}{dz^2}. \tag{3.22}$$

E' is replaced by E for plane stress, or $E/\left(1-\nu^2\right)$ for plane strain. $D(a)$ is the coefficient defined by the following equation for a strained beam having a transverse crack:

$$D(a) = \frac{18\pi F(a)^2 a^2}{E b_c h_c^4}, \tag{3.23}$$

In Equation (3.23), $F(a)$ is the function given for $a/h_c \le 0.6$ as follows:

$$F(a) = 1.12 - 1.4\left(a/h_c\right) + 7.33\left(a/h_c\right)^2 - 13.8\left(a/h_c\right)^3 + 14\left(a/h_c\right)^4. \tag{3.24}$$

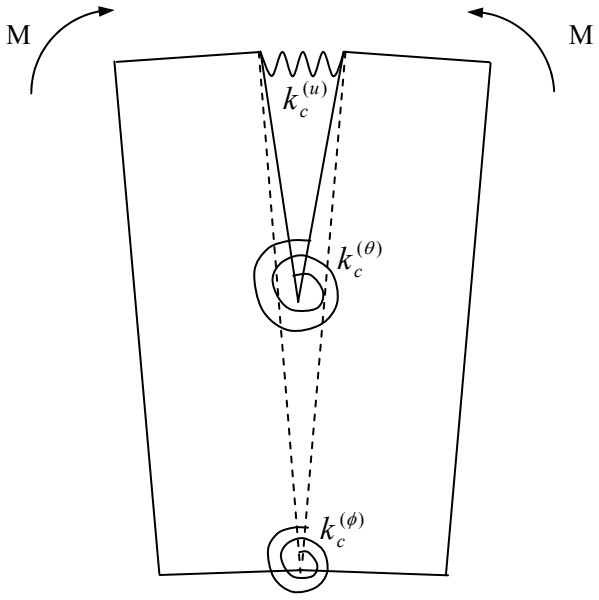

Figure 3.4 Spring models for the crack opening.

The crack opening results in additional angular displacement of the beam causing also tensile stresses in the vicinity of crack tips. The energy of the tensile stress can be considered as the energy of the rotational spring model located at the un-stretched side of the beam as shown in Figure 3.4. When this effect is considered, the energy

consumed is determined by taking the difference between the energy effects of the crack opening and tensile stress caused by the bending of the beam. In this case, the coefficient $D(a)$ is found as follows (Mazanoglu, Yesilyurt, & Sabuncu, 2009):

$$D(a) = \frac{18\pi F(a)^2 a^2}{E b_c h_c^4}\left(1 - a/h_c\right). \tag{3.25}$$

The energy consumed is distributed along the beam as follows (Yang, Swamidas, & Seshadri, 2001):

$$\Gamma^{CE} = \frac{Q(a, z_c)}{1 + \left[(z - z_c)/(q(a)a)\right]^2}, \tag{3.26}$$

where $Q(a, z_c)$ and $q(a)$ are the terms which can be defined as follow (Yang, Swamidas, & Seshadri, 2001);

$$Q(a, z_c) = \frac{D(a)\left[M(z_c)\right]^2}{q(a)a\left\{\arctan\left[(L - z_c)/(q(a)a)\right] + \arctan\left[z_c/(q(a)a)\right]\right\}}, \tag{3.27}$$

$$q(a) = \frac{3\pi\left[F(a)\right]^2 (h_c - a)^3 a}{\left(h_c^3 - (h_c - a)^3\right) h_c}. \tag{3.28}$$

If a crack exists on a beam, since the work is done by using the available maximum potential energy, the energy consumed results in a decrease of maximum potential energy with the assumption that there is no mass loss at the crack location. In this case, Equation (3.4) is modified by contributing the energy consumed as follows:

$$\int_{z=0}^{L} \left(\left(\Gamma^{PE} - \Gamma^{CE}\right) - \Gamma^{KE}\right) dz = 0 \tag{3.29}$$

Natural frequencies or mode shapes of cracked beams can be determined by using Equation (3.29) in one of the energy used numerical methods. In the cases of multiple cracks, stress/strain disturbances caused by different cracks are interacted with each other. When the cracks have reasonable distance from each other, interaction effect remains minor due to the exponentially decaying distribution form of the energy consumed. Since the cracks in close distance are not analysed in this chapter, interaction of consumed energies caused by different cracks is explained in the following chapters.

3.5 Results and Discussion

Vibration of the beams with additional masses are analysed by both the analytical and numerical methods considered and the commercial finite element program (ANSYS©). Comparative study between the methods is also carried out for multiple cracked beams with an additional mass. In the finite element program, cracks are considered as slots which are formed by subtracting thin transverse blocks from the "solid95" beam. Element size is set to 0.005 m with the "esize" command, and crack widths are chosen as 0.0004 m. The "solid95" block is used for modelling additional mass attached to the beam. Smaller element size requirements in the vicinity of discontinuous regions are provided by the "smrtsize,1" command, and free meshing procedures are applied. Finite element model of the beam is shown in Appendix B, Figure B.1. Natural frequencies are obtained by using the analysis type called "modal analysis" in the program. Changes in the element number caused by the variation of crack location and crack size, have negligible effects on the results.

3.5.1 Case Study: A Fixed–Fixed Beam with a Mass

A fixed–fixed steel beam is considered with the additional mass at the central location of the beam. Cross-section of the beam, having length 60 cm, is square with edge dimensions of 10 mm. Steel rectangular mass, with 30 mm edge dimensions and 10 mm thickness, symmetrically encloses the beam. Properties of steel material

are taken as: density $\rho = 7800\,\mathrm{kg/m^3}$, modulus of elasticity $E = 210\,\mathrm{GPa}$, and Poisson ratio $v = 0.3$.

Natural frequencies of the un-cracked uniform beam and the beam with additional mass are given in Table 3.2. Results of the analytical method and the Rayleigh–Ritz method employing the deflection function with six terms are compared with results of the finite element program. All methods give close values for the uniform beam. However, when the results obtained for the beam with additional mass are compared, it is seen that the Rayleigh–Ritz method employing solid mass model gives results better than the analytical method employing lumped mass model. Since a thin beam is used in the analysis, there are very small differences between the results of the Euler–Bernoulli and Rayleigh beam models.

Table 3.2 Natural frequencies of beam models obtained by several analysis methods.

Beam model	Analysis methods	First mode natural frequency (Hz)	Second mode natural frequency (Hz)
Uniform Euler–Bernoulli beam	Analytical method	148.156	408.398
	Rayleigh–Ritz method	148.156	408.398
Uniform Rayleigh beam	Rayleigh–Ritz method	148.135	408.180
Uniform finite element beam	The finite element program	148.174	407.467
Beam with additional lumped mass	Analytical method	126.05	409.003
Euler–Bernoulli beam with additional solid mass	Rayleigh–Ritz method	130.130	407.516
Rayleigh beam with additional solid mass	Rayleigh–Ritz method	130.115	407.300
Finite element beam with additional solid mass	The finite element program	129.420	406.586

If the vibration of the beam is analysed by simulating a transverse crack, natural frequencies fall down as one would expect. Analysis is repeated by considering the crack at different locations with the depth ratio of 0.3. Resulting natural frequency ratios obtained by the local flexibility model used in the analytical solution, the continuous flexibility model used in the Rayleigh–Ritz method, and the finite element model used in the commercial program are given in Figure 3.5. Results show that the methods in consideration present good agreement with each other. Small deviations are obtained near the additional mass and fixed end.

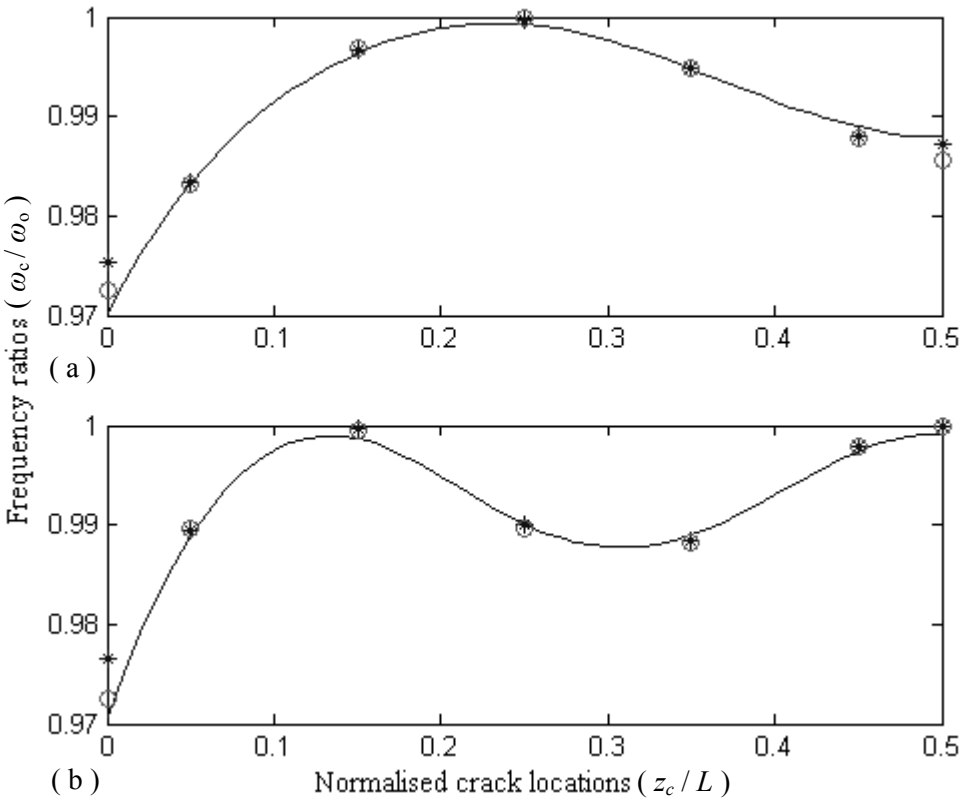

Figure 3.5 Natural frequency ratios for the (a) first and (b) second mode vibrations of the beam with variably located single crack having depth ratio of 0.3. Results of (*) the Ansys©, (o) analytical solution, and (——) Rayleigh–Ritz approximation.

Methods are also comparatively examined by considering the beam with two cracks. One of the cracks is simulated at the normalised location, 0.45, with the depth ratio, 0.3, and the other crack, moved along second half of the beam, is considered with the depth ratio of 0.2. Cracks are not considered in the same side of the

additional mass for neglecting the interaction effects of strain disturbances caused by different cracks. Description of these interaction effects required for the Rayleigh–Ritz method is given in the following chapters. There are good agreements between the results of the methods as shown in Figure 3.6. Expectedly, small deviations between the results for single crack at the normalised location of 0.45, are moved to frequency ratios determined for the double cracked beams.

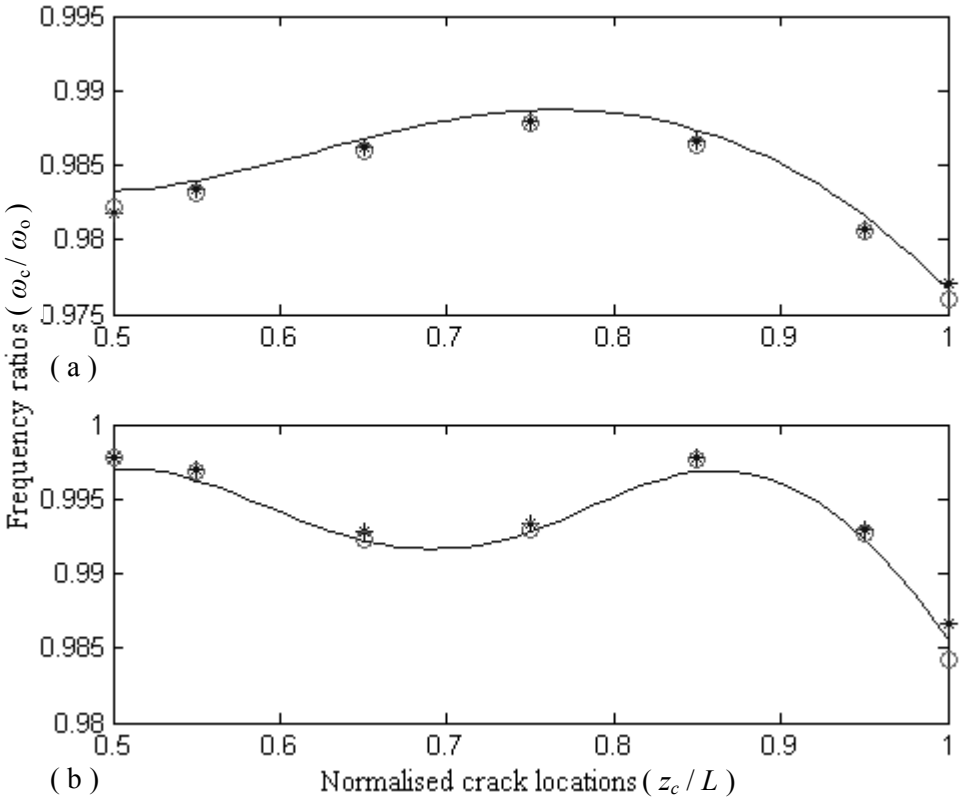

Figure 3.6 Natural frequency ratios for the (a) first and (b) second mode vibrations of the beam with two cracks; first crack at the normalised location, 0.45, with depth ratio of 0.3, and variably located second crack having depth ratio of 0.2. Results of (*) the Ansys©, (o) analytical solution, and (——) Rayleigh–Ritz approximation.

Ratios obtained by the finite element program can be assumed accurate near the additional mass, since the results of the analytical method deviate with the effect of simplified model using lumped mass. On the contrary, the analytical method can give accurate ratios near the fixed end, since the finite element results deviate with the effect of resolution problem in thin surface meshing. However, it should not be

forgotten that, errors in analytical solution for the vibration of un-cracked beams with lumped mass are moved to solution of the cracked beams. This means, although the local flexibility model presents well identification for flexibility change caused by the crack, analytical solution method requires additional flexibility identifications for other discontinuities like additional masses or steps on the beams. The Rayleigh–Ritz method also needs identifying flexibility changes in distributed form for providing continuity along the beam. But, results are quite satisfactory even if the additional mass caused stress fields are not considered. Small differences can be decreased more with the use of deflection function including higher number of terms.

In analytical solution, matrix size increases for each discontinuity requiring compatibility and continuity condition to describe. In example, vibration of a double cracked beam with a mass is analytically solved by finding singular values of 16×16 matrix. As the matrix size increases, determining singular values will be more difficult and will take more process time. However, vibration of that beam is analysed by using deflection function with 6 terms resulting in use of 6×6 matrix in the numerical solution. Therefore, analytical solution with local flexibility model can only be convenient for uniform beams with a few numbers of cracks.

3.6 Conclusion

In this chapter, the methods for continuous vibration analyses of the multiple cracked beams with the additional masses are presented. Lumped and solid mass models are employed in analytical and numerical solution methods respectively. Cracks are modelled by rotational springs describing the flexibility changes locally in analytical method and continuously in the energy method. Results of the methods are compared with the results of a commercial finite element program. Efficiencies of all methods are discussed on fixed–fixed beams. Good agreements are observed between the results of the methods.

In vibration analysis of the beam with additional mass, it is observed that error of the analytical method employing lumped mass model is larger than that of the

numerical method employing solid mass model. Description of the additional stiffness caused by the additional mass cannot be avoided for the analytical solution especially when the thickness of mass increases. However, the energy method gives quite satisfactory result without the use of additional stiffness model.

Low mode vibrations of beams are successfully analysed by using deflection function with a few terms even if the beams have multiple discontinuities including cracks and additional masses. However, number of terms in deflection function used for the analytical solution increases with each discontinuity. Normally, using more terms in deflection function causes larger matrix which requires more solution time for finding its singular values.

Types of the cracks are not separated by the commonly used rotational spring model. Because, flexibility change is modelled by using only one rotational spring located at the centre of beam. This needs the explanation of flexibility change for each different type of cracks. On the other hand, as will be shown in the following chapters, crack types can be identified by the rotational springs located at crack tips.

It is seen that, analytical method with local flexibility model can only be convenient for the analyses of uniform beams with a few numbers of cracks. It is almost impossible to analyse vibration of non-uniform beams by using analytical method. On the contrary, the energy method can be successfully used in different conditions of beam shaped structures. Therefore, energy used numerical solution is proposed in this thesis and it is employed in following chapters for non-uniform beams with different types of cracks.

CHAPTER FOUR
FLEXURAL VIBRATION ANALYSIS OF NON-UNIFORM BEAMS WITH MULTIPLE TRANSVERSE CRACKS

This chapter is reorganization of the paper published as "VIBRATION ANALYSIS OF MULTIPLE CRACKED NON-UNIFORM BEAMS" in *Journal of Sound and Vibration* (Mazanoglu, Yesilyurt, & Sabuncu, 2009).

4.1 Introduction

Flaws in the components of a structure can influence upon the dynamic behaviour of the whole structure. It is well known from the literature that one form of damage that can lead to catastrophic failure if undetected is transverse cracking of the structure elements. The recognition of the vibration effects of cracks is important in practise since vibration monitoring has revealed a great potential for investigation of cracks in the last three decades.

This chapter presents the vibration analysis of multiple cracked non-uniform beams using the distributions of the energies consumed caused by the transverse open cracks. The energy consumed is obtained by the change of the strain energy distribution given by Yang, Swamidas, & Seshadri (2001) for cracked surface of the beam together with the effect of stress field due to the angular displacement of the beam. The energy consumed is also determined by arranging the variation of the strain disturbances for defining the vibration of the multiple cracked non-uniform beams. Results obtained by the present method are compared with the results of Zheng & Fan (2001) and a commercial finite element program (ANSYS©) for several non-uniform cantilever beams.

4.2 Vibration of the Beams with a Crack

According to fracture mechanics theory, structural strain energy increases with the crack growth. Increase in strain energy, which is assumed equal to the energy

consumed, under the constant external bending moment is defined as follows (Sih, 1973; Tada, Paris, & Irwin, 1973);

$$\Delta U = CE = \int_0^a G\, b_c\, da\,. \tag{4.1}$$

G is called the strain energy release rate that can be written as $G = K_1^2 / E'$ for the transverse vibration of the beam by taking only the effects of bending stresses into account and neglecting the effects of shear stresses on the crack. E' is equal to E for plain stress, or $E/\left(1-\nu^2\right)$ for plain strain. Stress intensity factor for the first mode crack $\left(K_1\right)$ is given as:

$$K_1 = \frac{6M(z_c)\sqrt{\pi a}}{b_c {h_c}^2} F(a), \tag{4.2}$$

where $M(z_c)$ and $F(a)$ are given in Equations (3.22) and (3.24). Finally, the energy consumed can be written using the Equation (4.1) as:

$$CE = D(a)\left[M(z_c)\right]^2, \tag{4.3}$$

where the coefficient, $D(a)$, is also given in Equation (3.23).

The expressions given above for the energy consumed (Yang, Swamidas, & Seshadri, 2001) are valid only when the increase in strain energy through the cracked side of beam is taken into account. Increase in strain energy through the cracked beam surface can correspond to the energy of linear springs located along the crack-edge that can be transformed into the energy of rotational springs placed along the crack tip.

$$\Delta U = \frac{1}{2b_c} \int_{\tilde{y}=0}^{b_c} k_c^{(u)} \left(\Delta u_c\right)^2 d\tilde{y}, \tag{4.4}$$

$$\Delta U = \frac{1}{2b_c} \int_{\tilde{y}=0}^{b_c} k_c^{(\theta)} \left(\Delta\theta_c\right)^2 d\tilde{y}. \tag{4.5}$$

However, when slope change at the crack location of the beam is considered, angular displacement of the crack $\left(\Delta\theta_c\right)$ also results with the angular displacement of the beam $\left(\Delta\phi_c\right)$ at the crack location as shown in Figure 4.1. Angular displacement of the beam causes the additional stress field in the vicinity of crack tip. Similar to the additional strain energy definitions, stress energy change $\left(\Delta V\right)$ can also be defined by using linear or rotational spring models $\left(k_c^{(v)}, k_c^{(\phi)}\right)$ seen in Figure 4.1. As the strain caused by the crack decreases the potential energy, additional stress field increases it. Thus, angular displacement of the beam due to the bending decreases the energy consumed. Here, it should be noted that negative compressive strain field required to be considered under the neutral layer in the vicinity of crack, is assumed to be approximately equal to strain at the crack tip. These minor effects neutralise each other and thus can be neglected in the model. Resultantly, the energy consumed can be written as follows:

$$CE = \frac{1}{2b_c} \int_{\tilde{y}=0}^{b_c} \left(k_c^{(\theta)} \left(\Delta\theta_c\right)^2 - k_c^{(\phi)} \left(\Delta\phi_c\right)^2\right) d\tilde{y}\,, \tag{4.6}$$

where, $\Delta\phi_c = \frac{a}{h_c}\Delta\theta_c$. The stiffness relation can also be established by providing bending moment equivalence as:

$$\frac{1}{b_c} \int_{\tilde{y}=0}^{b_c} \left(k_c^{(\theta)}\Delta\theta_c - k_c^{(\phi)}\Delta\phi_c\right) d\tilde{y} = 0\,, \tag{4.7}$$

which results in $k_c^{(\phi)} = \frac{h_c}{a} k_c^{(\theta)}$.

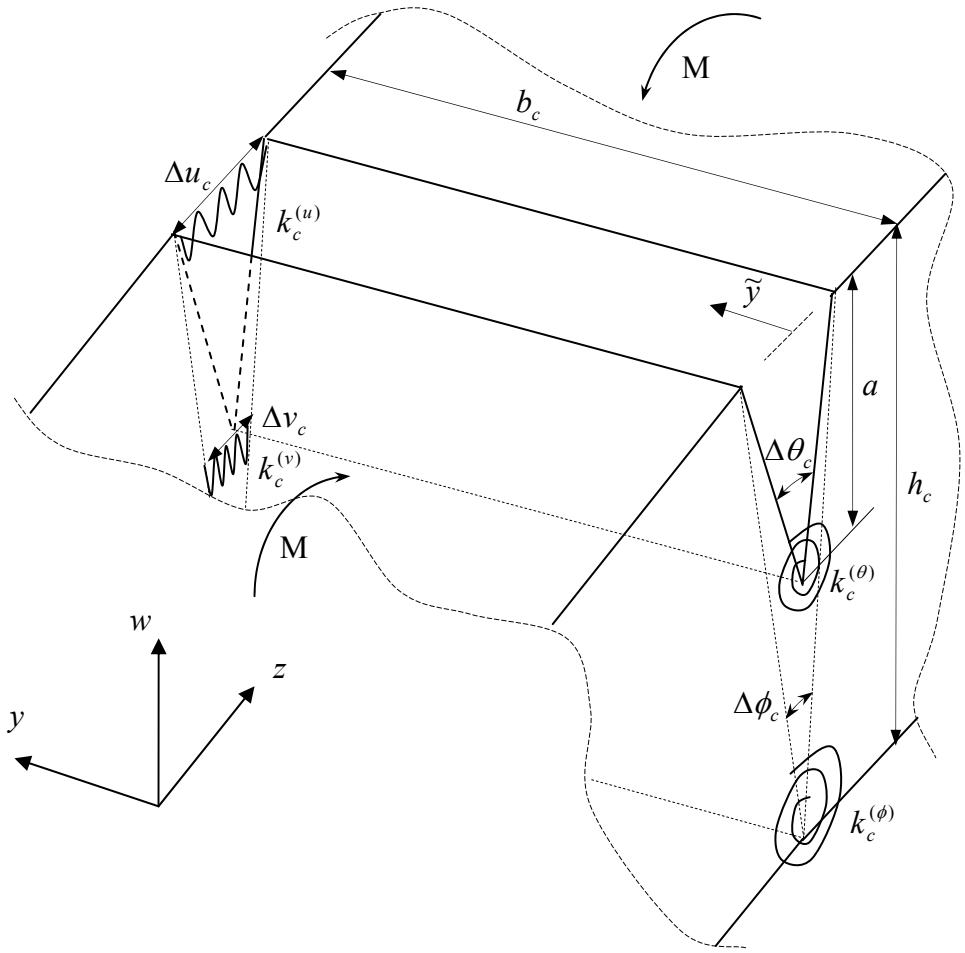

Figure 4.1 Angular displacement of the beam caused by a crack.

Thus, Equation (3.23) can be redefined for $a/h_c \le 0.5$, to include the effects of stress field caused by the angular displacement of the beam.

$$D(a) = \frac{18\pi F(a)^2 a^2}{E b_c h_c^4}\left(1 - a/h_c\right). \tag{4.8}$$

The energy consumed is distributed along the beam as given in Equations (3.26), (3.27), and (3.28) (Yang, Swamidas, & Seshadri, 2001).

According to the principle of conservation of energy, maximum potential and kinetic energies should be equal along the beam when there is no crack. If a crack

exists on a beam, the energy consumed results with the decrease in maximum potential energy with the assumption of no mass loss at the crack location. As a consequence, balance of maximum energies can be obtained as follows:

$$\int_{z=0}^{L}\left(\left(\Gamma^{PE}-\Gamma^{CE}\right)-\Gamma^{KE}\right)dz=0\,, \tag{4.9}$$

where, Γ^{PE} and Γ^{KE} represent the distributions of the maximum potential and kinetic energies as:

$$\Gamma^{PE}=\frac{1}{2}EI(z)\left(\frac{d^2W(z)}{dz^2}\right)^2, \tag{4.10}$$

$$\Gamma^{KE}=\frac{1}{2}\rho A(z)\omega^2\left(W(z)\right)^2. \tag{4.11}$$

Equation (4.9) can be approximated to zero using the Rayleigh–Ritz method explained in Section 3.2.2. Equation (3.8) is rewritten as follows:

$$\partial\left(\int_{z=0}^{L}\left(\left(\Gamma^{PE}-\Gamma^{CE}\right)-\Gamma^{KE}\right)dz\right)\Big/\partial\kappa_j=0\,. \tag{4.12}$$

4.3 Energy Balance in Multiple Cracked Beams

In the case of multiple cracks, parameters in Equations from (4.1) to (4.8) can be modified as $r_i, a_i, z_{c(i)}, h_{c(i)}, b_{c(i)}$ where $i=1\ to\ n$. The effect of interference of cracks on the distribution of the energy consumed for a multiple cracked beam is considered throughout the beam length. Typical distributions are shown in Figure 4.2 for the case of three cracks as an example. It can be noticed that, the distributions cannot be directly superposed, because the overlap of the distributions is considerably influential on the result especially when the cracks approach each other. Therefore,

the contribution of each crack to the maximum potential energy can be arranged according to the change of strain disturbance at other crack locations. In this respect, although the energy consumed caused by crack 1 results with the decrease of maximum potential energy in part 1 and part 2, strain disturbance as a result of crack 1 changes phase at $z_{c(2)}$, and the energy consumed caused by crack 1 results with the increase of maximum potential energy in part 3. Strain disturbance changes phase again at $z_{c(3)}$, and crack 1 negatively effects the maximum potential energy in part 4. Similarly, contributions of other cracks on maximum potential energies are seen in Figure 4.2.

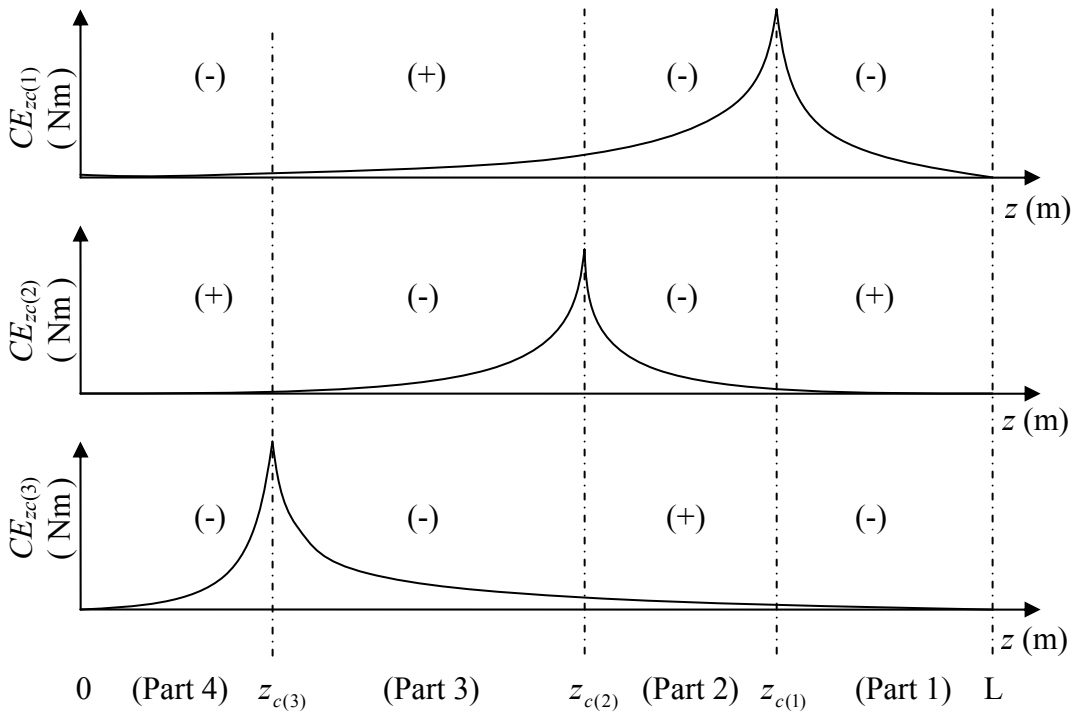

Figure 4.2 Example distributions of the energies consumed caused by three cracks and contributions of these distributions to the maximum potential energy.

As a consequence, if n cracks exist on the beam surface, the following equations can be written for $n+1$ parts;

$$BE_1 = \int_{Zc(1)}^{L}\left(\left(\Gamma^{PE} - \Gamma^{CE}_{c(1)} + \Gamma^{CE}_{c(2)} - \ldots\ldots\ldots \pm \Gamma^{CE}_{c(n)}\right) - \Gamma^{KE}\right)dz$$

$$BE_2 = \int_{Zc(2)}^{Zc(1)}\left(\left(\Gamma^{PE} - \Gamma^{CE}_{c(1)} - \Gamma^{CE}_{c(2)} + \Gamma^{CE}_{c(3)} - \ldots\ldots\ldots \mp \Gamma^{CE}_{c(n)}\right) - \Gamma^{KE}\right)dz$$

$$BE_3 = \int_{Zc(3)}^{Zc(2)}\left(\left(\Gamma^{PE} + \Gamma^{CE}_{c(1)} - \Gamma^{CE}_{c(2)} - \Gamma^{CE}_{c(3)} + \Gamma^{CE}_{c(4)} - \ldots\ldots\ldots \pm \Gamma^{CE}_{c(n)}\right) - \Gamma^{KE}\right)dz$$

$\ldots\ldots\ldots\ldots\ldots$ (4.13)

$$BE_{n-1} = \int_{Zc(n-1)}^{Zc(n-2)}\left(\left(\Gamma^{PE} \pm \Gamma^{CE}_{c(1)} \mp \ldots\ldots + \Gamma^{CE}_{c(n-3)} - \Gamma^{CE}_{c(n-2)} - \Gamma^{CE}_{c(n-1)} + \Gamma^{CE}_{c(n)}\right) - \Gamma^{KE}\right)dz$$

$$BE_n = \int_{Zc(n)}^{Zc(n-1)}\left(\left(\Gamma^{PE} \mp \Gamma^{CE}_{c(1)} \pm \ldots\ldots\ldots + \Gamma^{CE}_{c(n-2)} - \Gamma^{CE}_{c(n-1)} - \Gamma^{CE}_{c(n)}\right) - \Gamma^{KE}\right)dz$$

$$BE_{n+1} = \int_{0}^{Zc(n)}\left(\left(\Gamma^{PE} \pm \Gamma^{CE}_{c(1)} \mp \ldots\ldots\ldots + \Gamma^{CE}_{c(n-1)} - \Gamma^{CE}_{c(n)}\right) - \Gamma^{KE}\right)dz$$

Thus, the energy balance can be obtained by satisfying the following equation:

$$\sum_{i=1}^{n+1} BE_i = 0\,. \tag{4.14}$$

Equation (4.14) can also be approximated to zero by using the Rayleigh–Ritz method.

4.4 Results and Discussion

Results are represented by applying the method on several non-uniform cantilever beams which are dimensioned as seen in Figure 4.3. Relations between heights and length, or widths and length for tapered beams can be defined as follows;

$$h(z) = h_2 + (h_1 - h_2)z/L\,, \tag{4.15}$$

$$b(z) = b_2 + (b_1 - b_2)z/L\,. \tag{4.16}$$

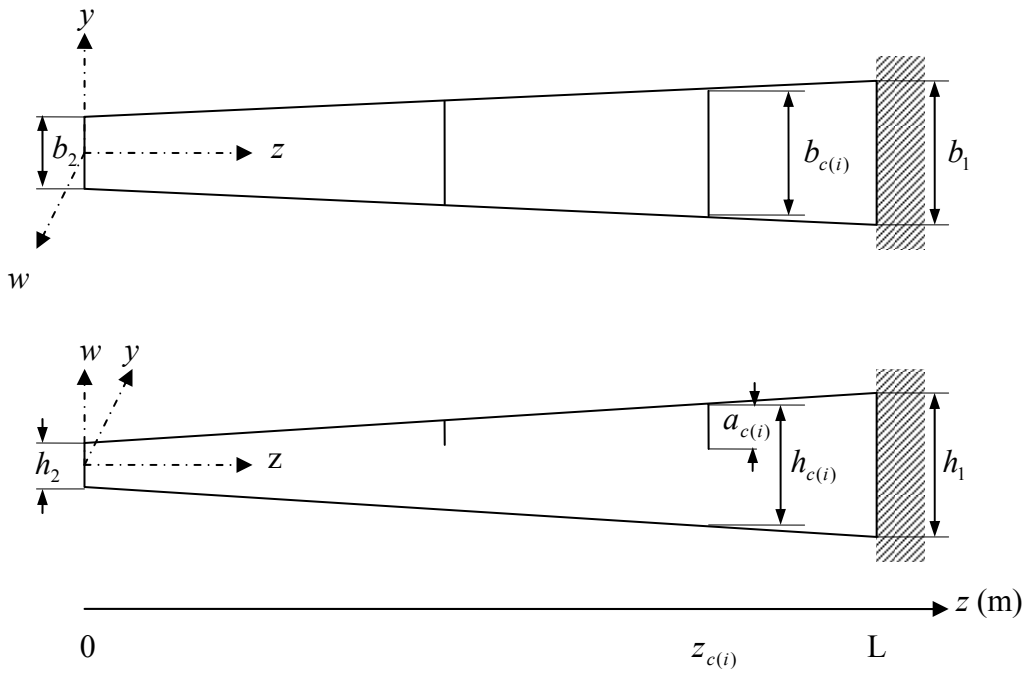

Figure 4.3 Geometry of a beam.

Four different cantilever beams have the same density, $\rho = 7800\,\mathrm{kg/m^3}$ and modulus of elasticity, $E = 210\,\mathrm{GPa}$. The beams have also the following geometric and material properties;

Beam1; $L = 0.6\,\mathrm{m}$, $h_1 = b_1 = 0.02\,\mathrm{m}$, $\alpha_h = h_2/h_1 = 0.25$, $\alpha_b = b_2/b_1 = 1$, $\nu = 0.3$

Beam2; $L = 0.6\,\mathrm{m}$, $h_1 = b_1 = 0.02\,\mathrm{m}$, $\alpha_h = 2$, $\alpha_b = 1$, $\nu = 0.3$

Beam3; $L = 0.6\,\mathrm{m}$, $h_1 = b_1 = 0.02\,\mathrm{m}$, $\alpha_h = 0.25$, $\alpha_b = 0.5$, $\nu = 0.3$

Beam4; $L = 0.8\,\mathrm{m}$, $h_1 = b_1 = 0.02\,\mathrm{m}$, $\alpha_h = 0.5$, $\alpha_b = 1$, $\nu = 0$ (Zheng & Fan, 2001).

The mode shape function of the beams is given in Table 3.1.

Results of the method are compared with the results of commercial finite element program (ANSYS©) for Beam1, Beam2, and Beam3. Cracks are considered as the slots causing discontinuities on the beams. They are formed by subtracting thin

transverse blocks from “solid95” beams in the program. Element size is set to 0.009 m with the “esize” command, and crack widths are chosen as 0.0004 m. Much smaller sized elements are unavoidable in the vicinity of cracks to observe the effects of discontinuities. Smaller sizes are automatically provided by the use of “smrtsize,1” command in the free meshing procedures. As a result, modal frequencies are obtained by using “modal analysis” as the analysis type. It should be noted that, changes in the element number caused by variation of crack location and crack size, have negligible effects on the results. Natural frequencies of the un-cracked beams obtained by the Rayleigh–Ritz approximations and the finite element program can be seen in Table 4.1.

Table 4.1 Natural frequencies of the un-cracked beams.

Beams	Vibration modes	Frequencies (Hz) obtained by Rayleigh–Ritz (4 terms)	Frequencies (Hz) obtained by Rayleigh–Ritz (5 terms)	Frequencies (Hz) obtained by Rayleigh–Ritz (6 terms)	Frequencies (Hz) obtained by finite element program
Beam1	1	55.3163	55.3157	55.3153	55.350
	2	215.4652	214.4026	214.4007	214.183
	3	-	520.6647	514.4896	511.814
Beam2	1	43.4178	43.3889	43.3870	43.4305
	2	374.8819	373.7616	373.7518	369.933
	3	-	1146.4491	1146.4276	1114.86
Beam3	1	66.0191	66.0146	66.0144	66.036
	2	230.7768	228.8314	228.8170	228.550
	3	-	540.6372	529.9834	527.355
Beam4	1	28.4894	28.4866	28.4863	-
	2	136.7583	136.6345	136.4713	-
	3	-	355.5734	354.0987	-

Vibrations of the beams defined above are inspected in the cases of single, double, and multiple cracks as represented in the following examples.

4.4.1 Example 1: Tapered Beams with a Crack

Beam1, Beam2, and Beam3 are examined by following crack properties;

$a_c = 0.15h_1, 0.3h_1, \quad z_c$ (variable)

Results of the method are in good agreement with the results of the finite element program for single crack cases of different beams as shown in Figures 4.4, 4.5, and 4.6. The method is valid for the crack depth ratio, $a/h_c \leq 0.5$ as defined before. It is for this reason that, normalised crack locations of Beam1 and Beam3 are considered between 0.2 and 1 for $a = 0.15h_1$, and between 0.5 and 1 for $a = 0.3h_1$. Application of the Rayleigh-Ritz approximation with 4, 5, and 6 terms is sufficient to obtain the best agreement with the first, second, and third mode of vibrations respectively. It is clear that higher vibration modes require the use of larger number of terms.

If the trends of the natural frequency ratios are comparatively examined for the cracks on Beam1 and Beam2, some distinctions can be obtained. Natural frequency reductions of Beam1 is lower than that of Beam2 when non-dimensional crack locations are lower than 0.8. Besides, node points, where no natural frequency reduction is obtained, are shifted from root to tip with the decreasing truncation factor. On the other hand, relatively minor influences of second taper on natural frequency ratios can be observed when Figure 4.4 is compared with Figure 4.6. Variation of the mass and inertia moment together with the variation of crack depth ratio along the beam are all influential on the observation of the natural frequency ratios seen in the figures.

4.4.2 Example 2: Tapered Beam with Two Cracks

Beam3 is examined by following crack properties;

$$a_1 = 0.3h_1, \quad a_2 = 0.15h_1, 0.3h_1, \quad z_{c(1)} = 0.91L, \quad z_{c(2)} \text{(variable)}$$

Natural frequency ratios obtained by the method are also quite agreeable with those obtained by the finite element program for double cracked Beam3 as shown in Figure 4.7. It can be observed that, as crack 2 comes closer to crack 1, the natural

frequency ratios of the double cracked beams have a tendency of approaching the natural frequency ratio of beams having single crack at $z_{c(1)}$.

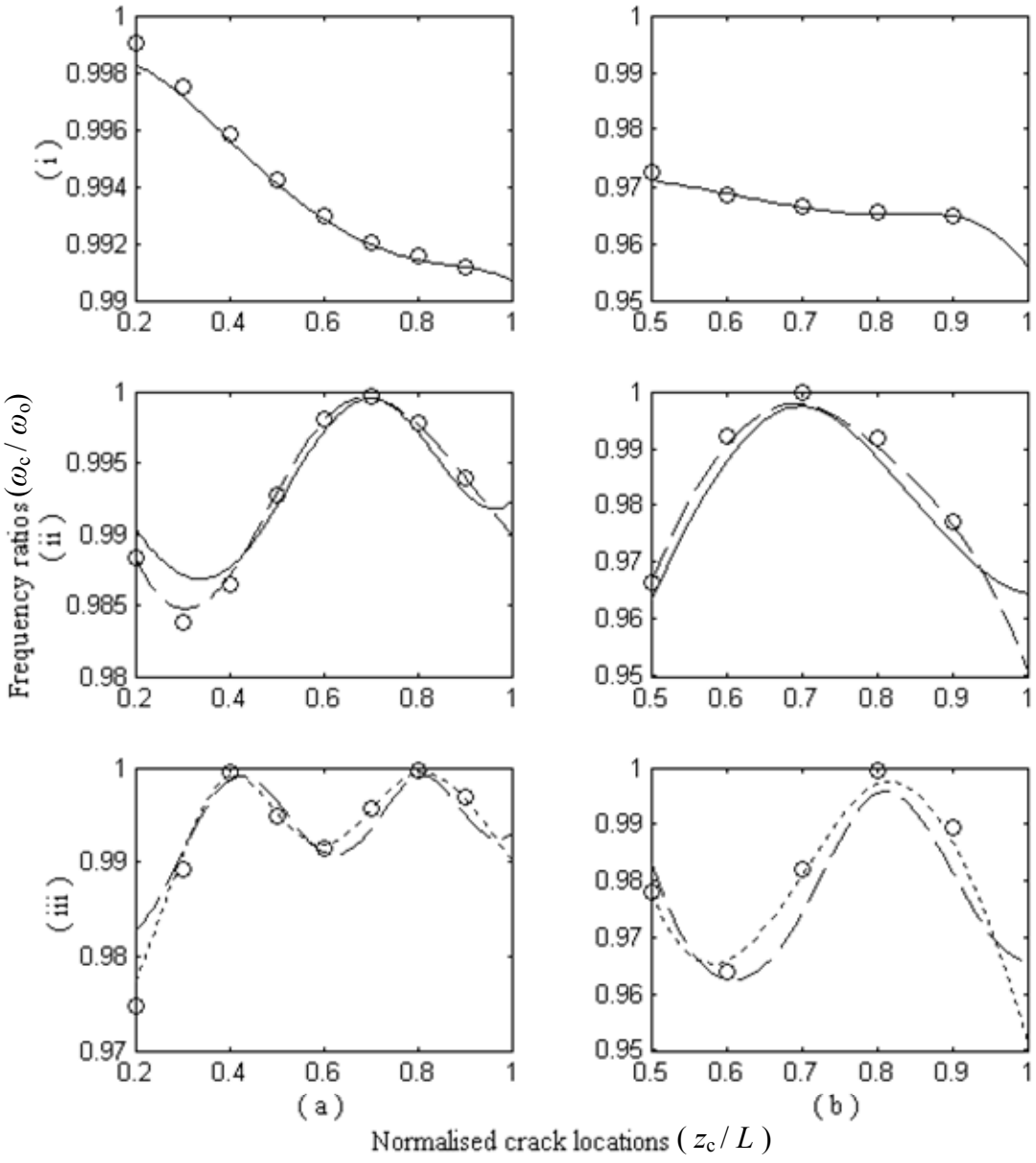

Figure 4.4 Natural frequency ratios for the (i) first, (ii) second and (iii) third mode vibration of Beam1 with variably located crack having depths (a) $a = 0.15h_1$, and (b) $a = 0.3h_1$. (o) Ansys results, (——) approximation with 4 terms, (– –) approximation with 5 terms, (---) approximation with 6 terms.

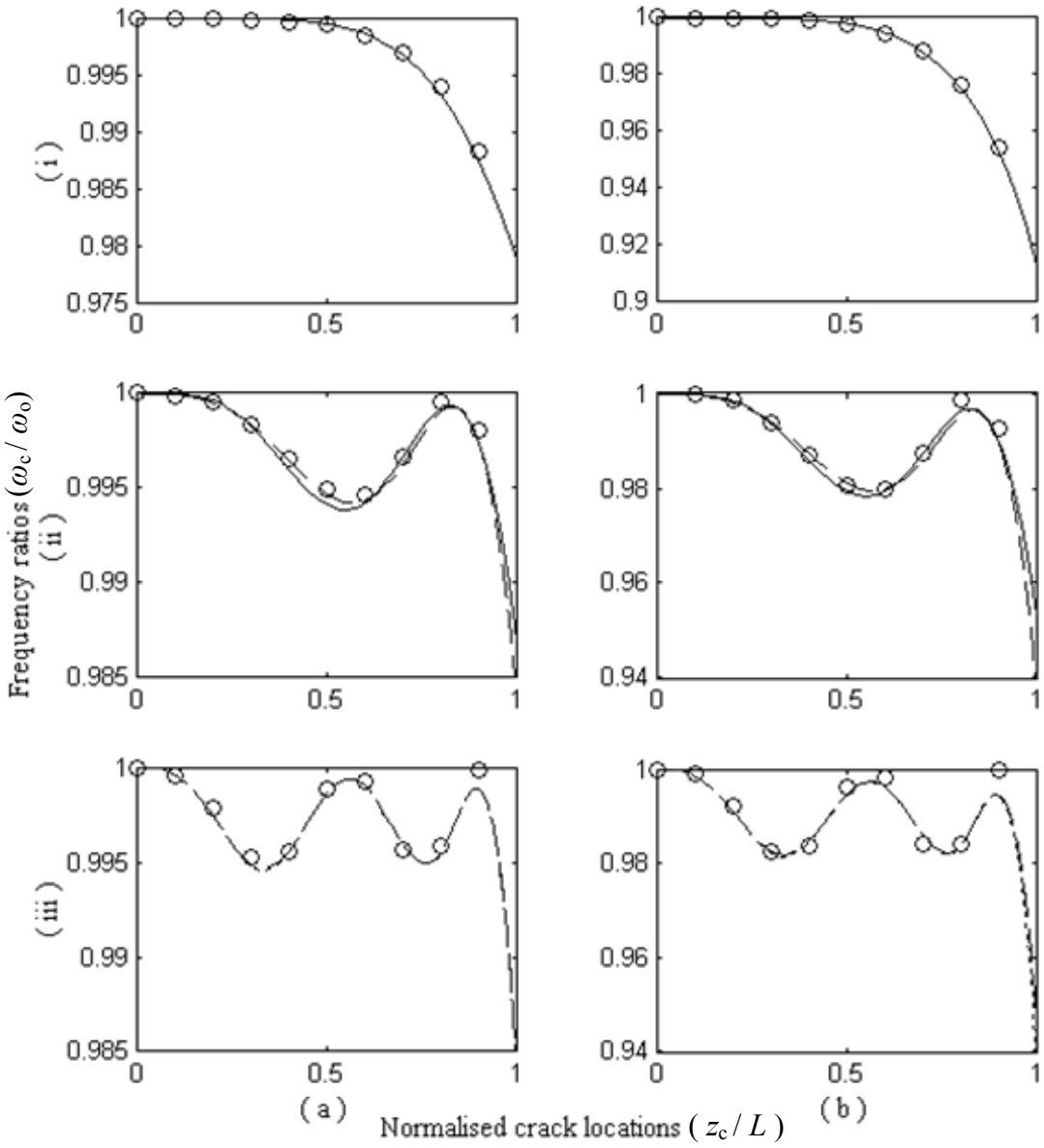

Figure 4.5 Natural frequency ratios for the (i) first, (ii) second and (iii) third mode vibration of Beam2 with variably located crack having depths (a) $a = 0.15h_1$, and (b) $a = 0.3h_1$. (o) Ansys results, (——) approximation with 4 terms, (– –) approximation with 5 terms, (---) approximation with 6 terms.

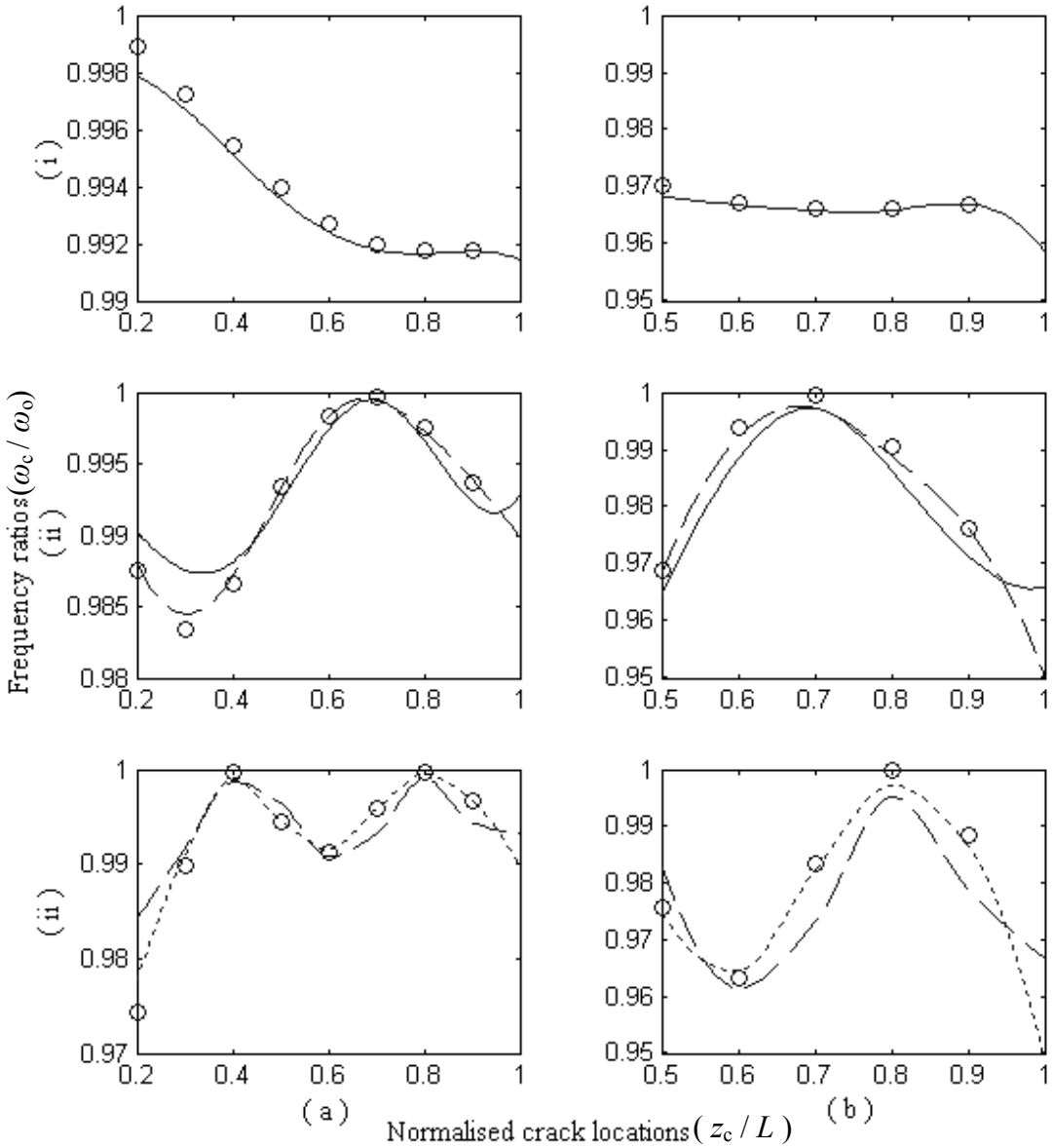

Figure 4.6 Natural frequency ratios for the (i) first, (ii) second and (iii) third mode vibration of Beam3 with variably located crack having depths (a) $a = 0.15h_1$, and (b) $a = 0.3h_1$. (o) Ansys results, (——) approximation with 4 terms, (– –) approximation with 5 terms, (---) approximation with 6 terms.

4.4.3 Example 3: Tapered Beam with Four Cracks

Beam4 has the following crack properties;

$a_1 = 0.3h_1, \quad a_2 = 0.2h_1, \quad a_3 = 0.1h_1, \quad a_4 = 0.1h_1, 0.2h_1, 0.3h_1,$ (variable)

$z_{c(1)} = 0.95L, \quad z_{c(2)} = 0.9L, \quad z_{c(3)} = 0.85L, \quad z_{c(4)}$ (variable)

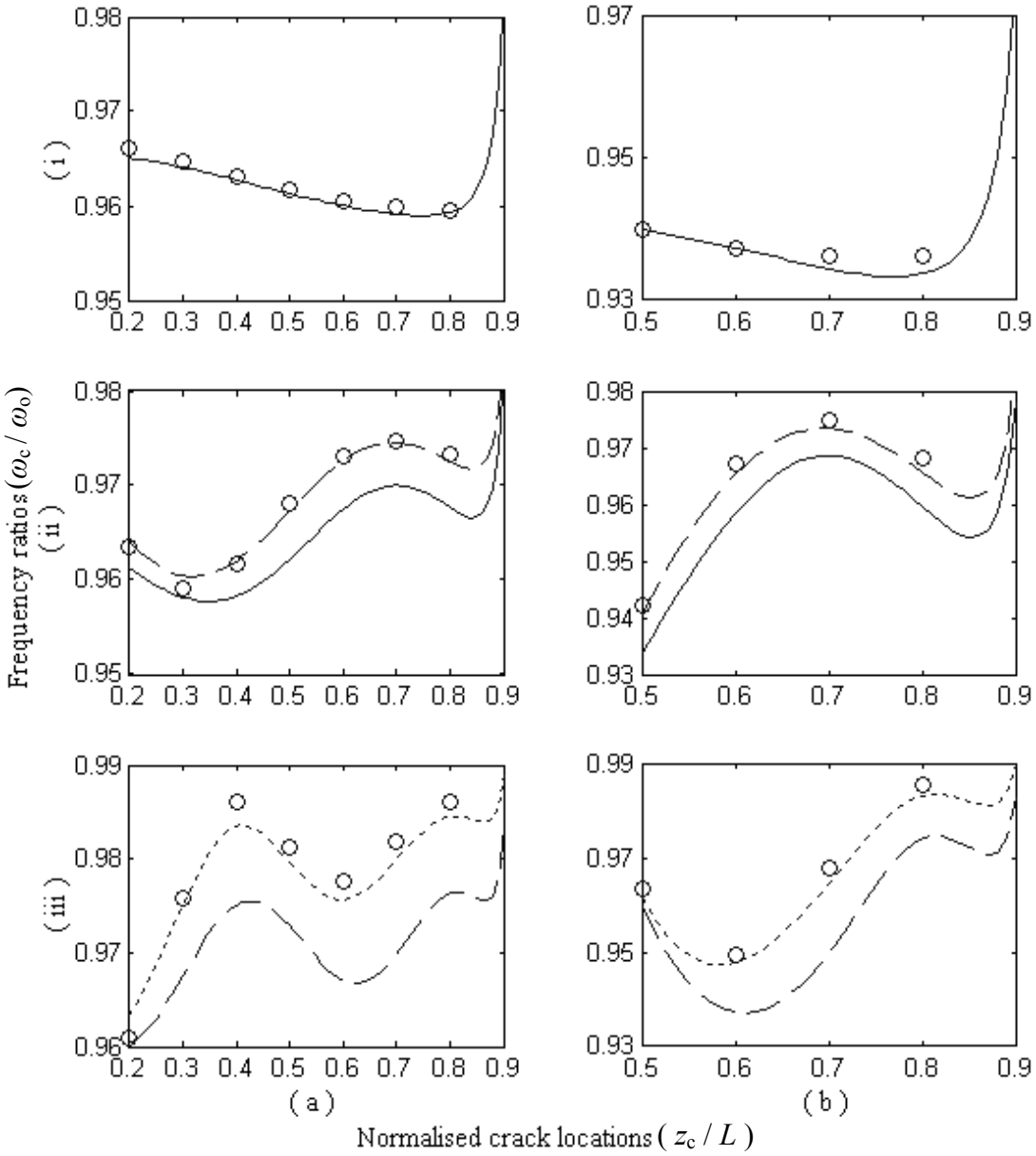

Figure 4.7 Natural frequency ratios for the (i) first, (ii) second and (iii) third mode vibration of double cracked Beam3 with variably located second crack having depths (a) $a_2 = 0.15h_1$, and (b) $a_2 = 0.3h_1$. (o) Ansys results, (——) approximation with 4 terms, (– –) approximation with 5 terms, (---) approximation with 6 terms.

Natural frequency ratios of Beam4 having four cracks are seen in Figures 4.8 and 4.9 for the first and second mode of vibration respectively. Good agreement with the results of Zheng & Fan (2001) is obtained by using four term approximation for the

first mode of vibration as seen in Figure 4.8. However, small differences between the results of two methods for a beam with four cracks can be seen in Figure 4.9 which depicts the second mode natural frequency ratios. Negligible differences increase as the crack depth increases. It can be observed that, as the number of terms in deflection function increases, the difference between the results decreases as expected. In Figure 4.9, the natural frequency ratios coincide for all considered crack depths at the normalised locations 0 and 0.75.

It should be noted that performing the finite element program with the acceptable number of elements that results with the correct solution is not possible for the Beam4 having four cracks. Furthermore, processes can exceed the memory limitations of computers with the previously defined crack and meshing properties, especially when the cracks are too close each other.

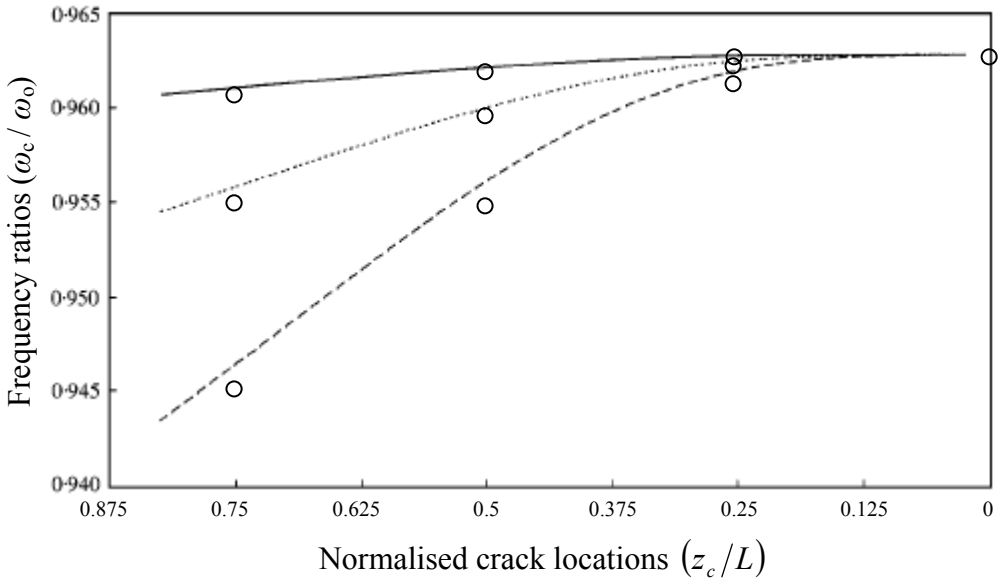

Figure 4.8 Natural frequency ratios of the first mode vibration of Beam4 with variably located fourth crack having depths (——) $a_4 = 0.1h_1$, (····) $a_4 = 0.2h_1$, (---) $a_4 = 0.3h_1$ as given in the paper of Zheng & Fan (2001); and findings of method with 4 terms (o).

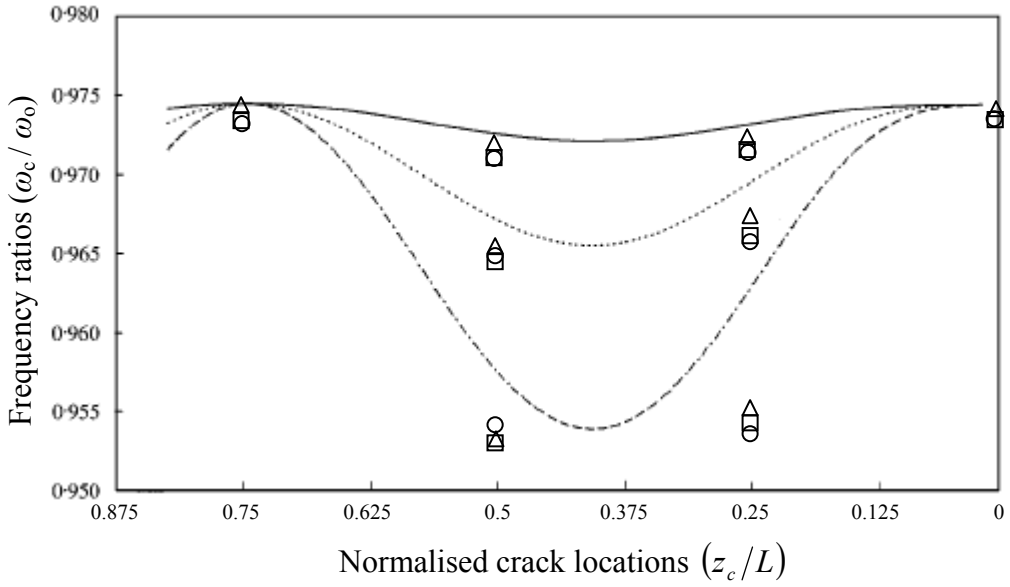

Figure 4.9 Natural frequency ratios of the second mode vibration of Beam4 with variably located fourth crack having depths (——) $a_4 = 0.1h_1$, (····) $a_4 = 0.2h_1$, (---) $a_4 = 0.3h_1$ as given in the paper of Zheng & Fan (2001); and findings of method with 4 terms (o), 5 terms (□), and 6 terms (Δ).

4.5 Conclusion

The energy based method presented by Yang, Swamidas, & Seshadri (2001) is modified to obtain the vibration of multiple cracked non-uniform Euler–Bernoulli beams. Effects of the stress field caused by the angular displacement of the beam in addition to strain energy change caused by the crack are both taken into account in the energy consumed. In the cases of multiple cracks, the energy consumed caused by one crack varies with the influence of other cracks. Examples are presented on several tapered cantilever beams. The results of the method presented agree well with the results of the finite element program when the beam has single or double cracks. Additionally, the first mode frequencies obtained for the multiple cracked Beam4 has an excellent agreement with the results of Zheng & Fan (2001), although small differences are obtained in the second mode.

Instead of the analytical methods, uses of the energy distributions in numerical approaches simplify the solution of non-uniform beams. However, these approaches

suffer from the interaction of crack effects in multiple cracked beams. Proposal for the solution of this problem is presented in this chapter. It is observed that double cracked beam behaves like a single cracked beam when both cracks come closer to each other, as one would expect.

Coupling effects are neglected in this study. It should be remembered that bending-torsion coupling cannot be influential on lower vibration modes of non-uniform Euler–Bernoulli beams. Furthermore, when the beams have cracks with acceptable depth ratios, bending-torsion coupling has still negligible influence on lower vibration modes as seen in the figures representing the comparatively examined method results. However, this coupling may be more influential on the vibration of the stepped beams.

Significant advantage of the method can be performing the processes in quite short durations in the order of seconds. Thus, natural frequencies required for the frequency based inverse methods like prediction schemes or contour graphs can be easily obtained for each different beam. In practical applications, natural frequencies may be measured in some error interval that can be kept in minimum by taking large sampling frequencies.

Effects of truncation factors are evaluated with respect to variation of the natural frequency ratios. Results show that cracks cause lower natural frequency ratios when the beam has lower truncation factor except for the cracks near the root of beam. It is clear that, the truncation factor of beam's height is much more effective than the truncation factor of beam's width. Another finding can be the shift of node points from root to tip with decreasing truncation factor.

CHAPTER FIVE
FLEXURAL VIBRATION ANALYSIS OF NON-UNIFORM BEAMS WITH MULTIPLE CRACKS ON UNUSUAL EDGE

This chapter is reorganization of the paper published as "VIBRATION ANALYSIS OF NON-UNIFORM BEAMS HAVING MULTIPLE EDGE CRACKS ALONG THE BEAM'S HEIGHT" in *International Journal of Mechanical Sciences* (Mazanoglu & Sabuncu, 2010a).

5.1 Introduction

All damages instantaneously change the vibration characteristics of the structures. It is for this reason that, definition of changes in vibration parameters is essential key for identification of damages. In existing literature, almost all researchers deal with the bending vibration of beams having width-edge crack at the stretched surface. More endurance fall and consequently more natural frequency decrease may be the reason of this interest. However, vibration of beams having height-edge crack may also be significant if the external forces bend the beam in the plane of crack tip axis. Stress/strain behaviour of the cracked planes under tension is given in a handbook presented by Tada, Paris, & Irwin (1973) together with many cases of the cracked structures. A thin slender beam can be considered in this scope to analyse its vibration in both planes. If the cracked beam has considerable thickness, vibration effects of the height-edge cracks should be different from those of width-edge cracks. This issue is not presented in existing literature.

This chapter presents a vibration analysis of non-uniform beams having multiple height-edge open cracks. The method uses the changes in the strain energy distribution caused by the cracks. Change of the strain energy distribution given by Yang, Swamidas, & Seshadri (2001) is modified for height-edge crack to obtain the distribution of the energy consumed. The effect of additional bending of the beam due to the crack is determined by developing a simple spring model at the crack location. Coupling effects are neglected for low bending vibration modes of the

Euler–Bernoulli beam. In the case of multiple cracks, a strain disturbance model is presented to overcome the problem of the methods based on a variational principle, which can be described as interaction of the crack effects. Results obtained by the present method are compared with the results of a commercial finite element program (ANSYS©) for several tapered cantilever beams and a fixed–fixed beam. Influences of the taper, boundary and crack location on modal frequencies are given in the figures.

5.2 Theoretical Explanations

According to fracture mechanics theory, structural strain energy increases with the crack growth. Increase in strain energy, which is equal to the energy consumed, under the constant external bending moment is defined as follows:

$$\Delta U = CE = \int_0^a G\, h_c\, da\,. \tag{5.1}$$

G is called the strain energy release rate that can be written as $G = K_1^2 / E'$ for the transverse vibration of the beam by taking the effects of only bending stresses into account and neglecting the effects of shear stresses on the crack. E' is equal to E for plain stress, or $E/\left(1-v^2\right)$ for plain strains (Tada, Paris, & Irwin, 1973).

Stress intensity factor for the first mode edge crack in semi-infinite body $\left(K_1\right)$ is given as:

$$K_1 = 1.12\,\frac{6M(z_c)\sqrt{\pi a}}{b_c h_c^{\,2}}, \tag{5.2}$$

where $M(z_c)$ is the bending moment that formulated in Equation (3.22). The energy consumed can be written using the Equation (5.1) as:

$$CE = D(a)\left[M(z_c)\right]^2, \tag{5.3}$$

where $D(a)$ can be formulated for the edge crack as follows:

$$D(a) = \frac{18\pi\, 1.12^2\, a^2}{E b_c^2 h_c^3}. \tag{5.4}$$

Equation (5.4) is true for the plane stresses or strains and consequently for the slender beam that has $h_c << b_c$. When the edge cracked beam has the considerable height, (h_c), Equation (5.4) is incomplete unless the beam is assumed to be only strained due to the crack as given in many works in the literature. However, opening of the crack also causes additional bending of the beam during the transverse vibration. In this case, average strain along the height of beam and thus stress amount should be half of the maximum values. This means, the stress intensity factor is halved for the considered opening mode of crack. Consequently, Equation (5.4) should be multiplied by the factor of $\varepsilon = 1/4$ for the rectangular beams.

Strains are neutralised by the tensile stresses at the un-cracked cross-sections. However, additional strains come into existence at the crack location. Since the open crack model is used, only additional strains are considered, that is why the neutral layer is not mentioned in this chapter. Nevertheless, E' is modified as $E/\left(1-0.5^2\nu^2\right)$ for a beam with height-edge open crack to contribute the effect of breathing. Increase in strain energy through the stretched surface can correspond to the energy of linear springs located at the opened side of the height-edge crack when the beam is under the effect of bending moment in $w-z$ plane. The energy of linear springs can be transformed into the energy of rotational springs placed at the closed side as shown in Figure 5.1.

$$\Delta U = \frac{1}{2a}\int_{\tilde{y}=0}^{a} k_{\tilde{y}}^{(u)}\left(\Delta u_{\tilde{y}}\right)^2 d\tilde{y}, \tag{5.5}$$

$$\Delta U = \frac{1}{2a}\int_{\tilde{y}=0}^{a} k_{\tilde{y}}^{(\theta)}\left(\Delta\theta_{\tilde{y}}\right)^2 d\tilde{y}\,. \tag{5.6}$$

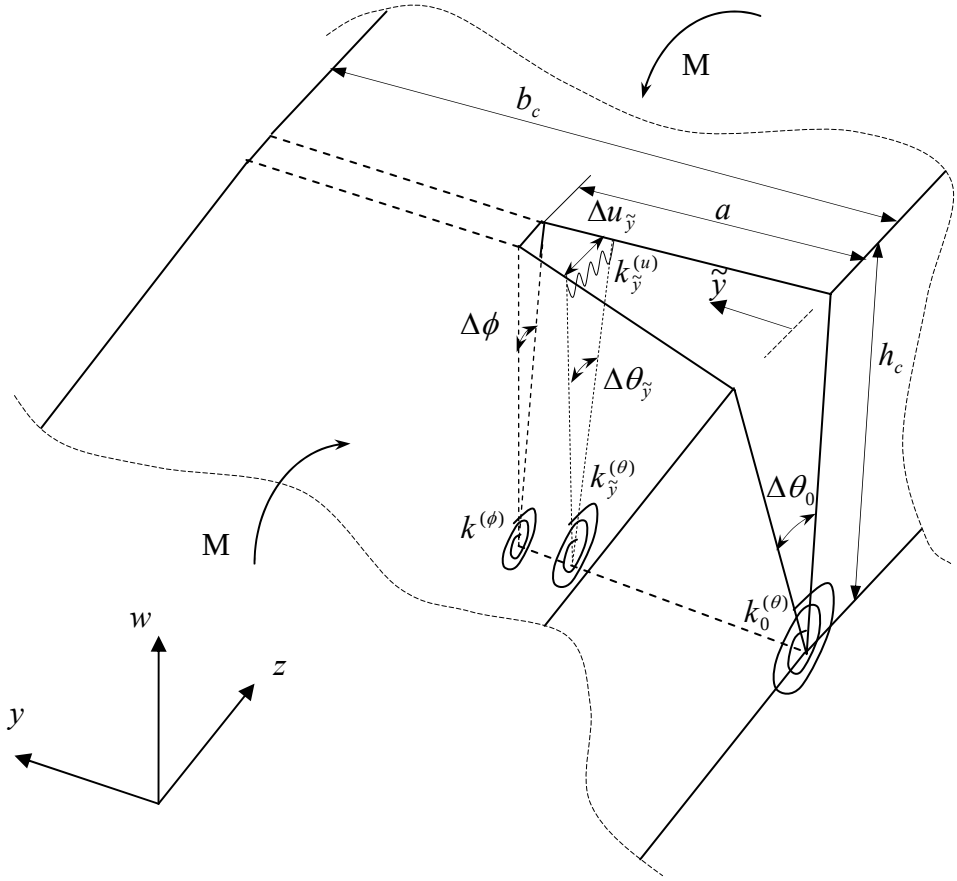

Figure 5.1 Assumed opening form of the crack as the external moment applied to the beam.

Since the cross-section decreases at the crack location, angular displacement of the crack $\left(\Delta\theta_{\tilde{y}}\right)$ results in the angular displacement of the beam $\left(\Delta\phi\right)$. Strain is neutralised by the tensile stress at the un-cracked part of crack location and thus energy is not consumed in this region. That means strain energy of $\left(\Delta\phi\right)$ should be a base for the additional strain energy at the crack location. At result, Equation (5.6) can be modified as follows:

$$\Delta U = \frac{1}{2a}\int_{\tilde{y}=0}^{a}\left(k_{\tilde{y}}^{(\theta)}\left(\Delta\theta_{\tilde{y}}\right)^2 - k^{(\phi)}\left(\Delta\phi\right)^2\right)d\tilde{y}\,. \tag{5.7}$$

Relation between the opening angles ($\Delta\phi$, $\Delta\theta_0$) at the tip ($\tilde{y} = a$) and mouth ($\tilde{y} = 0$) of the crack can be settled as:

$$\Delta\phi = \left(a/h_c\right)^3 \Delta\theta_0 . \tag{5.8}$$

Average angular displacement $\Delta\theta_{av}$ is equal to $\Delta\theta_0/2$. If bending moment equivalence is provided on the stretched surface, relation between the stiffness and angular displacements can be written as:

$$k^{(\phi)} = \frac{\Delta\theta_0}{\Delta\phi} k_0^{(\theta)} = \frac{\Delta\theta_{av}}{\Delta\phi} k_{av}^{(\theta)} . \tag{5.9}$$

Varying opening angles and stiffness can be defined by following equations:

$$\Delta\theta_{\tilde{y}} = 2\Delta\theta_{av}\left[\left(\left(a/h_c\right)^3 - 1\right)\frac{\tilde{y}}{a} + 1\right], \quad \text{for } 0 < \tilde{y} < a \tag{5.10}$$

$$k_{\tilde{y}}^{(\theta)} = \frac{k_{av}^{(\theta)}}{2} \Bigg/ \left[\left(\left(a/h_c\right)^3 - 1\right)\frac{\tilde{y}}{a} + 1\right], \quad \text{for } 0 < \tilde{y} < a \tag{5.11}$$

Thus, Equation (5.7) can be arranged using Equations (5.8)-(5.11) as follows:

$$\Delta U = \frac{1}{2} k_{av}^{(\theta)} \left(\Delta\theta_{av}\right)^2 \left[1 - \left(a/h_c\right)^3\right] \tag{5.12}$$

Consequently, Equation (5.4) can be redefined for $\left(a/h_c\right)^3 \le 0.5$ and $a/b_c \le 0.5$ as following equation:

$$D(a) = \frac{18\pi\left(1.12\right)^2 a^2}{E b_c^2 h_c^3} \varepsilon\left[1 - \left(a/h_c\right)^3\right]. \tag{5.13}$$

Increase in strain energy corresponding to the energy consumed is distributed along the beam length as formulated by Equations (3.26), (3.27) and (3.28) given in Chapter 3. The only difference is described in Equation (3.28) which is modified for the height-edge crack as follows:

$$q(a) = \frac{3\pi(1.12)^2 (h_c - a)^3 a}{\left(h_c^3 - (h_c - a)^3\right) b_c} \ . \tag{5.14}$$

If a crack exists on a beam, the energy consumed results in the decrease of maximum potential energy with the assumption of no mass loss at the crack location. As a consequence, balance of maximum energies can be obtained by Equation (4.9) that is approximated to zero by means of the Rayleigh–Ritz method. Resulting formulation for the mode shape function is given in Equation (3.9). The mode shape function includes series of functions satisfying the end conditions tabulated in Table 3.1.

5.3 Energy Balance in Beam with Multiple Height-Edge Cracks

In the case of multiple height-edge cracks, some parameters used in previous equations can be modified as $a_i, z_{c(i)}, h_{c(i)}, b_{c(i)}$ where $i = 1 \, to \, n$. Each height-edge crack partially interferes (as much as its depth ratio) the strain disturbances created by the other cracks. By means of this assumption, the distribution of the energy consumed throughout the beam length is modified for the multiple cracked beams by affecting the influence ratios described below.

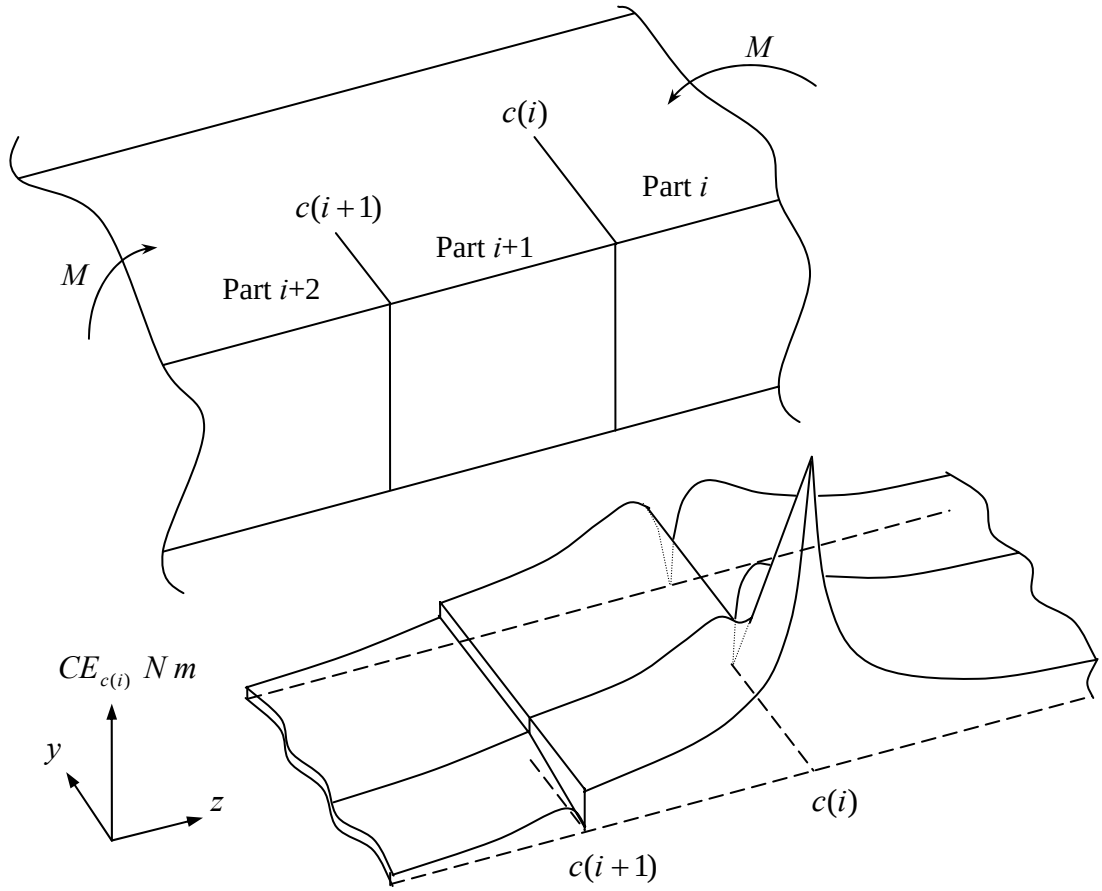

Figure 5.2 Distribution of the energy consumed caused by i^{th} crack.

Sketch of the distribution of the energy consumed caused by i^{th} crack is shown in Figure 5.2. It can be noticed that, the energy consumed is maximum at the crack mouth where there is no stress and maximum strain. Stress and strain values are approximately equal at the crack tip and remaining section of the beam's width at the crack location. Consequently, the energy consumed becomes zero on this line as seen in Figure 5.2. In our assumption, rotation of the beam around the *z* axis is neglected since the ratios ($a_i/b_{c(i)}$, $\left(a_i/h_{c(i)}\right)^3$) related with the crack depths are less than 0.5 and the rectangular beam bends in $w-z$ plane. Therefore, the energy consumed immediately spreads along the beam's width with the influences of the inner stresses of the beam. The energy consumed caused by i^{th} crack decreases at the other crack locations where the strain waves are partially damped. The ratio of strain waves

passing from the remaining un-cracked section of the location of crack i+1 is equal to $1-a_{i+1}/b_{c(i+1)}$. As a result, the energy consumed observed in the neighbour parts of i^{th} crack decreases at this ratio in part i+2 as shown in Figure 5.2. If $\gamma_{c(i),p(i)}$ defines the influence ratio of the energy consumed caused by crack i on part i, influence ratios of crack i on the neighbour parts can be written as follow:

$$\begin{aligned}
&\gamma_{c(i),p(i-1)} = 1-a_{i-1}/b_{c(i-1)},\\
&\gamma_{c(i),p(i)} = 1,\\
&\gamma_{c(i),p(i+1)} = 1,\\
&\gamma_{c(i),p(i+2)} = 1-a_{i+1}/b_{c(i+1)}
\end{aligned} \tag{5.15}$$

At this point of view, the influence ratios of the energy consumed in parts $i+\delta$ and $i-\delta$ are generalised as follow:

$$\begin{aligned}
&\gamma_{c(i),p(i+\delta)} = \gamma_{c(i),p(i+\delta-1)}\left(1-a_{i+\delta-1}/b_{c(i+\delta-1)}\right), && \delta \geq 2\\
&\gamma_{c(i),p(i-\delta)} = \gamma_{c(i),p(i-\delta+1)}\left(1-a_{i-\delta}/b_{c(i-\delta)}\right), && \delta \geq 1
\end{aligned} \tag{5.16}$$

The distributions of the energy consumed are obtained similarly for the other cracks also. Thus, the decrease of potential energy in each part of the beam is obtained by superposing the consumed energies caused by all cracks. If n height-edge cracks exist on the beam, the following energy balance equations can be written for $n+1$ parts:

$$\begin{aligned}
BE_1 &= \int_{Zc(1)}^{L}\left(\left(\Gamma^{PE} - \gamma_{c(1),p(1)}\Gamma^{CE}_{c(1)} - \gamma_{c(2),p(1)}\Gamma^{CE}_{c(2)} - \ldots - \gamma_{c(n),p(1)}\Gamma^{CE}_{c(n)}\right) - \Gamma^{KE}\right)dz\\
BE_i &= \int_{Zc(i-1)}^{Zc(i)}\left(\left(\Gamma^{PE} - \gamma_{c(1),p(i)}\Gamma^{CE}_{c(1)} - \gamma_{c(2),p(i)}\Gamma^{CE}_{c(2)} - \ldots - \gamma_{c(n),p(i)}\Gamma^{CE}_{c(n)}\right) - \Gamma^{KE}\right)dz\\
BE_{n+1} &= \int_{0}^{Zc(n)}\left(\left(\Gamma^{PE} - \gamma_{c(1),p(n+1)}\Gamma^{CE}_{c(1)} - \gamma_{c(2),p(n+1)}\Gamma^{CE}_{c(2)} - \ldots - \gamma_{c(n),p(n+1)}\Gamma^{CE}_{c(n)}\right) - \Gamma^{KE}\right)dz
\end{aligned} \tag{5.17}$$

Thus, the total energy given in Equation (4.14) is approximated to zero by using the Rayleigh–Ritz method.

5.4 Results and Discussion

Results are represented by applying the method on several fixed–fixed and cantilever beams of which dimensions are shown in Figure 5.3. Variation of the height and width of the beams is given in Equations (4.15) and (4.16) respectively.

Three different beams considered have the same density $\rho = 7800\,\mathrm{kg/m^3}$, modulus of elasticity $E = 210\,\mathrm{GPa}$, and Poisson ratio $\nu = 0.3$. The beams also have the following geometric properties:

Beam1; $L = 0.6\mathrm{m}, \quad h_1 = b_1 = 0.02\mathrm{m}, \quad \alpha_\mathrm{h} = h_2/h_1 = 0.5, \quad \alpha_\mathrm{b} = b_2/b_1 = 0.75$

Beam2; $L = 0.6\mathrm{m}, \quad h_1 = b_1 = 0.02\mathrm{m}, \quad \alpha_\mathrm{h} = 1.5, \quad \alpha_\mathrm{b} = 0.75$

Beam3; $L = 0.6\mathrm{m}, \quad h_1 = b_1 = 0.02\mathrm{m}, \quad \alpha_\mathrm{h} = 0.5, \quad \alpha_\mathrm{b} = 2.25$.

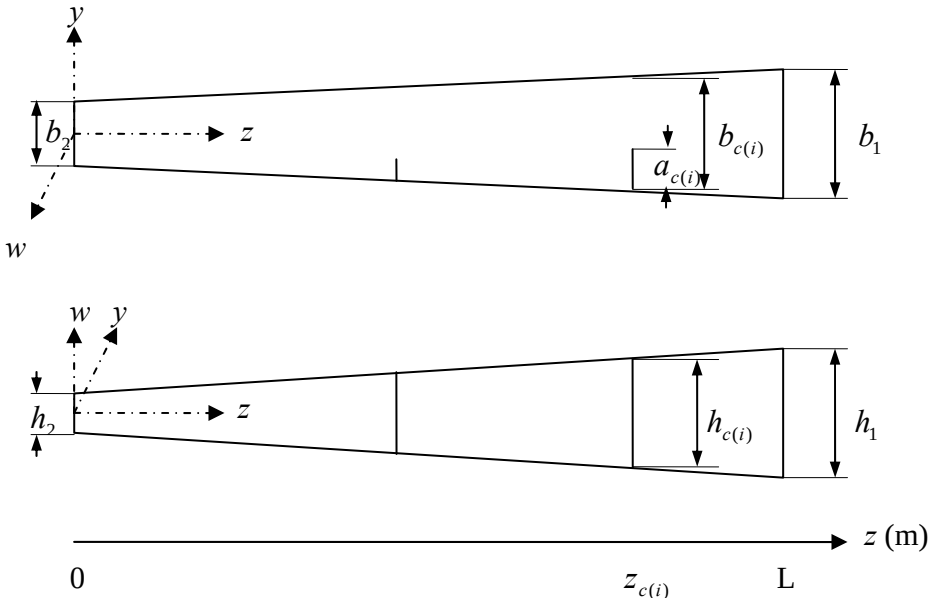

Figure 5.3 Geometry of a beam.

All these beams are considered as cantilevers fixed from $z = L$. In addition, Beam1 is reconsidered as fixed–fixed beam.

Results obtained by the present study are compared with the results of commercial finite element program (ANSYS©) for the beams considered. Properties of finite element program presented in Section 4.4 for modal analysis of the beam with transverse cracks are used also for modal analysis of the beam with height-edge cracks. Natural frequencies of the un-cracked beams obtained by Rayleigh–Ritz approximations and the finite element program can be seen in Table 5.1.

Table 5.1 Natural frequencies of the un-cracked beams.

Beams	Vibration Modes	Frequencies (Hz) obtained by Rayleigh-Ritz (4 terms)	Frequencies (Hz) obtained by Rayleigh-Ritz (6 terms)	Frequencies (Hz) obtained by Rayleigh-Ritz (8 terms)	Frequencies (Hz) obtained by Finite Element program
Cantilever Beam1	1	54.9031	54.8964	54.8963	54.945
	2	249.6583	249.2314	249.2008	248.75
	3	689.958	636.7900	632.941	629.05
Cantilever Beam2	1	48.8426	48.8420	48.8420	48.91
	2	344.3177	344.0024	344.0013	341.69
	3	1053.128	996.4606	995.1637	976.5
Cantilever Beam3	1	40.311	40.3082	40.3082	40.36
	2	225.5448	224.9975	224.9894	224.62
	3	633.242	609.3576	607.0943	603.60
Fixed Beam1	1	217.6039	217.6028	217.6027	217.6
	2	598.556	597.4309	597.4229	594.42
	3	1181.955	1169.652	1169.194	1155.6

Vibrations of the beams having single, double, and triple cracks are investigated as follows.

5.4.1 Example 1: Tapered Cantilever Beams with a Crack

Beam1, Beam2 and Beam3 are examined by following crack properties:

$a_c = 0.2b_1, 0.4b_1 \qquad z_c(\text{var}\,iable)$

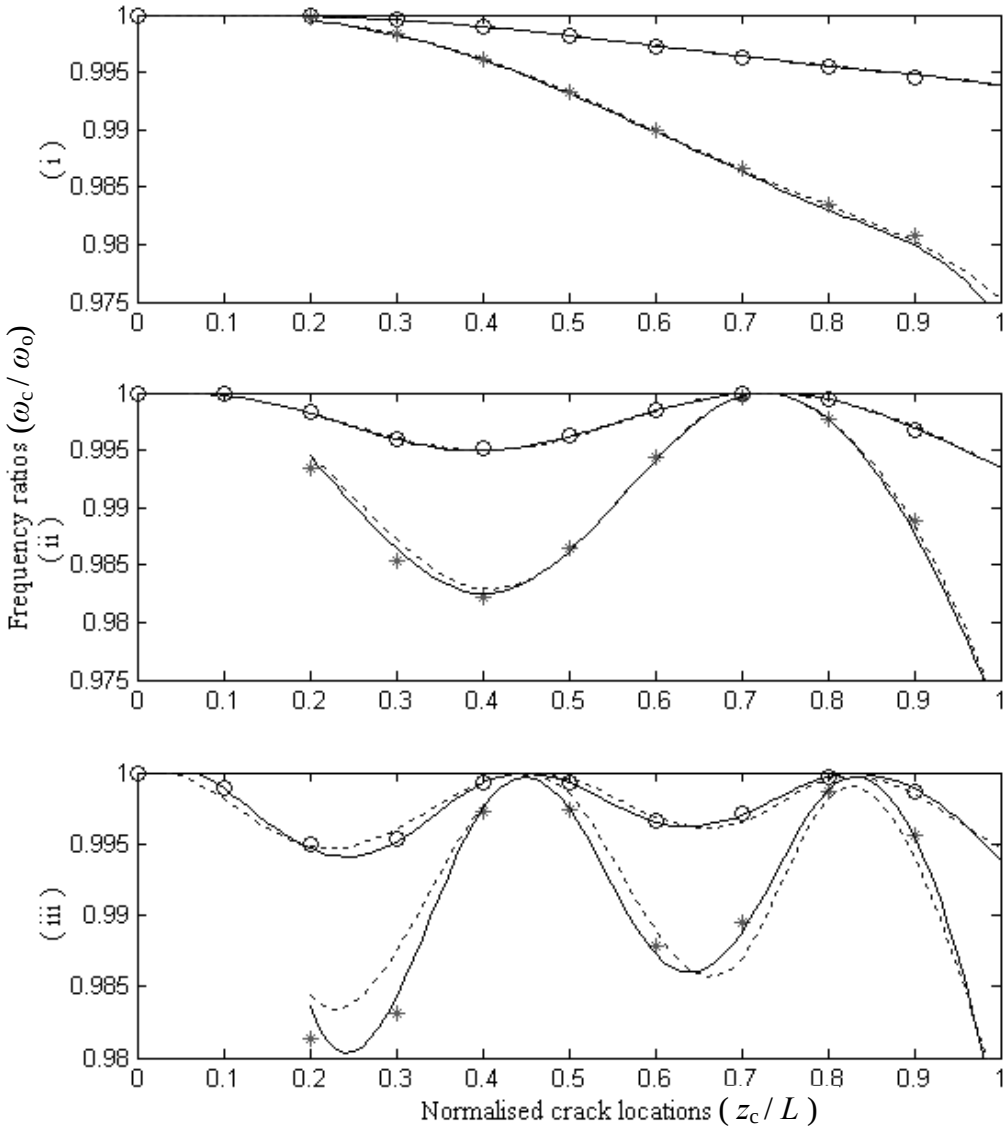

Figure 5.4 Natural frequency ratios for the (i) first, (ii) second and (iii) third mode vibration of cantilever Beam1 with variably located crack having depths $a = 0.2b_1$ and $a = 0.4b_1$. Results of Ansys for $a = 0.2b_1$ (o), and for $a = 0.4b_1$ (*). Results of approximations with 6 terms (---), and 8 terms (——).

Results of the present method are in good agreement with the results of the finite element program for single crack cases of three different tapered cantilever beams as shown in Figures 5.4, 5.5 and 5.6. The analyses are performed for different crack location intervals in which acceptable ratios of crack depths are provided.

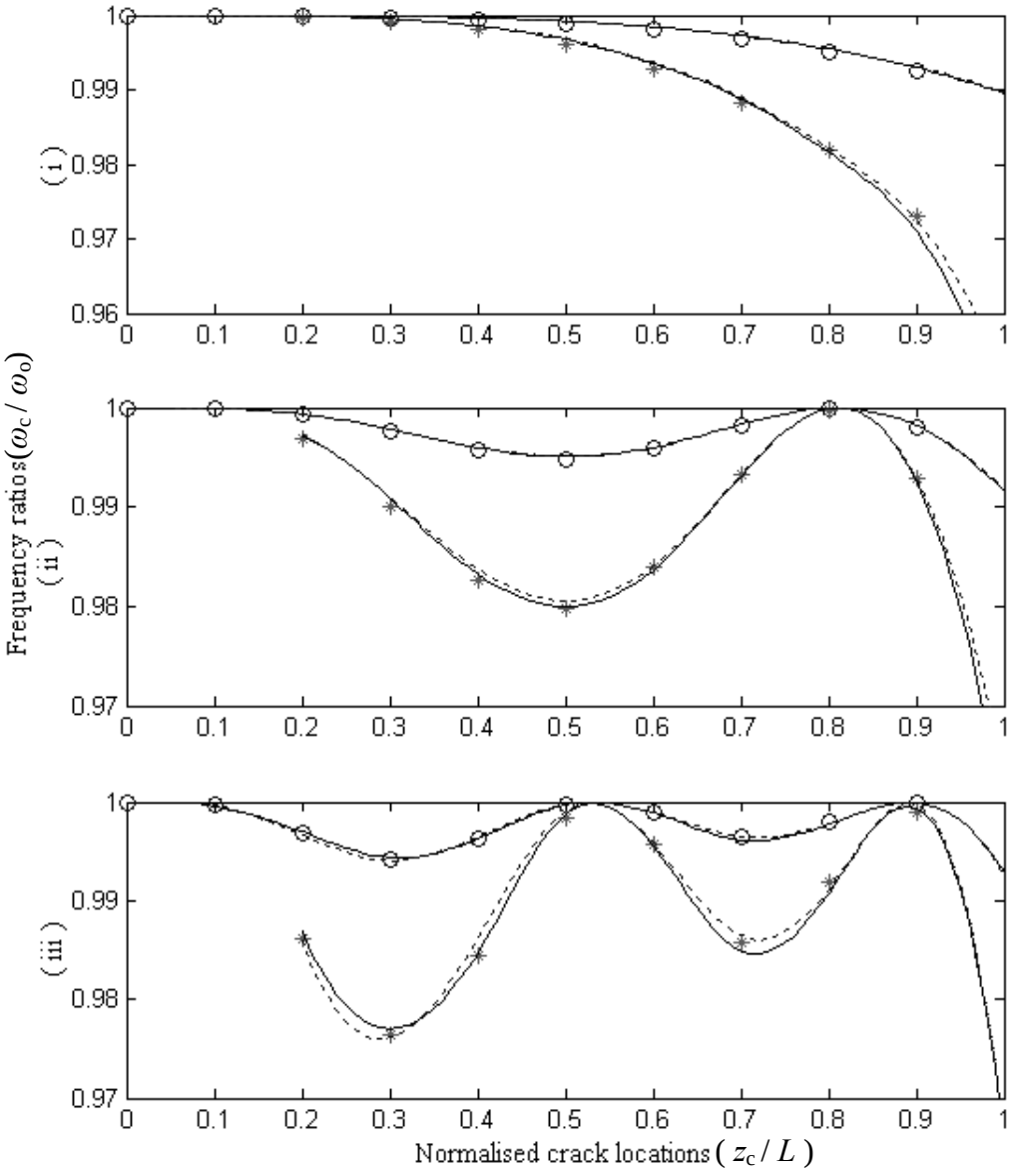

Figure 5.5 Natural frequency ratios for the (i) first, (ii) second and (iii) third mode vibration of cantilever Beam2 with variably located crack having depths $a = 0.2b_1$ and $a = 0.4b_1$. Results of Ansys for $a = 0.2b_1$ (o), and for $a = 0.4b_1$ (*). Results of approximations with 6 terms (---), and 8 terms (——).

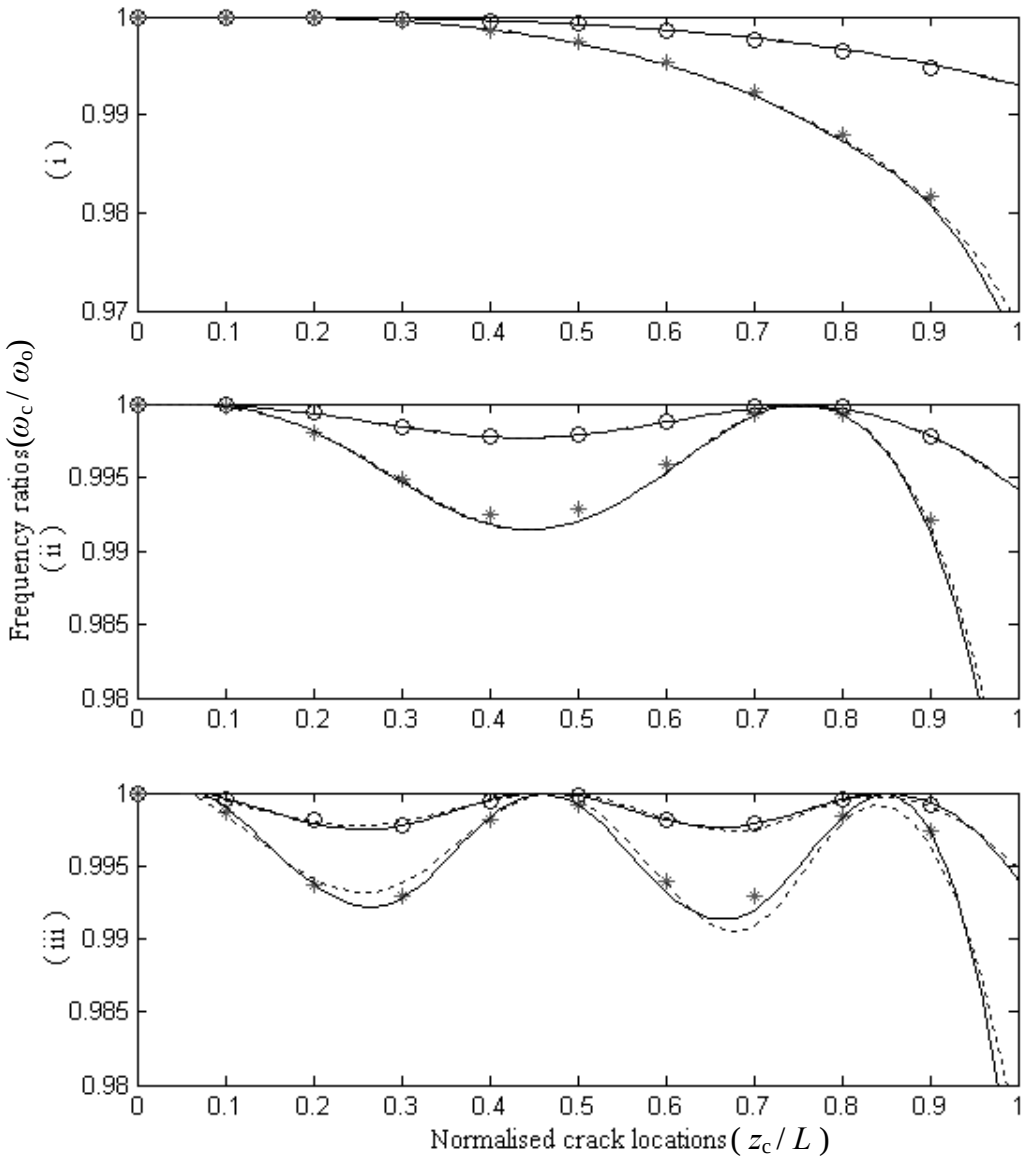

Figure 5.6 Natural frequency ratios for the (i) first, (ii) second and (iii) third mode vibration of cantilever Beam3 with variably located crack having depths $a = 0.2b_1$ and $a = 0.4b_1$. Results of Ansys for $a = 0.2b_1$ (o), and for $a = 0.4b_1$ (*). Results of approximations with 6 terms (---), and 8 terms (——).

Application of Rayleigh–Ritz approximation with six terms is sufficient to obtain good agreement with the natural frequency ratios of the first and second mode vibrations. However, use of the method with eight terms gives better results for the third mode of vibration as seen in the figures. Natural frequencies of the un-cracked beams given in Table 5.1 can be used to determine required number of terms to be

used in the method. It can be observed that, the number of terms, which is sufficient to obtain accurate natural frequencies for the un-cracked beams, also becomes sufficient for the cracked beams. In this sense, four termed approximation can be applicable for only the first vibration mode as can be observed in the table.

If the trends of the natural frequency ratios are comparatively examined for the cracks on the beams, some distinctions can be observed. Increase of the height taper factor, α_h, results in the highest natural frequency reduction near the root of the beam that can be seen by the comparison of Figures 5.4 and 5.5. Similarly, higher width taper factor, α_b, causes the more natural frequency reductions near the root as seen in Figure 5.6. In addition, node points, where no natural frequency reduction is obtained, are shifted from tip to root with the increasing taper factor. It can be clearly seen that α_h is more influential than α_b. Resultantly, variation of the mass and inertia moment together with the variation of crack depth ratio along the beam are all influential on the natural frequency ratios seen in the figures.

5.4.2 Example 2: Tapered Fixed–Fixed Beam with a Crack

Beam1 is fixed from both ends and it is examined by following crack properties:

$$a_c = 0.2b_1, 0.4b_1 \qquad z_c(\text{var}\,iable)$$

Figure 5.7 shows that the application of the method when analysing a beam whose both ends are fixed, gives good results that agree well with the results of the finite element program. Although the natural frequencies of the fixed–fixed beam are higher than those of cantilevers due to the increased rigidity, one sees that the accuracy of the present method does not depend on the different boundary conditions. Figure 5.7 also shows that the analysis of a fixed–fixed beam using six terms instead of eight suffices and gives results which agree with the finite element program. However, when the six termed function is used in the analysis of the cantilever, there is a discrepancy especially for the third mode frequency ratios. Maximum natural frequency drops are seen in Figure 5.7 when the cracks are located

near the ends of the beam where maximum bending moments occur. Comparing Figure 5.7 to Figures 5.4, 5.5, and 5.6 shows that there exists one more node points where there is no natural frequency reduction. This is a result of the bending moments at the two ends of the fixed–fixed beam.

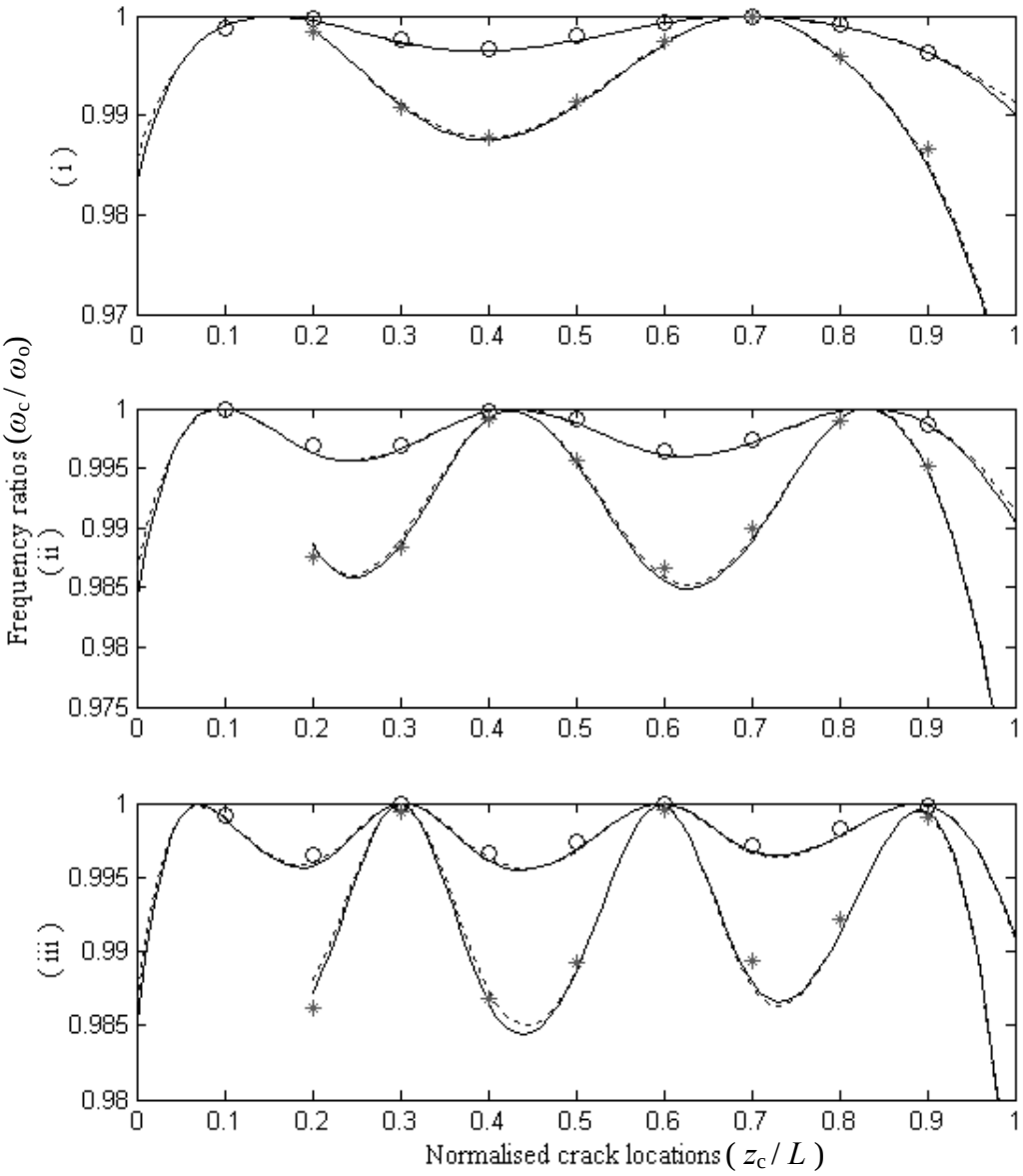

Figure 5.7 Natural frequency ratios for the (i) first, (ii) second and (iii) third mode vibration of fixed-fixed Beam1 with variably located crack having depths $a = 0.2b_1$ and $a = 0.4b_1$. Results of Ansys for $a = 0.2b_1$ (o), and for $a = 0.4b_1$ (*). Results of approximations with 6 terms (---), and 8 terms (——).

5.4.3 Example 3: Tapered Cantilever and Fixed–Fixed Beams with Two Cracks

Beam1 is examined by the following crack properties:

$a_1 = 0.2b_1, \quad a_2 = 0.2b_1, 0.4b_1 \qquad z_{c(1)} = 0.91L, \quad z_{c(2)}(\text{var}\,iable)$

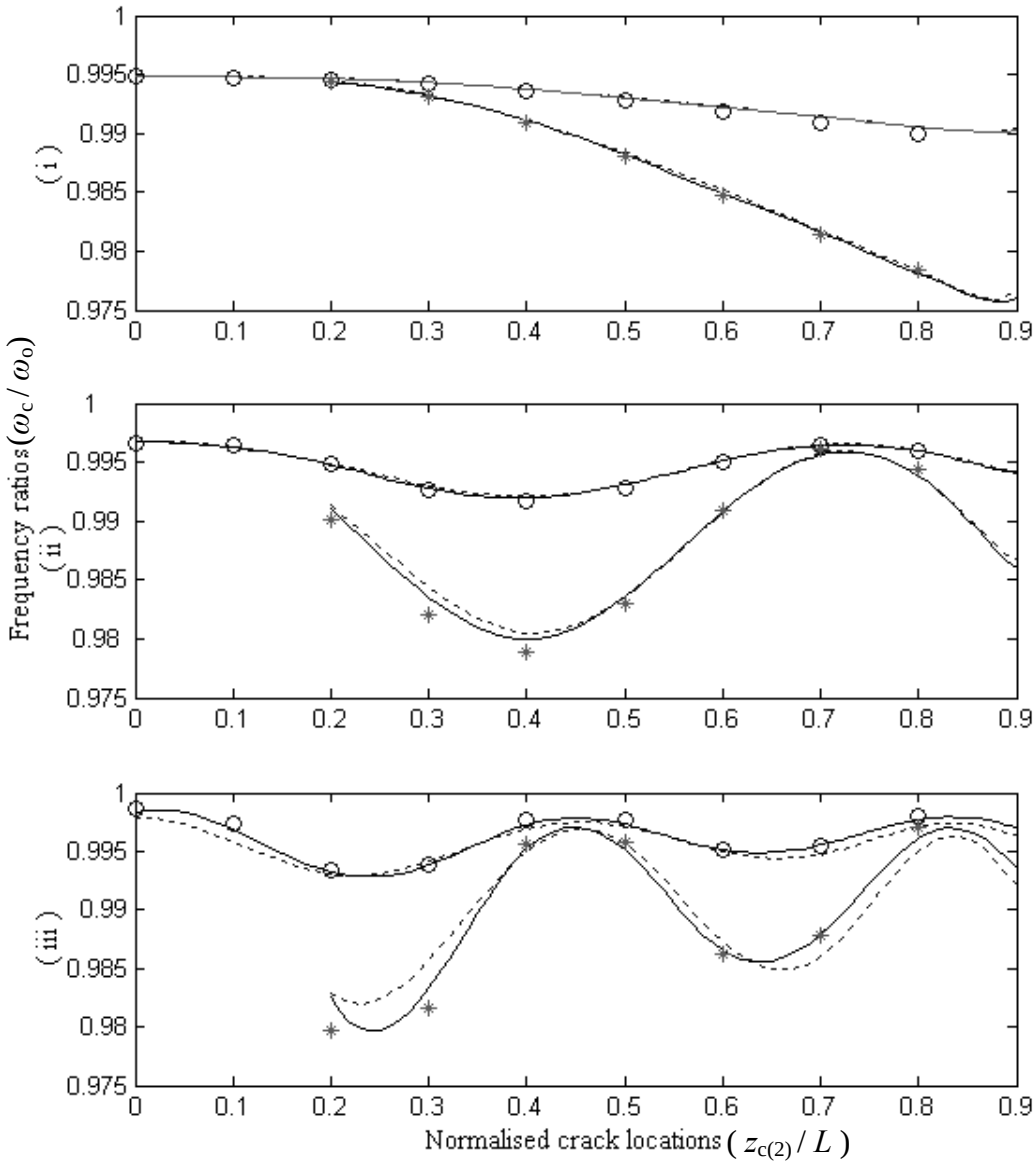

Figure 5.8 Natural frequency ratios for the (i) first, (ii) second and (iii) third mode vibration of double cracked cantilever Beam1 with variably located second crack having depths $a_2 = 0.2b_1$ and $a_2 = 0.4b_1$ as $a_1 = 0.2b_1$. Results of Ansys for $a_2 = 0.2b_1$ (o), and for $a_2 = 0.4b_1$ (*). Results of approximations with 6 terms (---), and 8 terms (——).

Natural frequency ratios obtained by the method agree with those obtained by the finite element program for the double cracked cantilever and double cracked fixed–fixed Beam1 as shown in Figures 5.8 and 5.9. Agreements are achieved with the same number of terms used for single cracked beams.

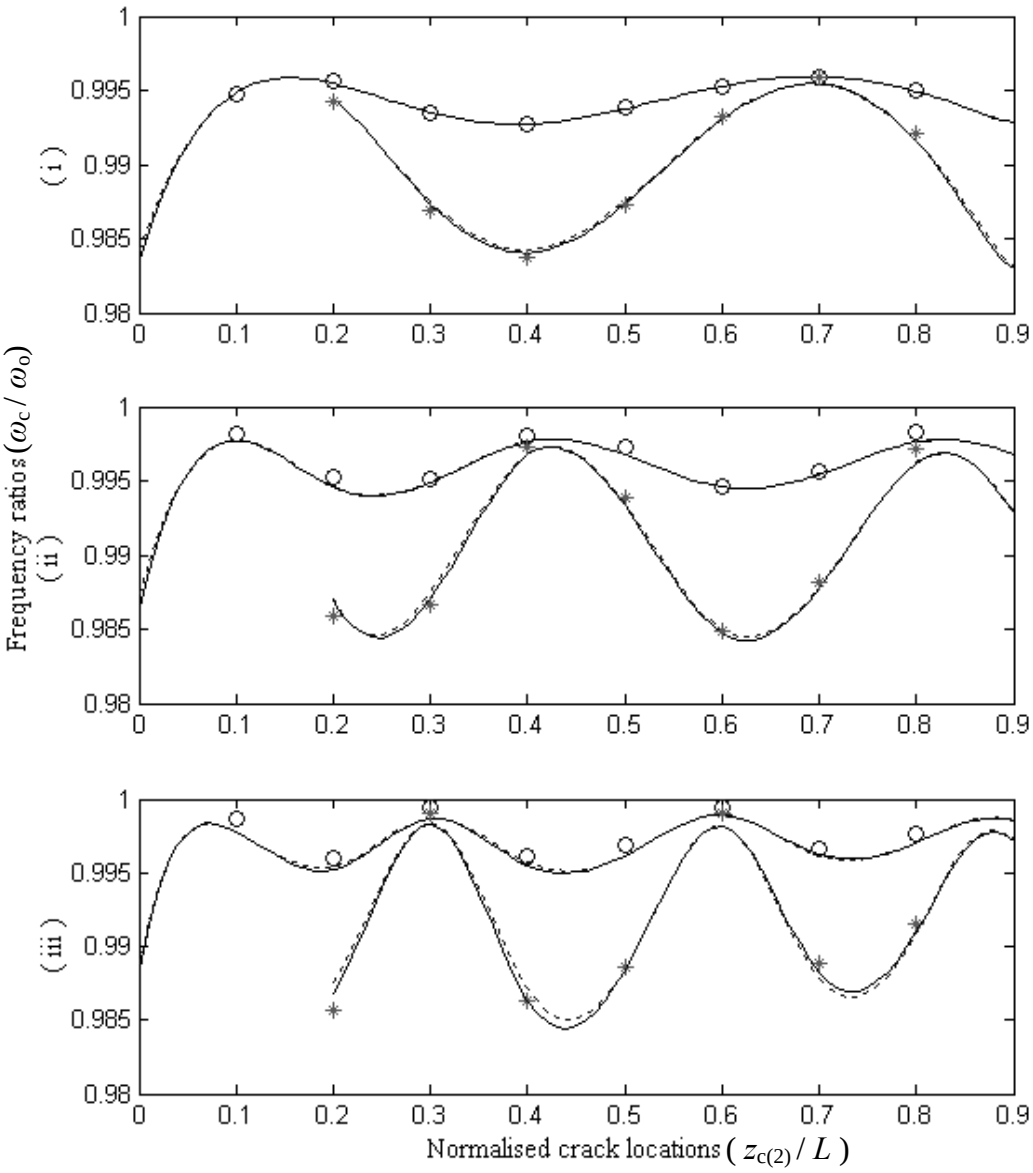

Figure 5.9 Natural frequency ratios for the (i) first, (ii) second and (iii) third mode vibration of double cracked fixed-fixed Beam1 with variably located second crack having depths $a_2 = 0.2b_1$ and $a_2 = 0.4b_1$ as $a_1 = 0.2b_1$. Results of Ansys for $a_2 = 0.2b_1$ (o), and for $a_2 = 0.4b_1$ (*). Results of approximations with 6 terms (---), and 8 terms (——).

Trends of the natural frequency reductions of the double cracked cantilever and both ends fixed beams are similar to the trends obtained from single cracked beams seen in Figures 5.4 and 5.7 except for the cases of proximity of the cracks. The difference arises from partially damped strain disturbances caused by the cracks which interact with each other.

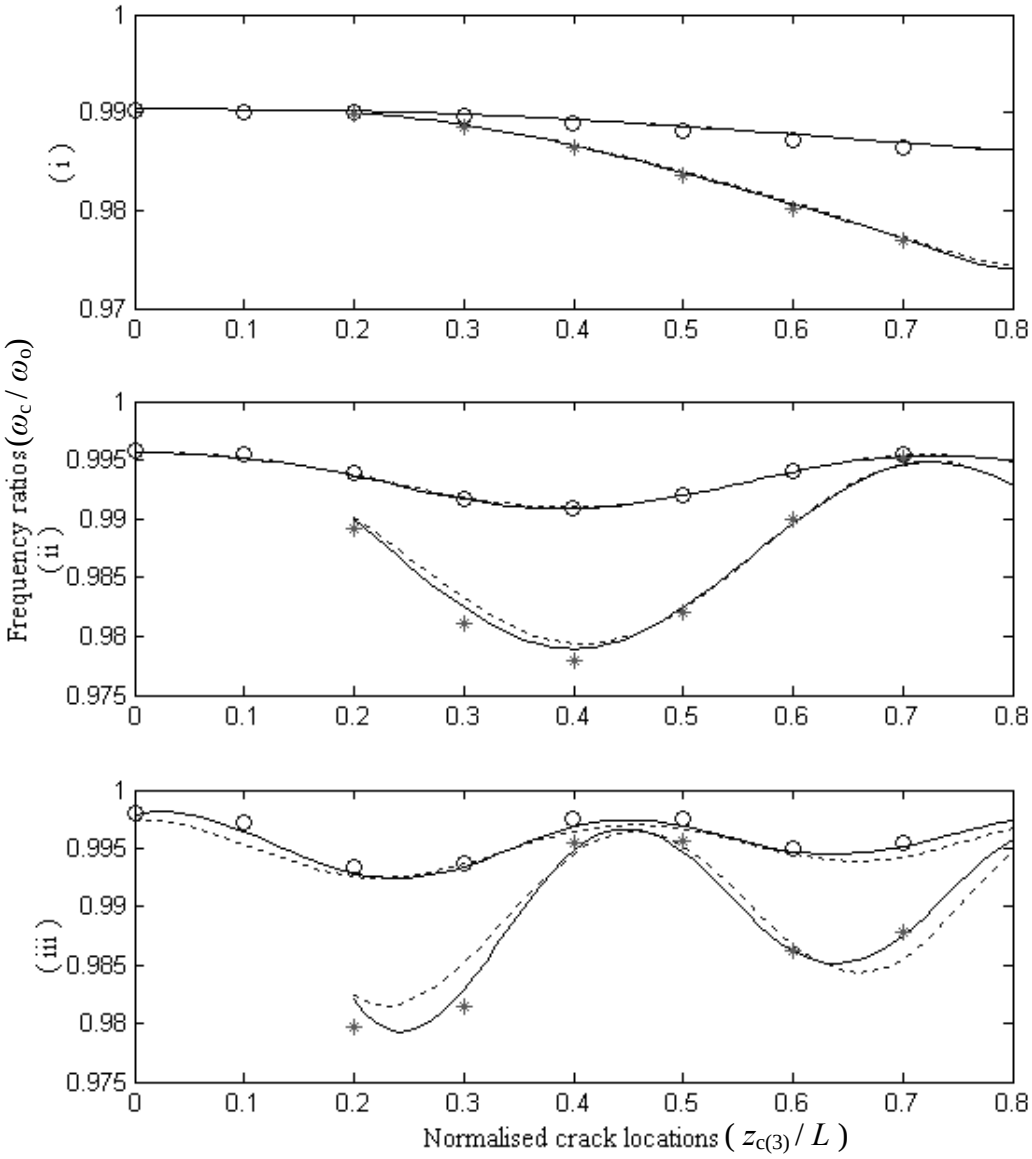

Figure 5.10 Natural frequency ratios for the (i) first, (ii) second and (iii) third mode vibration of triple cracked cantilever Beam1 with variably located third crack having depths $a_3 = 0.2b_1$ and $a_3 = 0.4b_1$ as $a_1 = a_2 = 0.2b_1$. Results of Ansys for $a_3 = 0.2b_1$ (o), and for $a_3 = 0.4b_1$ (*). Results of approximations with 6 terms (---), and 8 terms (——).

It is clear that, maximum frequency ratio of the double cracked Beam1 should be equal to the frequency ratio of the Beam1 having one crack located at the position, $z_{c(1)}$. Interestingly, using the presented method or the finite element program gives the same results, which indicates that there is no clear effect of coupling on the considered vibration modes even if the beams have two cracks.

5.4.4 Example 4: Tapered Cantilever Beam with Three Cracks

Beam1 has the following crack properties:

$$a_1 = 0.2b_1, \quad a_2 = 0.2b_1, \quad a_3 = 0.2b_1, 0.4\,b_1 \ (\text{var}\,iable)$$
$$z_{c(1)} = 0.91L, \quad z_{c(2)} = 0.82L, \quad z_{c(3)} (\text{var}\,iable)$$

Natural frequency ratios of cantilever Beam1 having three cracks are seen in Figure 5.10 for the first three modes of vibrations. Good agreements are also obtained. As seen in the figures for single, double and triple cracked beams, eight termed approximation is sufficient to obtain good agreement with the finite element program for the first three modes of vibration. Thus, it can be said that the number of cracks along the beam is not effective on the number of terms required to be used in the approximation. As seen in the figures, crack depths are also not influential over the number of terms required.

It should be noted that performing the finite element program with the acceptable number of elements that results in the correct solution requires very long computation time when the cracks are too close to each other for double and triple cracked beams. Processes can exceed the memory limitations of computers with defined cracks and meshing properties.

5.5 Conclusion

The energy method presented by Yang, Swamidas, & Seshadri (2001) is modified to obtain the vibration of multiple height-edge cracked non-uniform Euler–Bernoulli

beams. Fracture mechanics theory is adapted to the height-edge open cracks via a proposed model for the vibration behaviour of crack. The energy consumed is determined by forming the opening of the crack and distributing the strain disturbance along the beam's length. If the beam has multiple cracks, it is assumed that the strain disturbance caused by one of the cracks is damped as much as the depth ratio of the other cracks at their locations. Consumed energies caused by the cracks are superposed to obtain the overall energies consumed from the potential energy. Thus, interaction of the multiple crack effects, which is the problem for the methods based on a variational principle, is defined by the strain disturbance model presented in this chapter.

When the results of the method are compared with the results of a commercial finite element program for a fixed–fixed beam and the cantilever beams having different taper factors, good agreements are found. Significant advantage of the method can be performing the processes in quite short durations in the order of seconds when the method compared with the finite element program. Even if the beam has multiple cracks, the solution time of the method does not rise as much as the solution time of the finite element program, because the mode shape function used in the approximation method is not changed in the analysis of the multiple cracked beam. Thus, natural frequencies required for the frequency based inverse methods like prediction schemes or contour graphs can easily be obtained for each different beam. In practise, it is not impossible to obtain exact natural frequency ratios represented in figures. Sensitivity and resolution of the measurement system should be satisfactory. Restriction caused by the sampling can be kept to a minimum by the acquisition of long data with sufficient sampling frequency. Furthermore, sensitivity in the frequency domain can be improved by several statistical methods.

Vibration of the beam with height-edge cracks can also be described as the unique plane vibration of width-edge cracked beam. Vibrations in the plane perpendicular to crack tip axis are well-known with many papers presented in literature. Unique plane vibrations obtained by the present method can be critical in measuring and crack identification. Determination of the vibration characteristics in two planes results in

adequacy of lower frequency modes especially if the cross-section of the beam is not square.

Coupling effects are neglected in this chapter. Bending-torsion, which is probably the most coupling type, can have considerable influence if the cracks become deep enough. However, admissible sized cracks do not have clear influence of coupling on the lower modes of bending vibrations as obtained from the present results. It is certain that coupling is effective at the higher modes of vibration even if the beam is un-cracked.

CHAPTER SIX
FLEXURAL VIBRATION ANALYSIS OF NON-UNIFORM BEAMS HAVING DOUBLE-EDGE BREATHING CRACKS

This chapter is reorganization of the paper published as "FLEXURAL VIBRATION OF NON-UNIFORM BEAMS HAVING DOUBLE-EDGE BREATHING CRACKS" in *Journal of Sound and Vibration* (Mazanoglu & Sabuncu, 2010b).

6.1 Introduction

Understanding the vibration effects of cracks enables their recognition in practical applications of vibration monitoring. However until date, there has been no work analysing asymmetric double-edge crack in the literature, mainly because the definition of a crack advancement function for all different depth combinations of the double-edge crack would be quite a complicated task.

This chapter presents a method for the flexural vibration of non-uniform Rayleigh beams having double-edge transverse cracks which are symmetric or asymmetric around the central layer of the beam's height. The breathing crack models are employed because the external moments change direction in a period of vibration. Distribution of the energy changes along the beam's length is determined together with contributing the effects of tensile and compressive stress fields that occur in the vicinity of the crack tips due to the additional angular displacement of the beam. Effects of neutral axis deviations are also included in the model. The Rayleigh–Ritz method is applied on total energy distribution for analysing the vibration of the beam. Cantilever and simply supported beams are presented as examples and good agreements are obtained when the employed method results are compared with the results of the Chondros, Dimarogonas, & Yao (1998) and the results of the commercial finite element program (ANSYS©). The effects of crack's asymmetry and positions of cracks on the natural frequency ratios are shown graphically.

Finally, the results obtained by open and breathing crack models are discussed comparatively.

6.2 Vibration of Beams with a Single-Edge and Double-Edge Crack

Fracture mechanics theory describes the change of structural strain/stress energies with crack growth (Sih, 1973). The strain stored due to a crack is determined by means of the stress intensity factor for the Mode I crack and thus strain energy release rate. Clapeyron's Theorem states that only half of the work done by the external moment is stored as strain/stress energy when a crack exists on a beam. The remaining half is the energy consumed by the crack that is given in Chapter 3 by the Equations (3.21)-(3.24).

The energy consumed given in Equation (3.21) can also be explained by the spring model. The energy change due to crack opening can be balanced by the energy stored by a rotational spring model located at the crack tip. Since there is no spring in reality, the energy stored by the spring model is lost somewhere and is called 'the energy consumed'. The crack opening results in additional angular displacement of the beam causing also tensile stresses in the vicinity of crack tips. The energy of the tensile stress can be considered as the energy of the rotational spring model located at the un-stretched side of the beam as shown in Figure 6.1(a). When this effect is considered, the energy consumed is determined by taking the difference between the energy effects of the crack opening and tensile stress caused by the bending of the beam. In this case, the coefficient $D(a)$ is modified as given in Equation (4.8) (Mazanoglu, Yesilyurt, & Sabuncu, 2009).

In deriving Equation (4.8), minor effects of crack closing and compressive stresses caused by the bending of the beams are neglected. This open crack model can be sufficient for single-edge cracked beams vibrating in small amplitudes. When beams having double-edge cracks are bent, the crack on the stretched side opens up, and the crack on the compressed side of the beam closes. This makes it inevitable to use the breathing crack model for analysing the double-edge cracked beam. As

shown in Figure 6.1(b), this model covers the superposition of two cases: elongation of the beam due to crack opening and shortening of the beam due to crack closing. It is clear that, an additional crack will make the beam bend more, mainly because of the additional cross–section decrease and thus the stiffness loss of the beam. The beams will posses extra displacement near the open crack, in contrast to the displacement in negative direction near the closed crack. Tensile and compressive stresses also occur in the vicinity of the crack tips. Since some of the lost energy caused by the displacement changes is restored by the effect of the stress changes, the net energy consumed can be described by the following expression for the maximum deflection of a beam having double-edge breathing crack:

$$\begin{aligned} CE = &\left(Energy\ of\ the\ elongation - Energy\ of\ the\ tensile\ stress\right) \\ &-\left(Energy\ of\ the\ shortening - Energy\ of\ the\ compressive\ stress\right) \end{aligned} \tag{6.1}$$

The energy changes for the breathing crack can be obtained by the model including the equivalent rotational springs shown in Figure 6.1(b). Additional rotational springs are located on the tip of the crack opening, for obtaining the energy of the compressive stress and are located on the tip of the closed crack for obtaining the energy change due to the displacement in negative direction. This model, which includes the extensions to the open crack model, is valid for the total depth ratio of the cracks in pair, $(a_{op} + a_{cl})/h_c$, for less then 0.5. The energy consumed can be formulated by the energy of the equivalent springs as follows:

$$CE = \frac{1}{2b_c}\int_{\tilde{y}=0}^{b_c}\left[\left(k_{dc}^{(\theta)}\left(\Delta\theta_{dc}\right)^2 - k_{dc}^{(\phi)}\left(\Delta\phi_{dc}\right)^2\right) - \left(k_{dc}^{(\psi)}\left(\Delta\psi_{dc}\right)^2 - k_{dc}^{(\varphi)}\left(\Delta\varphi_{dc}\right)^2\right)\right]d\tilde{y}\,, \tag{6.2}$$

where,

$$\Delta\phi_{dc} = \frac{a_{op}}{h_c}\Delta\theta_{dc}\,, \tag{6.3}$$

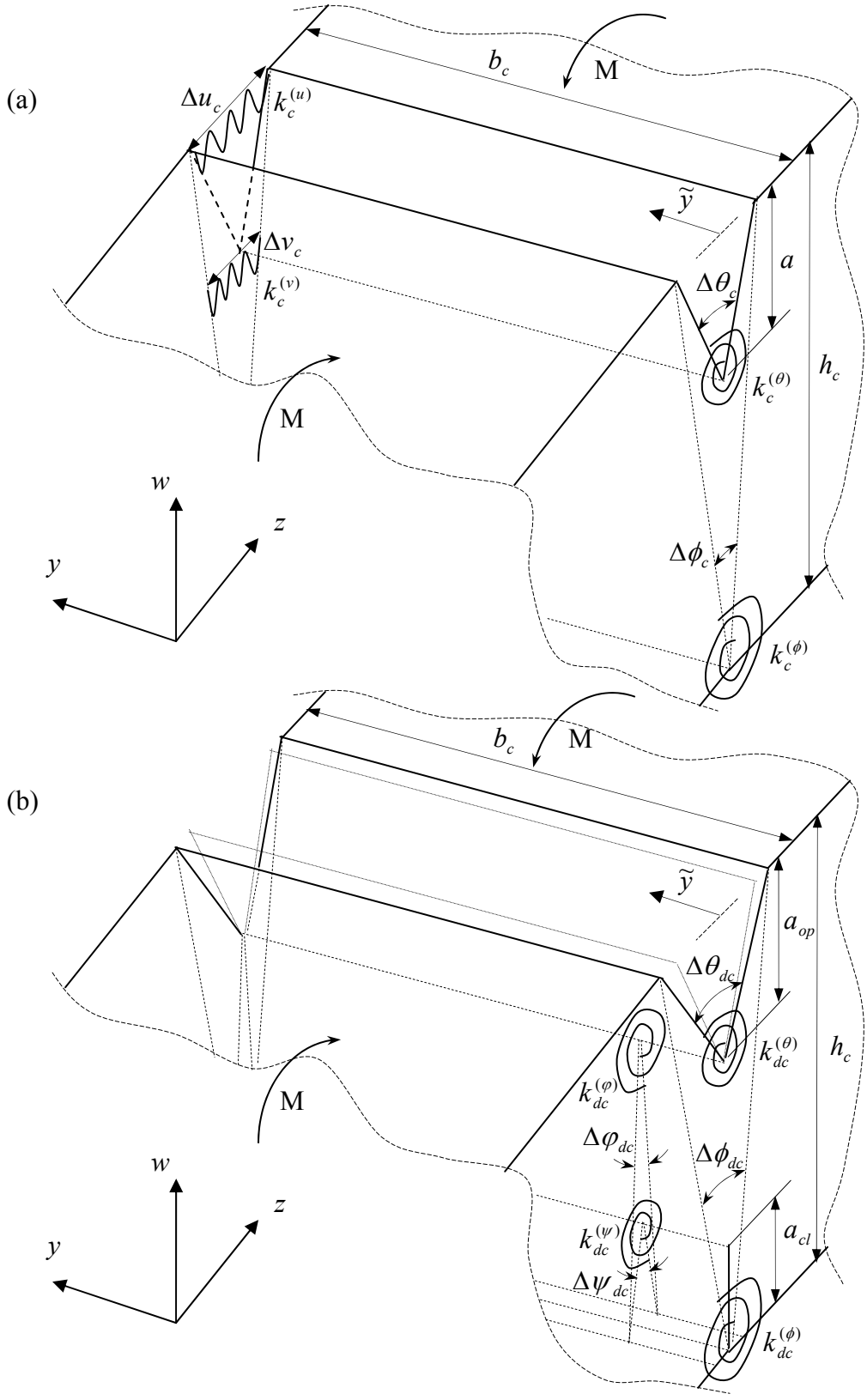

Figure 6.1 Models for (a) single-edge and (b) double-edge cracks.

$$\Delta\varphi_{dc} = \frac{a_{cl}}{h_c - a_{op}} \Delta\psi_{dc} . \tag{6.4}$$

The stiffness relation can also be established by providing bending moment equivalences at the stretched and compressed sides of the beam.

$$k_{dc}^{(\phi)} = \frac{h_c}{a_{op}} k_{dc}^{(\theta)}, \tag{6.5}$$

$$k_{dc}^{(\varphi)} = \frac{h_c - a_{op}}{a_{cl}} k_{dc}^{(\psi)} . \tag{6.6}$$

If Equations (6.3)-(6.6) are substituted into Equation (6.2), the following equation is obtained:

$$CE = \frac{1}{2b_c} \int_{\tilde{y}=0}^{b_c} \left[k_{dc}^{(\theta)} \left(\Delta\theta_{dc}\right)^2 \left(1 - \frac{a_{op}}{h_c}\right) - k_{dc}^{(\psi)} \left(\Delta\psi_{dc}\right)^2 \left(1 - \frac{a_{cl}}{h_c - a_{op}}\right) \right] d\tilde{y} . \tag{6.7}$$

The additional rotations of the open ($\Delta\theta_{ad}$) and closed ($\Delta\psi_{ad}$) cracks are influenced by three parameters which can be stated as; the cross-section decrease ($_d$), the neutral axis yawing ($_y$) due to the angular displacement difference between the cracks opening and closing, and the neutral axis shift ($_s$) due to the crack's asymmetry. Thus, the additional rotations are formulated as follows:

$$\Delta\theta_{ad} = \Delta\theta_{dc} - \Delta\theta_c = \Delta\theta_d + \Delta\theta_y + \Delta\theta_s , \tag{6.8}$$

$$\Delta\psi_{ad} = \Delta\psi_{dc} = \Delta\psi_d - \Delta\psi_y + \Delta\psi_s \tag{6.9}$$

where $\Delta\theta_d$ and $\Delta\psi_d$ are the additional rotations caused by the direct effect of the cross-section decreases. The depth of a crack on one edge influences the opening and

closing amounts of the crack on the other edge. Thus, additional rotation of the open crack due to the closed crack based cross-section drop is defined as follows:

$$\Delta\theta_d = \left(\frac{a_{cl}}{h_c - a_{op} - a_{cl}} \right) \Delta\theta_c , \tag{6.10}$$

Similarly, the additional rotation of the closed crack is written as follows:

$$\Delta\psi_d = \frac{a_{op}}{a_{cl}} \Delta\theta_d . \tag{6.11}$$

Neutral axis is not mentioned in the determination of the coefficient, $D(a)$, given in Equation (4.8), since the crack is assumed always open and hence the beam bends with extra displacement and tensile stress only (Mazanoglu, Yesilyurt, & Sabuncu, (2009). However, the breathing crack model makes it also necessary to take both the crack closing and the compressive stress effects into consideration. Nonlinear effects of the breathing cracks arise with the neutral axis modulation around the central axis during the period of vibration. The relation between the $\Delta\theta_d$ and $\Delta\psi_d$ can also be described by using yawing of the neutral axis X_y, which is caused by the difference between these additional rotations. Thus, yawing of the neutral axis is obtained as follows:

$$X_y = \frac{h_c}{2} - \left(h_c - a_{op}\right) \frac{\Delta\psi_d}{\Delta\theta_d + \Delta\psi_d} \tag{6.12}$$

Yawing of the neutral axis leads to another additional rotation symbolised by $\Delta\theta_y$ and $\Delta\psi_y$ in Equations (6.8) and (6.9). The sign of the $\Delta\psi_y$ in Equation (6.9) is negative, since the angular displacement due to the closed crack is always less then that caused by the crack opening. This means that the neutral axis always moves towards the closed crack during the bending. It is clear that, yawing effects reach a maximum when the cracks are located at the centre of mass of the beam and decrease

as the cracks approach to the beam's ends. The yawing effects function can be represented by multiplying the maximum yawing with a Normalised Gaussian function, G_N, having unit amplitude. The mean value of this function is then located on the mass centre and the standard deviation of the function is $L/6$. As a consequence, additional rotation of the beam due to the yawing of the neutral axis can be defined by the following relations:

$$\Delta\theta_y = \Delta\theta_d \left(\frac{X_y G_N}{h_c/2} \right), \tag{6.13}$$

$$\Delta\psi_y = \Delta\psi_d \left(\frac{X_y G_N}{h_c/2} \right). \tag{6.14}$$

The neutral axis will deviate from the central axis if there is an asymmetry in the depths of the open and closed cracks. The neutral axis shift is given by the parameter X_s;

$$X_s = \left(a_{cl} - a_{op}\right)/2, \tag{6.15}$$

and the additional rotations due to this shift is described by the following equations:

$$\Delta\theta_s = \Delta\theta_d \left(\frac{X_s}{h_c/2} \right), \tag{6.16}$$

$$\Delta\psi_s = \Delta\psi_d \left(\frac{X_s}{h_c/2} \right). \tag{6.17}$$

The signs of $\Delta\theta_s$ and $\Delta\psi_s$ are determined by the sign of X_s. If Equations (6.10)-(6.17) are considered together with Equations (6.8) and (6.9), the relations for additional angular displacement effects for open and closed cracks can be easily found as:

$$\Delta\theta_{dc} = \Delta\theta_c\left[1+\left(1+\frac{X_y G_N}{h_c/2}+\frac{X_s}{h_c/2}\right)\left(\frac{a_{cl}}{h_c-a_{op}-a_{cl}}\right)\right] = \Delta\theta_c\gamma\,, \tag{6.18}$$

$$\Delta\psi_{dc} = \Delta\theta_c\left[\left(1-\frac{X_y G_N}{h_c/2}+\frac{X_s}{h_c/2}\right)\left(\frac{a_{op}}{h_c-a_{op}-a_{cl}}\right)\right] = \Delta\theta_c\beta\,. \tag{6.19}$$

Resistances to these additional rotations, which are modelled by the rotational springs, can be determined by equating the bending moments at the stretched and compressed sides of the beam which in return gives us the following stiffness equations:

$$k_{dc}^{(\theta)} = \frac{k_c^{(\theta)}}{\gamma}, \tag{6.20}$$

$$k_{dc}^{(\psi)} = \frac{k_c^{(\theta)}}{\beta}. \tag{6.21}$$

Hence, the energy consumed is obtained by substituting the additional rotation and stiffness expressions into Equation (6.7):

$$CE = \frac{1}{2b_c}\int_{\tilde{y}=0}^{b_c}\left[k_c^{(\theta)}\left(\Delta\theta_c\right)^2\left(1-\frac{a_{op}}{h_c}\right)\gamma\right]d\tilde{y} - \frac{1}{2b_c}\int_{\tilde{y}=0}^{b_c}\left[k_c^{(\theta)}\left(\Delta\theta_c\right)^2\left(1-\frac{a_{cl}}{h_c-a_{op}}\right)\beta\right]d\tilde{y} \tag{6.22}$$

Extensions to the open crack model, seen in Figure 6.1, are extracted from Equation (6.22) and added into Equation (4.8) which should be modified as the formulations below, for opening and closing cases of single-edge or double-edge breathing cracks.

$$D(a_{op}) = \frac{18\pi F(a_{op})^2 a_{op}^{\ 2}}{Eb_c h_c^4}\left(1 - \frac{a_{op}}{h_c}\right)\gamma\,, \tag{6.23}$$

$$D(a_{cl}) = \frac{18\pi F(a_{cl})^2 a_{cl}^{\ 2}}{Eb_c h_c^4}\left(1 - \frac{a_{cl}}{h_c - a_{op}}\right)\beta\,. \tag{6.24}$$

Of course when a beam vibrates, it will be bending in two opposite directions which will result in the exchange of the positions of the open and closed cracks. If the open and closed cracks are subscripted by the numbers also, Equation (3.21), defining the energy consumed for a single-edge open crack, is modified as below for the single-edge and double-edge breathing cracks:

$$CE_{a1} = D(a_{op,1})\left[M(z_c)\right]^2 - D(a_{cl,1})\left[M(z_c)\right]^2 \tag{6.25}$$

$$CE_{a2} = D(a_{op,2})\left[M(z_c)\right]^2 - D(a_{cl,2})\left[M(z_c)\right]^2 \tag{6.26}$$

It should be remembered that the moment terms in Equations (6.25) and (6.26) include different expressions for open and closed cracks due to the difference in E'. The energy consumed is distributed along the beam length as follows (Yang, Swamidas, & Seshadri, 2001):

$$\Gamma^{CE} = \frac{Q(a_1, z_c)}{1 + \left[(z - z_c)/(q(a_1)a_1)\right]^2} + \frac{Q(a_2, z_c)}{1 + \left[(z - z_c)/(q(a_2)a_2)\right]^2} \tag{6.27}$$

where

$$Q(a_1, z_c) = \frac{CE_{a1}}{q(a_1)a_1\left\{\arctan\left[(L - z_c)/(q(a_1)a_1)\right] + \arctan\left[z_c/(q(a_1)a_1)\right]\right\}}, \tag{6.28}$$

$$q(a_1) = \frac{3\pi\left(F(a_1)\right)^2\left(h_c - a_1 - a_2\right)^3\left(a_1 + a_2\right)}{\left(h_c^3 - \left(h_c - a_1 - a_2\right)^3\right)h_c}\,. \tag{6.29}$$

Equations (6.28) and (6.29) can be modified for the crack at the second edge.

The conservation of energy law dictates that, for a beam with no cracks, the maximum potential energy should be equal to maximum kinetic energy. If a crack exists on a beam, the energy consumed results in the decrease of maximum potential energy with the assumption of no mass loss at the crack location. As a consequence, balance of maximum energies can be obtained by Equation (4.9) that is approximated to zero by means of the Rayleigh–Ritz method. Since the Rayleigh beam model is used in this chapter, kinetic energy distribution given in Equation (4.11) is modified as follows:

$$\Gamma^{KE} = \frac{1}{2}\rho A(z)\omega^2 \left(W(z)\right)^2 + \frac{1}{2}\rho I(z)\omega^2 \left(\frac{dW(z)}{dz}\right)^2 . \tag{6.30}$$

The second term in Equation (6.30) describes the effect of rotary inertia around the axis perpendicular to the bending plane. Resulting formulation for the mode shape function is given in Equation (3.9). The mode shape function includes series of functions satisfying the end conditions tabulated in Table 3.1.

6.3 Results and Discussion

Results are presented by applying the developed method on simply supported and cantilever beams. Simply supported aluminium and steel beams having single-edge or symmetric double-edge cracks at the mid-span range are analysed and the results are compared. The aluminium beam has the following geometric properties; length $L = 0.235\,\mathrm{m}$, width $b = 0.006\,\mathrm{m}$, and height $h = 0.0254\,\mathrm{m}$. The material properties of the beam are $\rho = 2800\,\mathrm{kg/m^3}$ as density, $E = 72\,\mathrm{GPa}$ as modulus of elasticity, and $\nu = 0.35$ as poisson ratio. A double-edge cracked steel beam of length, width, and height are given as $L = 0.575\,\mathrm{m}$, $b = 0.00952\,\mathrm{m}$, and $h = 0.03175\,\mathrm{m}$ respectively. The beam has the following material properties; density $\rho = 7800\,\mathrm{kg/m^3}$, modulus of elasticity $E = 206\,\mathrm{GPa}$, and poisson ratio $\nu = 0.35$. A

six termed deflection function is employed in the Rayleigh–Ritz method, and a breathing crack model is used in the analysis. Frequency ratios obtained by the method agree with the results of the models presented by Chondros, Dimarogonas, & Yao (1998) as seen in Figures 6.2 and 6.3.

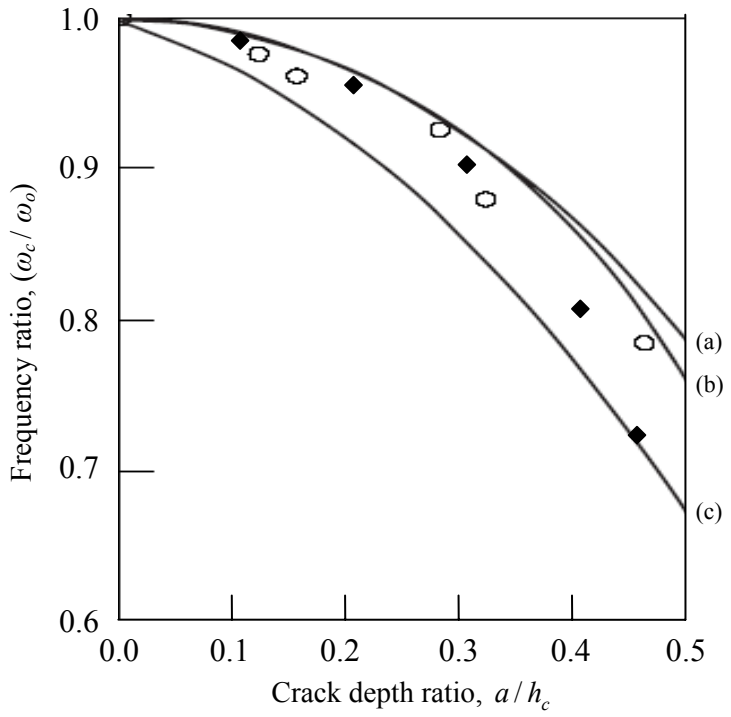

Figure 6.2 First mode vibration frequency ratios of the simply supported aluminium beam with mid-span single-edge crack. (a) Lumped crack flexibility model (Chondros, Dimarogonas, & Yao, 1998), (b) continuous crack model (Chondros, Dimarogonas, & Yao, 1998), (c) model of Christides & Barr (1984), (o) experimental results (Chondros, Dimarogonas, & Yao, 1998), and (♦) the present model.

The method is also applied to a tapered cantilever beam having density $\rho = 7800\,\mathrm{kg/m^3}$, modulus of elasticity $E = 210\,\mathrm{GPa}$, and poisson ratio $\nu = 0.3$. Variation of the height and width of the tapered beam can be expressed by the functions in Equations (4.15) and (4.16). The beam has also geometric properties as $L = 0.6\,\mathrm{m}$, $h_1 = b_1 = 0.02\,\mathrm{m}$, $\alpha_h = h_2/h_1 = 0.5$, and $\alpha_b = b_2/b_1 = 0.75$. The geometry of the tapered beam is shown in Figure 6.4.

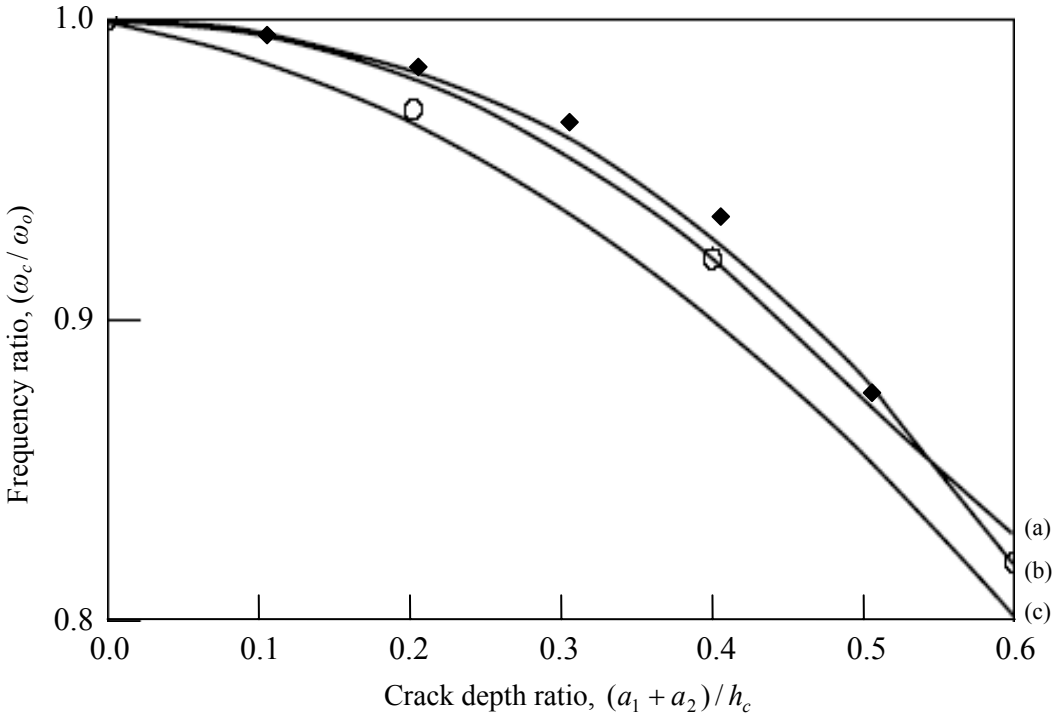

Figure 6.3 First mode vibration frequency ratios of the simply supported steel beam with mid-span symmetric double-edge crack. (a) Lumped crack flexibility model (Chondros, Dimarogonas, & Yao, 1998), (b) continuous crack model (Chondros, Dimarogonas, & Yao, 1998), (c) model of Christides & Barr (1984), (o) experimental results (Chondros, Dimarogonas, & Yao, 1998), and (♦) the present model.

Results obtained by the present method are compared with the results of the commercial finite element program (ANSYS©) for the tapered beam in consideration. Analysis properties of the finite element program presented in Section 4.4 for the beam with transverse cracks are used also for the beam with double-edge cracks. Finite element model of the double–edge cracked beam considered is given in Appendix B, Figure B.2. It should be remembered that, changes in the element number caused by the variation of crack location and crack size, have negligible effects on the results. Natural frequencies of the un-cracked beams obtained by the Rayleigh–Ritz approximations and the finite element program closely agree with each other as shown in Table 6.1.

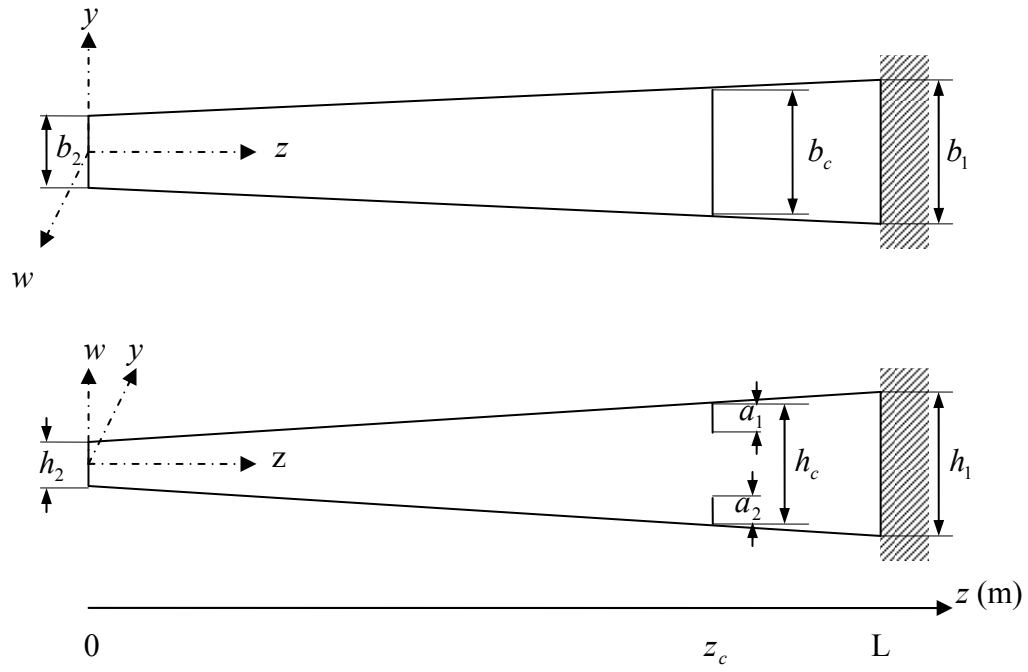

Figure 6.4 Geometry of a beam.

Table 6.1 Natural frequencies of the un-cracked beam.

Vibration Modes	Frequencies (Hz) obtained by Rayleigh–Ritz (6 terms)	Frequencies (Hz) obtained by Rayleigh–Ritz (9 terms)	Frequencies (Hz) obtained by Finite Element program
1	54.8890	54.8890	54.935
2	249.059	249.029	248.75

The vibration of a beam having different combinations of symmetric and asymmetric double-edge breathing cracks with the same total depth $(a_1 + a_2 = 0.3h_1)$ is investigated as an example. The vibration of a single-edge cracked beam is also examined. The following crack cases are examined for the beam considered with variable crack locations:

Case 1: $a_1 = 0.15h_1, \quad a_2 = 0.15h_1;$ Case 2: $a_1 = 0.20h_1, \quad a_2 = 0.10h_1;$

Case 3: $a_1 = 0.25h_1, \quad a_2 = 0.05h_1;$ Case 4: $a_1 = 0.30h_1, \quad a_2 = 0.00h_1.$

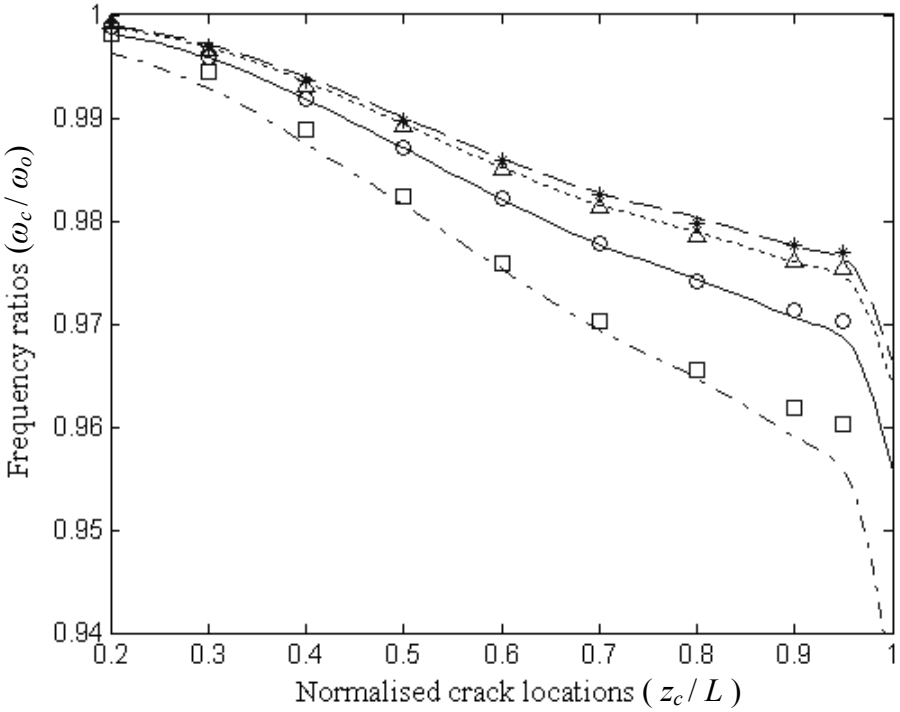

Figure 6.5 First mode vibration frequency ratios of the tapered cantilever beam with several depth combinations of cracks in pair. (– –), (---),(—), and (– -) are the results obtained by the method with six termed deflection function in Case 1, Case 2, Case 3, and Case 4 respectively. (*), (Δ), (o), and (□) are the results of the Ansys© for mentioned cases.

The analyses are performed for the beams having the cracks located through $0.2L - L$ in which the total crack depth ratio remains under 0.5. The results of the present method, which uses the six termed deflection function, agree well with the results of the finite element program for the first mode of vibration as shown in Figure 6.5. Second mode frequencies obtained by the method also match with the results of the finite element program for the beam having single-edge crack. However, in the cases of double-edge cracks, the matching of the second mode frequencies decreases when cracks exist through the $0.2L - 0.4L$ as seen in Figure 6.6. Better agreement can be observed in higher vibration modes when the deflection function used in the analysis is expanded with the larger number of terms (Mazanoglu, Yesilyurt, & Sabuncu, 2009). As shown in Figure 6.7, improved matching of the second mode frequencies is obtained by a nine termed approximation function for the beam with a double-edge crack. This result shows

that in the analysis of the double-edge cracked beam, the number of terms used in the deflection function should be more than the size of the function used in the analysis of the single-edge cracked beam. It is also seen from the figures that natural frequency ratios decrease with increasing asymmetry of the cracks in pair.

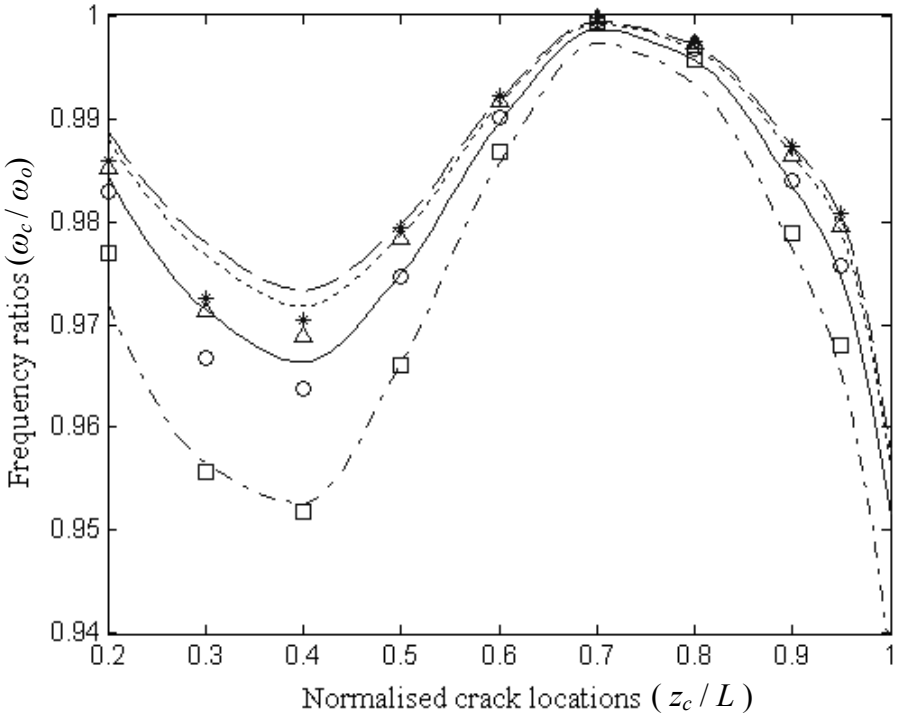

Figure 6.6 Second mode vibration frequency ratios of the tapered cantilever beam with several depth combinations of cracks in pair. (– –), (---),(—), and (– -) are the results obtained by the method with six termed deflection function in Case 1, Case 2, Case 3, and Case 4 respectively. (*), (Δ), (o), and (□) are the results of the Ansys© for mentioned cases.

The differences between the results of open and breathing crack models are shown in Figure 6.8. The effects of crack closing, compressive stresses, additional rotations, and neutral axis changes are not included in the open crack model. Results show that better matching with the finite element program can be obtained when the breathing crack model is used in the analysis of a double-edge cracked beam. It is also seen from the figure that the differences between the results of open and breathing crack models become smaller when larger asymmetry exists between the cracks.

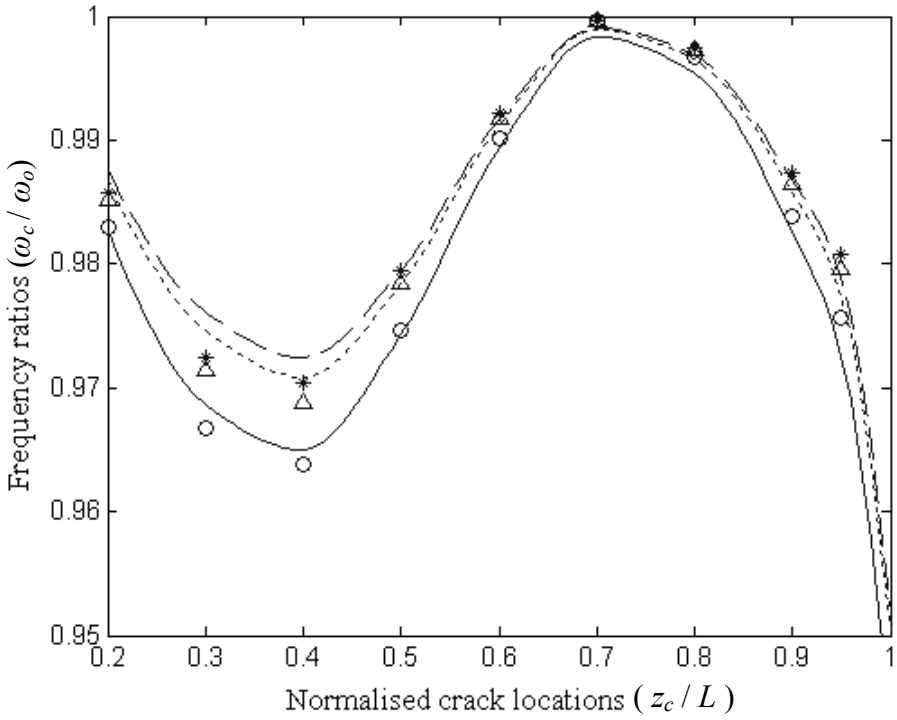

Figure 6.7 Second mode vibration frequency ratios of the tapered cantilever beam with several depth combinations of cracks in pair. (– –), (---), and (—) are the results obtained by the method with nine termed deflection function in Case 1, Case 2, and Case 3 respectively. (*), (Δ), and (o) are the results of the Ansys© for mentioned cases.

6.4 Conclusion

A method is presented to obtain the vibration of non-uniform beams having symmetric and asymmetric double-edge breathing cracks. The open crack model presented by Mazanoglu, Yesilyurt, & Sabuncu (2009) is modified by taking into account the effects of crack closing and compressive stress in addition to crack opening and tensile stress for modelling the breathing cracks. In addition to the direct effect of extra cross-section decrease, the effects of neutral axis yawing due to the difference between the opening and closing amounts and neutral axis shift due to the depth difference of the cracks in pair are also included in the model. The energy effects of the rotary inertia are also taken into consideration. Overall energy is analysed by the Rayleigh–Ritz approximation method.

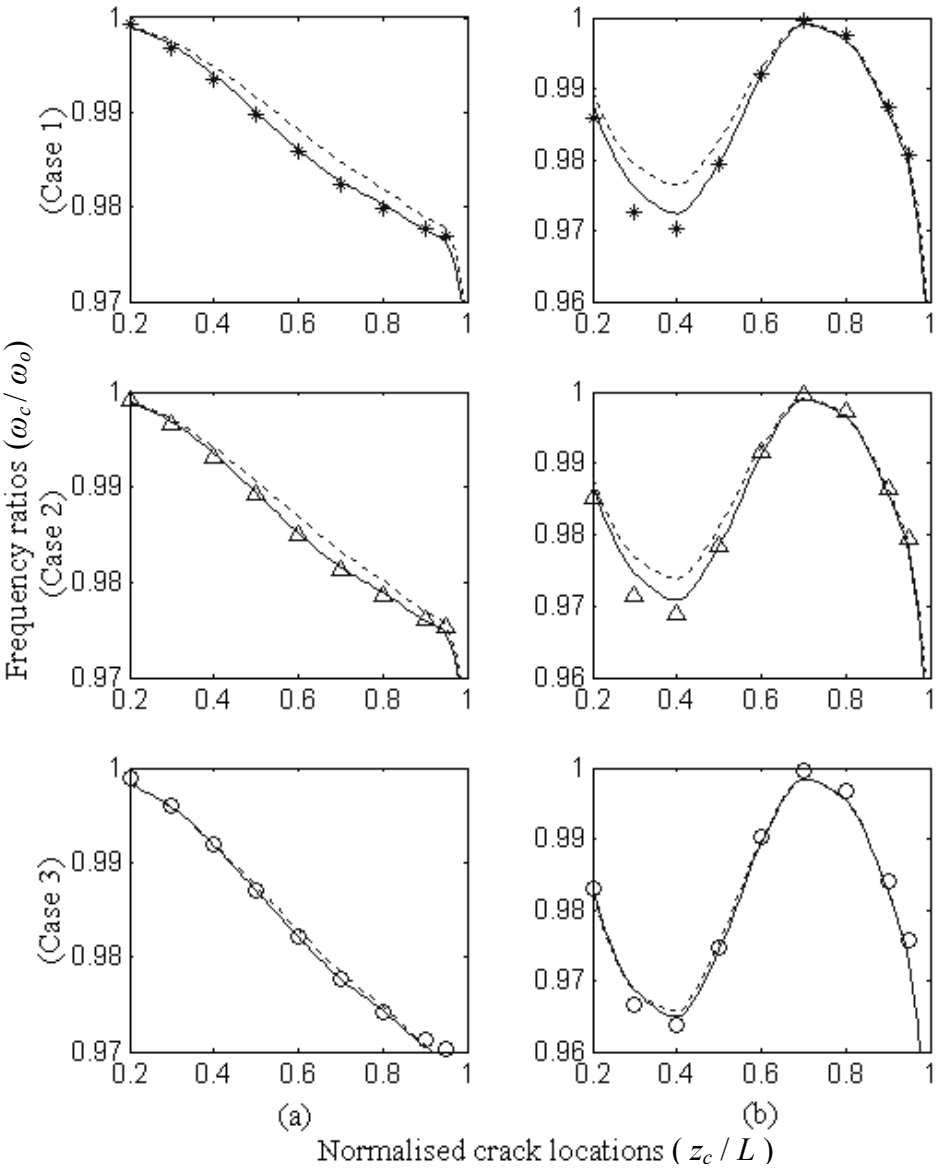

Figure 6.8 (a) First mode and (b) second mode natural frequency ratios obtained by the method using (a) six termed and (b) nine termed deflection functions. The method including breathing (—), and open (---) crack models are compared with the results of the Ansys© figured by (*), (Δ), and (o) representing Case 1, Case 2, and Case 3 respectively.

This chapter presents the first application of the vibration analysis of non-uniform beams having double-edge cracks. Up until now, there has been no work in existing literature for analysing the vibration of beams with asymmetric double-edge crack although symmetric double-edge crack models have been presented for uniform beams. The model presented in this chapter is valid for both single-edge and

symmetric double-edge cracks. The model has also the capability of analysing the vibration of beams with different depth combinations of asymmetric double-edge cracks.

Results of the method including open and breathing crack models are compared and examined in this chapter. When the results we obtain for the double-edge cracked beams are compared with the results of the finite element program, we see that the results of the breathing crack model are more accurate than that of the open crack model. The differences between the results of open and breathing crack models become negligible for the single-edge cracks.

In the chapter, it is shown that higher modes of vibration frequencies require larger number of terms to use in the deflection function. It is also observed that an extended number of terms are required for analysing the vibration of double-edge cracked beams. This means vibration analysis of the double-edge cracked beams needs more time than that of the single-edge cracked beams. However, a significant advantage of the method is the performing of the calculation process in a short period of seconds when the method compared with the finite element program. Thus, natural frequencies required for the frequency based inverse methods can be easily obtained for different beams.

CHAPTER SEVEN
A FREQUENCY BASED ALGORITHM FOR DETECTING DOUBLE CRACKS ON THE BEAM VIA A STATISTICAL APPROACH USED IN EXPERIMENT

7.1 Introduction

Any physical or chemical influences can result in flaws that lead to change of the dynamic behaviour of the structures. Exact identification of these changes is significantly important for the success of vibration based crack identification methods which are supported by the theoretical vibration models. Crack identification methods on direct use of several practical applications of measurements and vibration monitoring may not need a theoretical vibration model. These methods are generally based on the inspection of mode shape changes and need measurements with very high quality. They require expensive data acquisition and monitoring systems having the properties such as multiple sensors, high sensitivity, large hard disc capacity, and fast processing. Ideal system for the crack identification should be inexpensive, non-invasive and automated, so that subjective operator differences are avoided.

This chapter presents a method for identification of double cracks in beams and the processes minimising the measurement errors in experiment. Energy based numerical method is used in the vibration analyses for determining the natural frequencies of the cracked beam. Prediction tables including the natural frequency ratios are prepared by using the theoretical model for different depth and location of single crack on the beam. Prediction table is expanded by interpolating the data in both crack location and crack size directions. In resulting frequency map, contour lines representing the measured frequency ratios are easily utilised for identification of a single crack. However, if the beams have two cracks, contour lines cannot be directly used due to the necessity of plotting contours for all different location and depth combinations of cracks. This problem is solved by an algorithm presented in this chapter. Algorithm makes it available the approximation to the exact location

and size of both cracks after initial estimation done for one of the crack. Efficiency of the algorithm is checked by both experimental frequency ratios and the ratios obtained by commercial finite element program (ANSYS©). Errors in measured natural frequencies are minimised by means of presented statistical approach called 'Recursively scaled zoomed frequencies (RSZF)'. In this approach, measured frequencies are corrected by mean value of the natural frequencies observed from the interpolated frequency data determined in different frequency scales. A process called 'Derivative aided spline interpolation (DASI)' is used as an interpolation method for obtaining changes in peak characteristics in the frequency spectra. Methods are verified by the experimental natural frequencies measured from the cantilever beams. Measured natural frequency ratios, which will be obtained more sensitively by means of RSZF, are given as inputs into the algorithm. Experiments show that both cracks are detected with acceptable deviations.

7.2 Algorithm for Detecting Double Cracks

A prediction table formed by the natural frequency ratios obtained for all location and depth ratio of single crack is used as base data. Any correct cracked beam vibration model can be utilised for preparing the prediction table. However, speed of solution method and its adaptation to the automation is critically significant. Map of the frequency falling ratios is formed by interpolating prediction table in both location (z_c) and depth ratio (r_c) directions. Measured frequency ratios are meshed with the frequency ratios in the map and corresponding contour lines are plotted. If the contour lines for the first three modes are intersected at the same position in the map, it is known that there is one crack at that position which gives the location and depth ratio of the crack. However, if the contour lines intersect at the different positions, it can be judged that there is more than one crack. In this case, a position for one of the crack is predicted under the contour lines of measured frequency ratios. Because, the frequency ratio caused by one predicted crack should be found higher than the frequency ratio caused by two cracks. Remaining frequency fall should be the effect of the second crack and helps for determining the position of that crack in the map.

Here, the relation between the frequency ratios of a double cracked beam and the frequency ratios of two beams each sharing those cracks should be described. In most cases, minor effect of cracks interaction can be neglected such that a local flexibility model is used. Thus, the frequency ratio of the double cracked beam can be simply formulated as:

$$r_{f(dc)} = r_{f(c1)} r_{f(c2)}, \tag{7.1}$$

where $r_{f(c1)}$ and $r_{f(c2)}$ are the frequency ratios obtained from the separate single cracked beams.

When one of the positions is selected for the first crack, frequency ratios corresponding to this position, $r_{f(c1)}$, are found. Frequency ratio caused by the second crack, $r_{f(c2)}$, can be determined by using the ratio of measured frequencies as the ratio of double cracked beam, $r_{f(dc)}$, in Equation (7.1). Since the estimated crack position is not exactly true, contour lines plotted for the second crack caused frequency ratios of different vibration modes will intersect at the different positions in the map. Four contour lines corresponding to four natural frequencies are used in the algorithm. If the first four natural frequencies are used, intersection positions of the contour lines for the mode couples 1-2, 1-3, and 1-4 are determined. Sometimes, there can be more than one intersection points for one mode couple. In this case, intersection points causing the trio having minimum positional variance are selected as critical intersection points. Positional variance values are calculated by multiplying the standard deviations in both location and depth ratio directions. In the inner loop, minimum positional variances are calculated for the first crack's selected position and four surrounding positions of it. Distance from the surrounding positions to the selected position is identified by the step size.

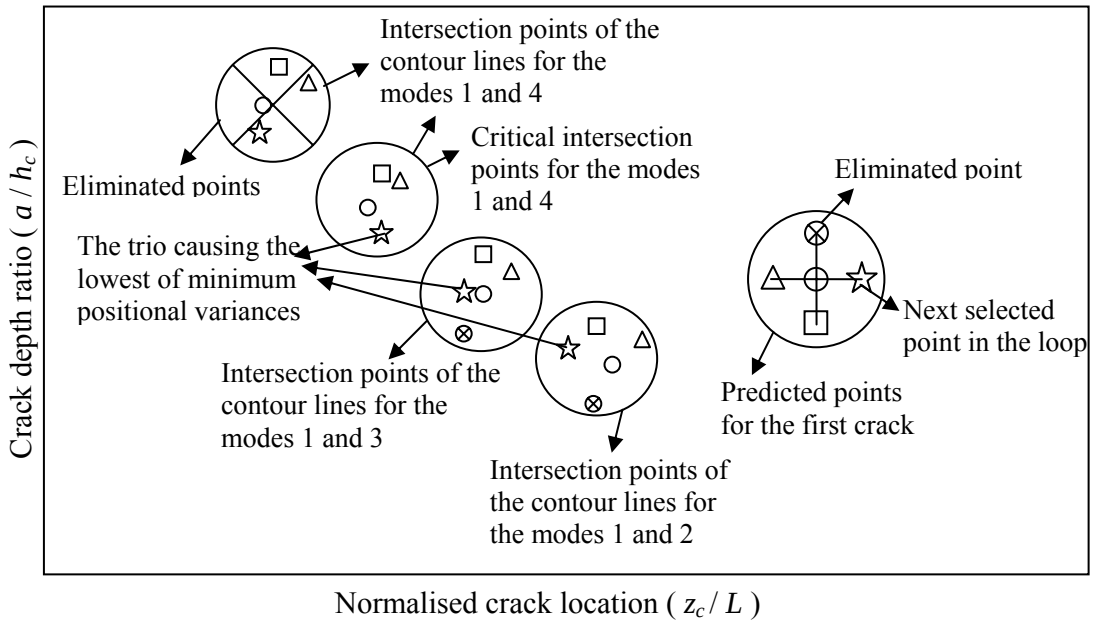

Figure 7.1 Schematic example for the selection of the new converged position in the loop.

The new converged position of the first crack and the next step size are determined in the judge module. Normally, the position, which results in the lowest of the minimum positional variance, should be the next selected position in the loop logically closer to the first exact crack position. If the lowest of minimum positional variances is obtained for the selected or previously selected first crack's positions, new position is selected through the remaining surrounding points. In the inner loop, sometimes contour lines for one of the mode couples may not be intersected, and thus the intersection point is not observed for that mode couple. Therefore, this point is also eliminated in selection. This case is represented in Figure 7.1 as an example. In the figure, the point of first crack symbolised by cross-circle does not cause intersection of the contour lines for the modes 1 and 4. It is also seen that the other first crack's points result in two possible intersection points of contour lines for the modes 1 and 4. Through them, the points causing minimum positional variances are selected for the mode couple 1-4. Since the lowest of the minimum positional variances is obtained by the point symbolised by a star, this will be the next selected point in the loop as shown in Figure 7.1. When the contour lines of all mode couples are not intersected, which means there is no corresponding frequency ratio of the

predicted position in the map, second crack is positioned out of map. In this case, first crack is directed toward contra position which causes the second crack come into the map.

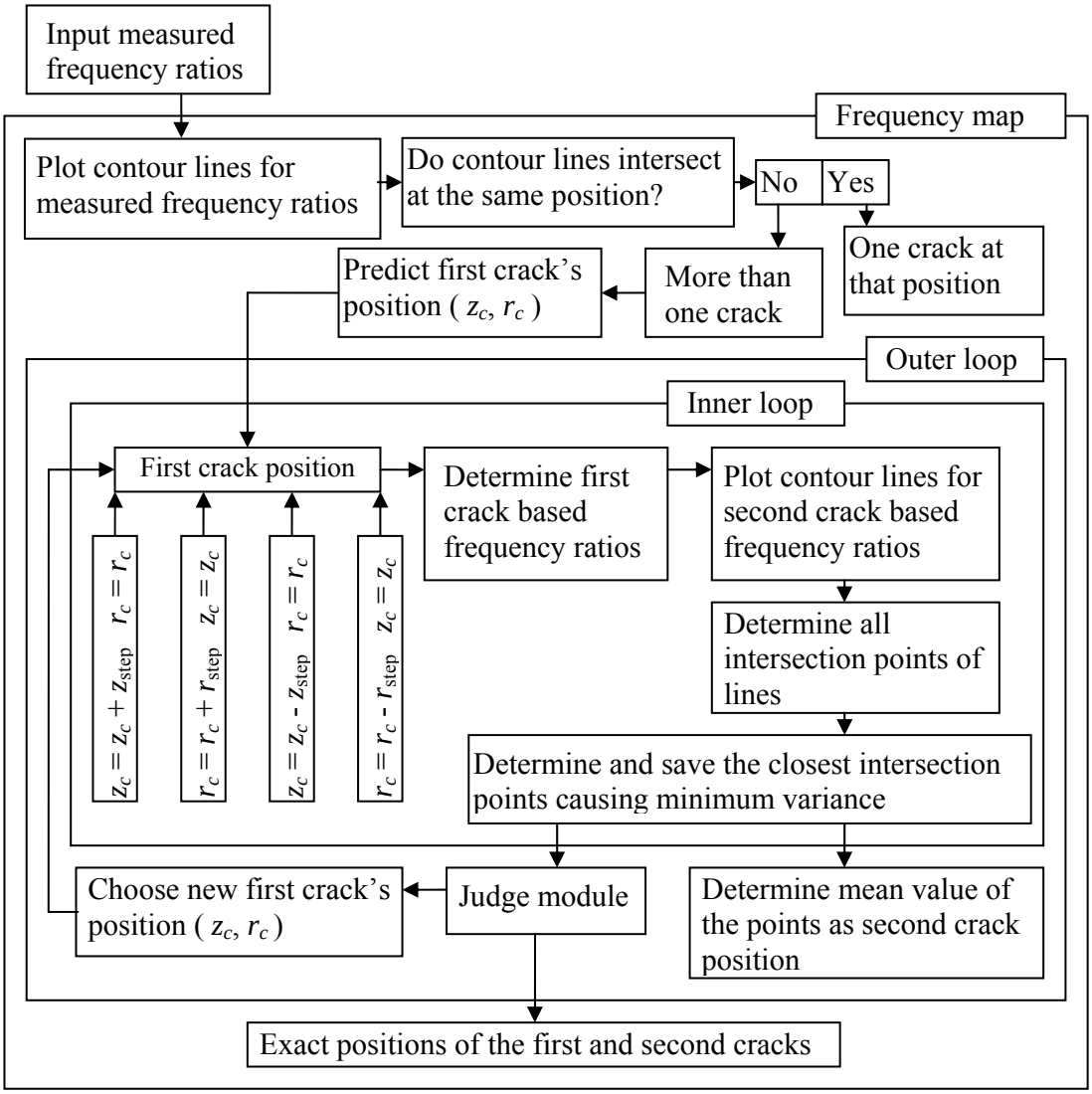

Figure 7.2 Schematic representation of the algorithm for detecting double cracks.

Two threshold values are prescribed by using minimum positional variances. First threshold sets the size of the step. Step size is multiplied or divided by two if the lowest of the minimum positional variances is respectively higher or lower than the first threshold. However, step size should be limited from the top and the bottom. Upper limit can be varied according to user preference, but base step size should be

equal to the distance between the neighbour points in the map. For each estimated first crack position, corresponding second crack position can be determined as mean of the mode intersection points. Process continues until the lowest of the minimum positional variances decreases under the second threshold value defined for stopping the outer loop. Schematic representation of the algorithm is presented in Figure 7.2.

7.3 Processes for Obtaining the Best Frequency Ratios in Measurement

It is well known that natural frequencies of the structure can be easily found by the frequency response function (FRF) which gives the relation between the excitation and response in frequency domain. FRF can be simply defined as the ratio of the Fourier transform of response to the Fourier transform of the excitation. Discrete Fourier transform of any signal can be formulated as follows:

$$S(k) = \sum_{n=0}^{N-1} s(n) e^{-2\pi i k \frac{n}{N}} \qquad k = 0 \text{ to } N-1 \tag{7.2}$$

However, measured frequencies are bounded by several limits such as sensor sensitivity and resolution. In the frequency spectra, the frequency index spacing can be minimised by using many samples or low sampling frequency. Nyquist criterion states that half of the sampling frequency cannot be lower than the aimed measured frequencies. Moreover, even if this criterion is satisfied, sensitivity decreases as the frequency approaches to the Nyquist limit. In addition, long time data requires more disk capacity for storing and more memory for processing.

A statistical method supported by interpolation of the frequency data can be useful for minimising the measurement errors even if larger sampling frequency and shorter time data are used. The method of RSZF presented in this chapter minimises the measurement errors without the need of repeating the experiments for taking statistical data. Several frequency spectra are obtained in one experiment by decreasing the length of time data N to $N - X$. Correspondingly, in the interval $0 \le f < f_s/2$, while there are N equidistant samples with spacing $\delta f = f_s/(2N)$ at

first, reduced data include $N-X$ samples with spacing $\delta f = f_s/(2(N-X))$. Observed natural frequencies change due to the use of different frequency scale. In addition, there can be changes in peak characterisation for all different frequency scales. More approximate peak values are obtained by interpolating the frequency data. Classical spline interpolation may be utilised directly on the frequency data, but changes in peak characterisation are obtained better by applying the DASI method. If $S(k)$ is the frequency data indexed by $k=0$ to $N-1$ derivative of $S(k)$ can be written as follows:

$$dS(k) = \frac{1}{\delta f}\big(S(k+1) - S(k)\big), \qquad k = 0 \text{ to } N-2 \tag{7.3}$$

Dyadic spline interpolation is applied on the derivative of the frequency data and interpolated derivative, $dS_{\text{int}}(k)$ is obtained for $k=0$ to $2(N-1)-1$. Then, inverse differentiation gives the interpolated frequency data, $S_{\text{int}}(k)$ having length $2N-1$.

$$S_{\text{int}}(0) = S(0),$$

$$S_{\text{int}}(k) = S_{\text{int}}(k-1) + \frac{f_s}{2N-1} dS_{\text{int}}(k-1), \qquad k = 1 \text{ to } 2N-2. \tag{7.4}$$

This process is repeated as long as the frequency data reach to the length meeting required sensitivity. After R reputation of the dyadic interpolation, length of the interpolated data will be $N_{\text{int}} = 2^R(N-1)-1$.

As a result, frequency data are rescaled by reducing data length for each return and different natural frequencies are obtained for all different frequency scales, although the interpolation minimise the discrepancies. Therefore, mean value of the natural frequencies found in each return is taken as exact natural frequency. The processes for the RSZF and DASI are schematically summarised in Figure 7.3.

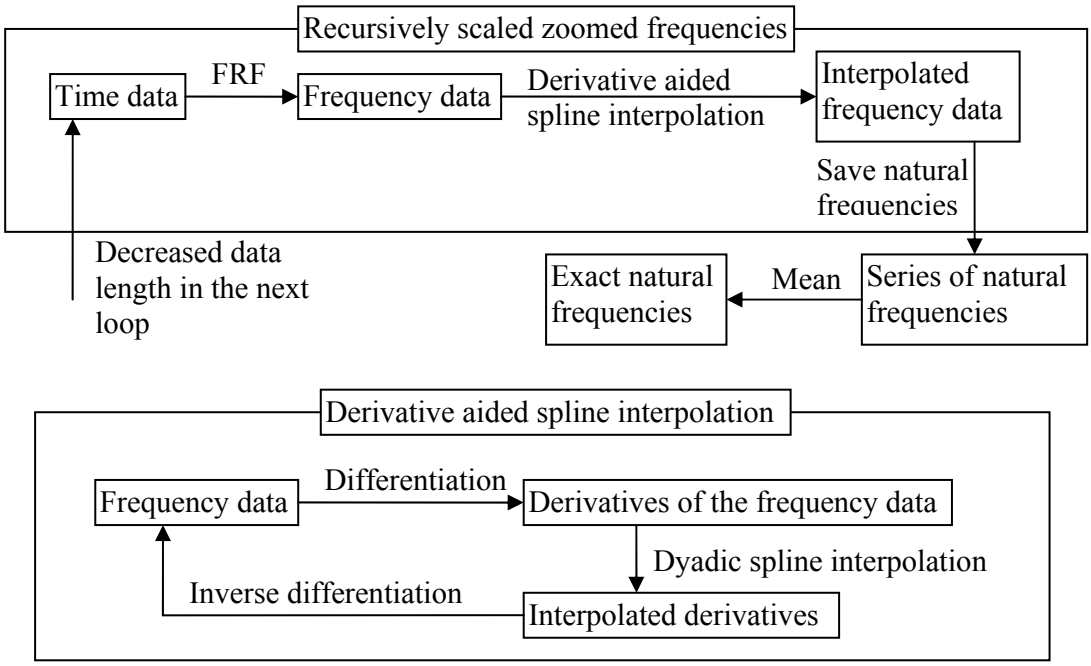

Figure 7.3 Schematic representations for RSZF and DASI processes.

7.4 Results and Discussion

Success of the algorithm is checked by using the natural frequency ratios of the double cracked cantilever beam obtained by the commercial finite element program. These ratios are given as inputs into the algorithm which uses prediction tables prepared by theoretical frequency ratios. Modal properties used in the finite element program are given in Section 3.5.

An aluminium alloy cantilever beam, which is utilised in the experiment, is also simulated in the finite element program for checking the efficiency of the algorithm. In the first example, cracks are simulated at the normalised locations of 0.3 and 0.6 which are positioned from the free end. Their depth ratios are taken to be 0.35 and 0.25 respectively. These cracks are detected using the algorithm at the normalised location 0.63 with depth ratio 0.23 and the normalised location 0.31 with depth ratio 0.375. Small differences between the exact and detected positions are caused by the differences between the theoretical frequency ratios and the ratios obtained by the commercial finite element program. The algorithm is checked by selecting four

different starting positions in the map as shown in Figure 7.4. Contour lines represent the input frequency ratios of the first four modes. In another example, cracks are considered at the normalised locations 0.45 and 0.65 with the depth ratios 0.30 and 0.27 respectively. Figure 7.5 shows that cracks are successfully detected by the algorithm starting from three different positions. In a final example, cracks simulated at the normalised locations 0.25 and 0.80 are considered with depth ratios 0.35 and 0.15 respectively. Figure 7.6 shows the approximate detection of the cracks as a result of searching the crack positions by starting from four different predicted first crack positions.

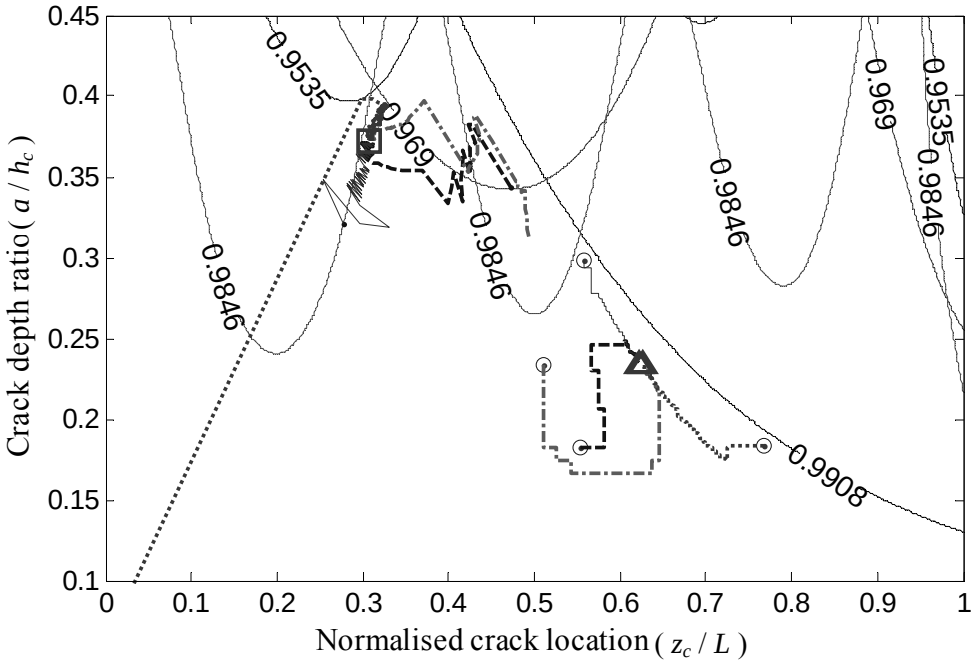

Figure 7.4 Results of the algorithm for simulated beam slotted from the normalised locations 0.3 and 0.6 with the depth ratios 0.35 and 0.25 respectively. (o) Initial predictions for the first crack, (—, – –, – · –, ····) paths from predicted points to resulting positions, (Δ) resulting first crack position, (□) resulting second crack position. Input frequency ratios: First mode 0.9908, second mode 0.969, third mode 0.9535, fourth mode 0.9846.

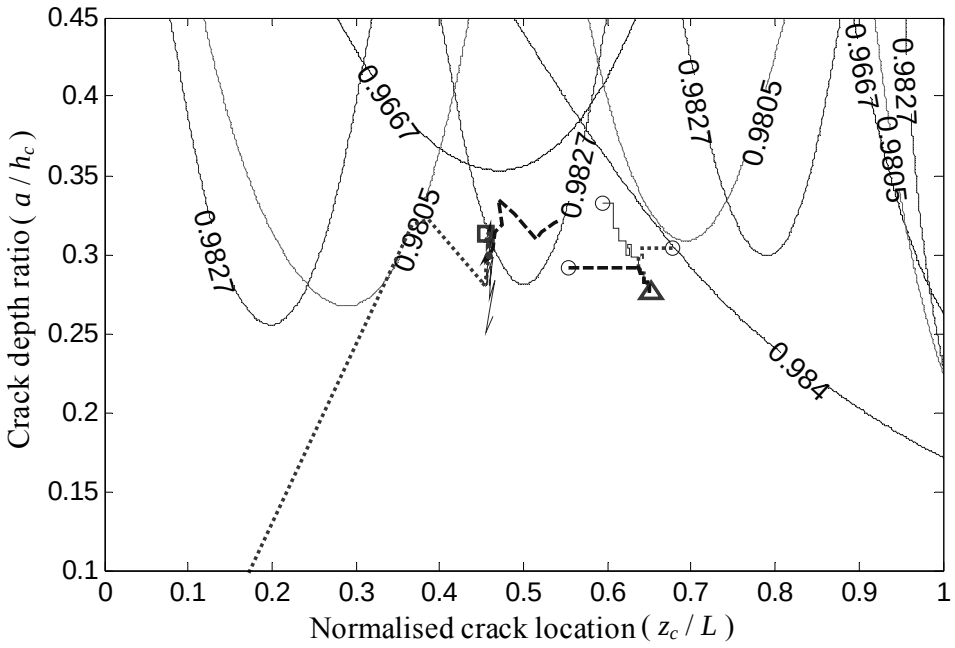

Figure 7.5 Results of the algorithm for simulated beam slotted from the normalised locations 0.45 and 0.65 with the depth ratios 0.30 and 0.27 respectively. (o) Initial predictions for the first crack, (—, – –, ····) paths from predicted points to resulting positions, (Δ) resulting first crack position, (□) resulting second crack position. Input frequency ratios: First mode 0.984, second mode 0.9667, third mode 0.9805, fourth mode 0.9827.

As seen in Figures 7.4, 7.5 and 7.6, the algorithm searches the suitable orbit of the first mode contour for the predicted crack, and then follows that orbit since the convenient contour lines for the second crack are investigated by using the first mode contour lines intersected with the lines of other modes. Searching continues on that orbit until the positional variance of possible second crack position decreases under the predetermined threshold for stopping the search. When second crack goes out of the map, it comes into the map by means of the first crack directed toward contra position.

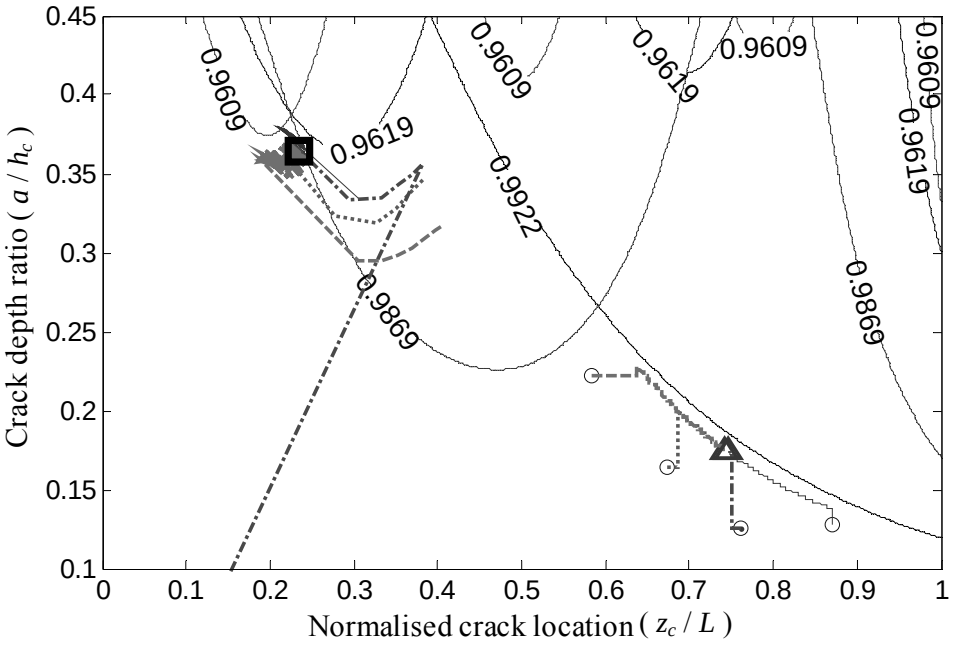

Figure 7.6 Results of the algorithm for simulated beam slotted from the normalised locations 0.25 and 0.80 with the depth ratios 0.35 and 0.15 respectively. (o) Initial predictions for the first crack, (—, – –, – · –, ····) paths from predicted points to resulting positions, (Δ) resulting first crack position, (□) resulting second crack position. Input frequency ratios: First mode 0.9922, second mode 0.9869, third mode 0.9619, fourth mode 0.9609.

RSZF and DASI methods, which increase the sensitivity and resolution of the measured data, are verified experimentally. An aluminium alloy cantilever beam is used in experiment. The beam has the following geometric properties: 10×10 mm^2 cross-section and $L = 0.36$ m length. Its elasticity module and density is determined as $E = 69$ GPa and $\rho = 2678$ kg/m^3 respectively. Poisson ratio is taken as $\nu = 0.3$. Cracks are simulated as slots sawed by a fretsaw on site for supplying stable test condition. Data acquisition is achieved by exciting the beam using impact hammer and by taking the vibration response using a miniature accelerometer with negligible weight 0.8g. Photos of test structure and measurement devices are given in Appendix C. 30000 samples are collected with 6000 Hz sampling frequency to observe the first four peaks of the natural frequencies in the frequency spectrum obtained from only one experiment. When there is no crack on the beam, measured natural frequencies

or the frequencies obtained after applying the presented processes are taken as reference frequencies.

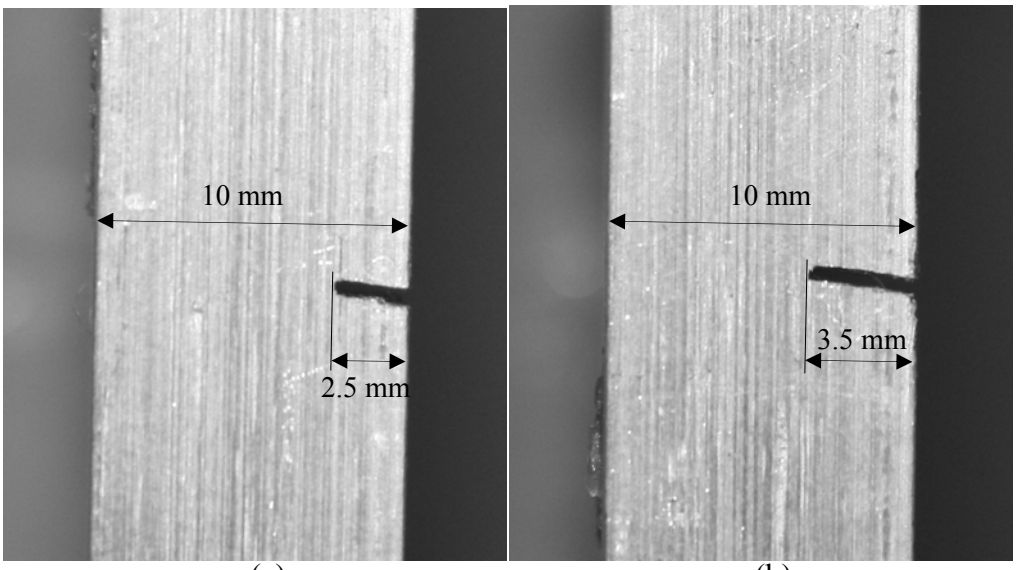

Figure 7.7 Photos of slots simulated as (a) first crack and (b) second crack.

First slot is constituted at the location having 0.27 m distance from the free end with an approximate depth ratio of 0.25 as shown in Figure 7.7(a). Natural frequency ratios are obtained and the crack is identified by the intersection position of the contour lines plotted for the first three natural frequency ratios. In Figure 7.8, the ratios determined from the direct FRF results are presented by using 30000 and 3000 samples without any additional processes of RSZF. Corresponding to these data lengths, frequency data are indexed by the spaces 0.2 Hz and 2 Hz respectively. Lower frequency index space requires larger data to store with more process time, memory and disk capacity. On the other hand, larger frequency index space causes insufficient resolution especially for detecting the decrease ratio of the lower mode frequencies. Results show that contour lines plotted for the measured natural frequency ratios cannot be intersected at the same position of the map due to the insufficient resolution even if the 30000 samples are used. When the data length is reduced to the 3000 samples, frequency resolution will be very poor for usage of FRF directly. Contour lines of the first and second mode frequency ratios are not seen in Figure 7.8(b), since the ratios are found “1” as a result of very poor frequency

resolution. The unchanged frequencies can be observed from the FRF results represented by zooming of the spectra around the first two natural frequencies shown in Figure 7.9(a).

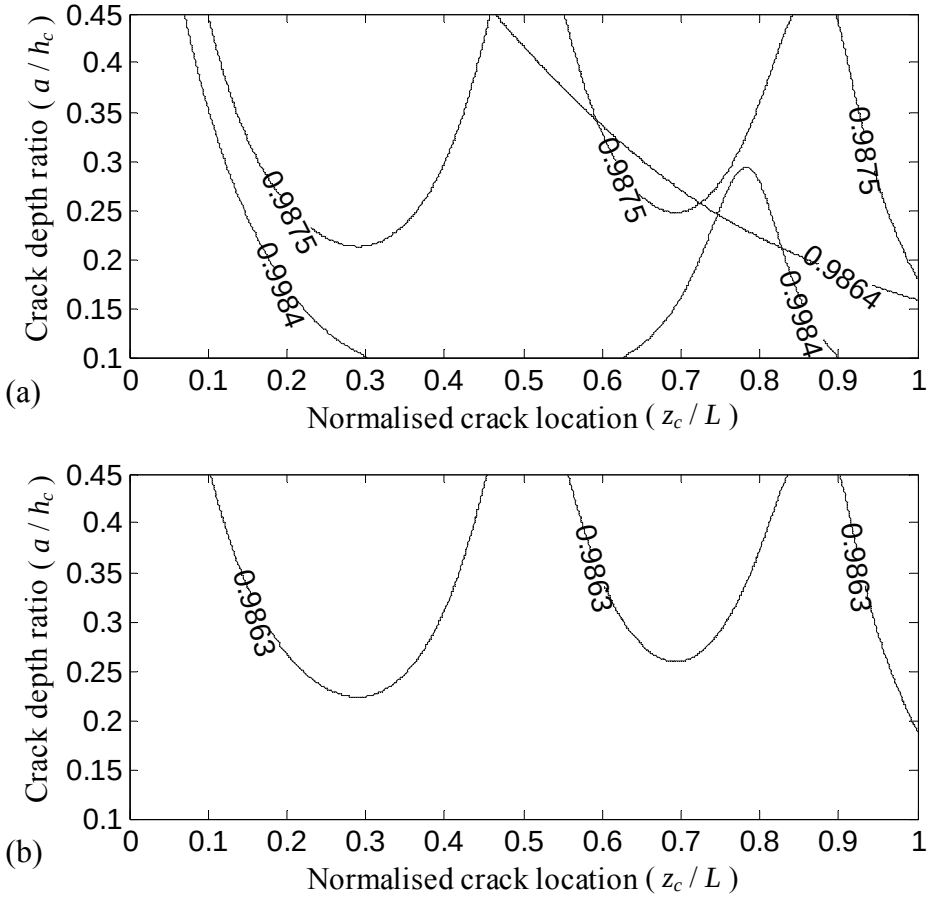

Figure 7.8 Contour lines of the measured natural frequency ratios obtained by the direct FRF applied to the (a) 30000 and (b) 3000 samples of data. Modal frequency ratios: (a) First mode 0.9864, second mode 0.9984, third mode 0.9875, (b) first mode 1, second mode 1, third mode 0.9863.

As a consequence, it is critically significant to obtain satisfactory results by additional processes applied to the lower sized data. When only zooming process using DASI is applied to the data having 3000 samples, measured frequencies are a little modified. This change is recognised in the interpolated frequency spectra seen in Figure 7.9(b) for the first two vibration modes.

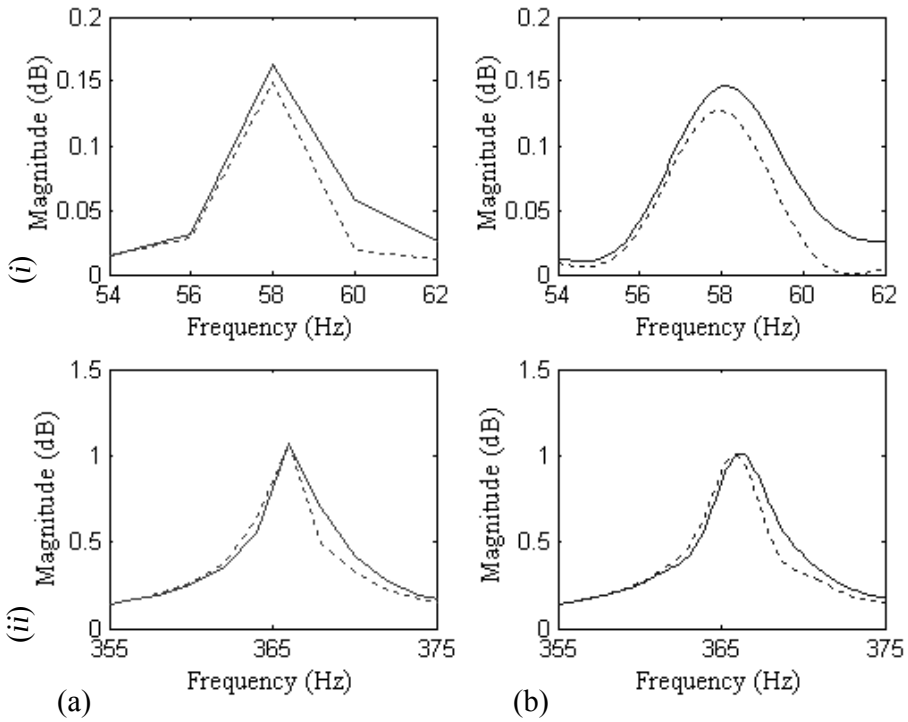

Figure 7.9 Frequency spectra of (—) un-cracked and (---) cracked beam's data zoomed around (*i*) first and (*ii*) second natural frequencies (a) without any additional process, (b) with DASI process**.**

However, contour lines are still apart from each other and do not intersect at the same position of map as shown in Figure 7.10(a). Here, the RSZF method including DASI gives the best results. In the application of methods, frequency data are interpolated 4 levels ($R = 4$), and time data are rescaled 20 times by decreasing the data length 15 samples in each return. Results show that the best approximation is observed for detecting the position of single crack in the map as shown in Figure 7.10(b).

Five different data are taken from the un-cracked and cracked conditions of the same beam to ensure robustness of the experiment. In each measurement, the observed natural frequencies change a little for higher vibration modes since the sensitivity decreases as the frequencies increase.

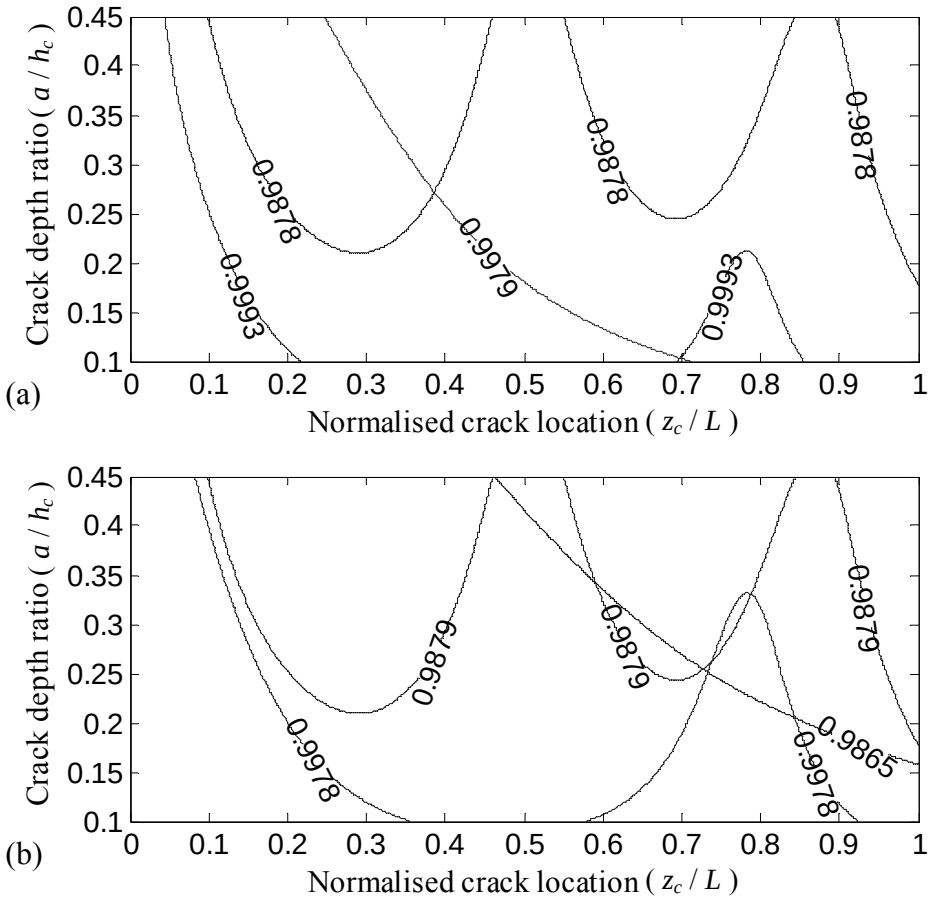

Figure 7.10 Contour lines of the natural frequency ratios obtained by (a) zooming process without rescaling and (b) RSZF method using 3000 samples of data. Modal frequency ratios: (a) First mode 0.9979, second mode 0.9993, third mode 0.9878, (b) first mode 0.9865, second mode 0.9978, third mode 0.9879.

Therefore, the success of the RSZF method can be rechecked by using the average natural frequency ratios obtained from the five experiments. Average natural frequency ratios obtained by FRF of the 30000 samples and RSZF of the first 3000 samples are shown in Figures 7.11(a) and 7.11(b) respectively. It is seen that the contour lines obtained by the RSZF method close to each other in the vicinity of crack position although the data are bounded by only 3000 samples. Furthermore, even if the first 1000 data samples are used, satisfactory results are obtained by using RSZF method as shown in Figure 7.11(c).

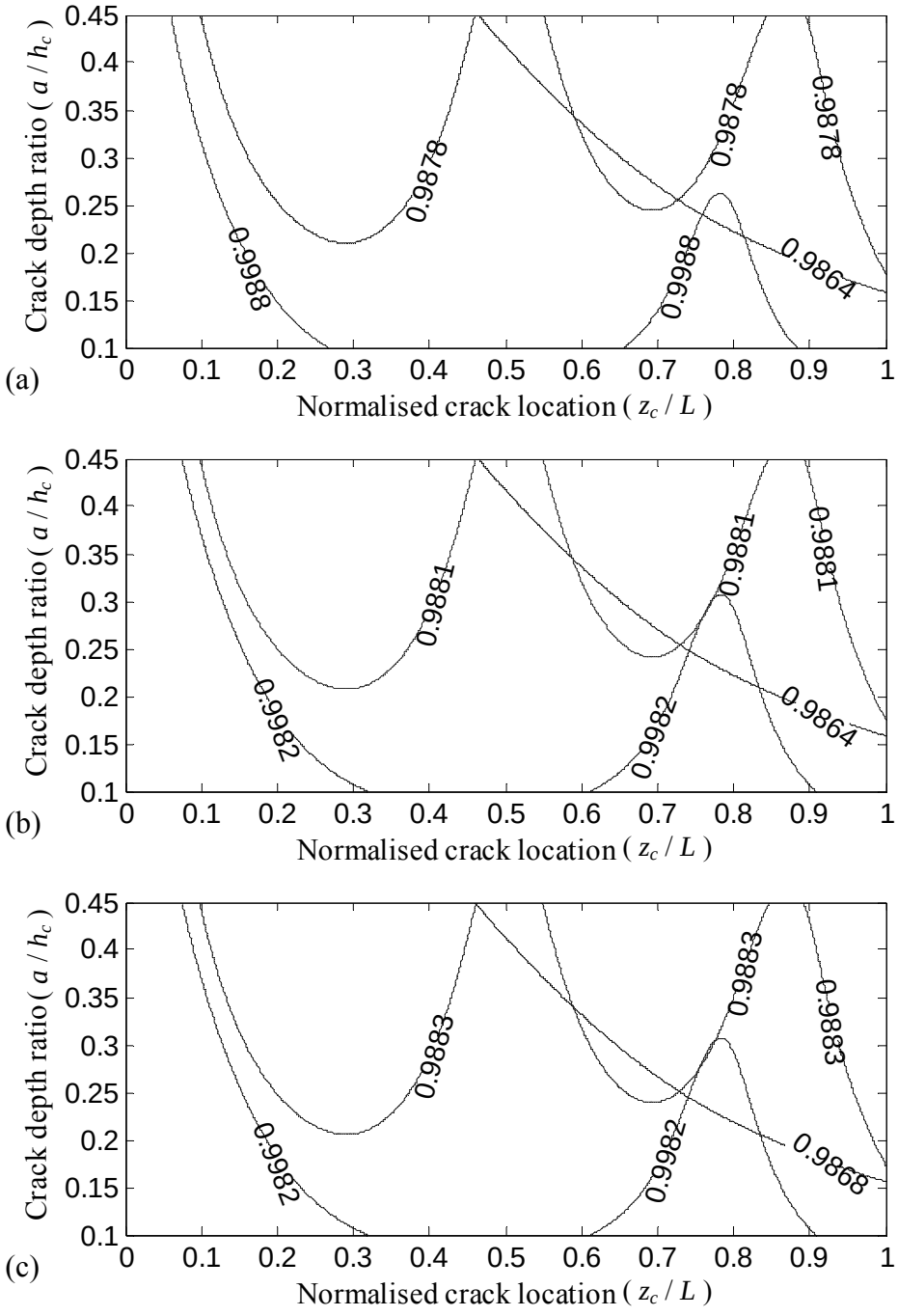

Figure 7.11 Contour lines of the natural frequency ratios obtained by (a) FRF using 30000 samples, (b) RSZF using 3000 samples and (c) RSZF using 1000 samples. Modal frequency ratios: (a) First mode 0.9864, second mode 0.9988, third mode 0.9878, (b) first mode 0.9864, second mode 0.9982, third mode 0.9881, (c) first mode 0.9868, second mode 0.9982, third mode 0.9883.

The beam is slotted again from the location having 0.20 m distance from the free end with approximate depth ratio 0.35. It is seen from the single crack results that the best approximations are obtained when the measured natural frequency ratios are corrected by RSZF. Therefore, when two cracks are investigated in the beam, RSZF results obtained by using 3000 samples of data are given as inputs into the presented algorithm. As shown in Figure 7.12, both cracks are positioned with acceptable deviations in the map by means of the first four natural frequency ratios used in the algorithm. The algorithm successfully approximates to the same crack positions although it is started from four different predicted positions. Deviations from the accurate crack positions are caused by the difference between the theoretical model and the experiment.

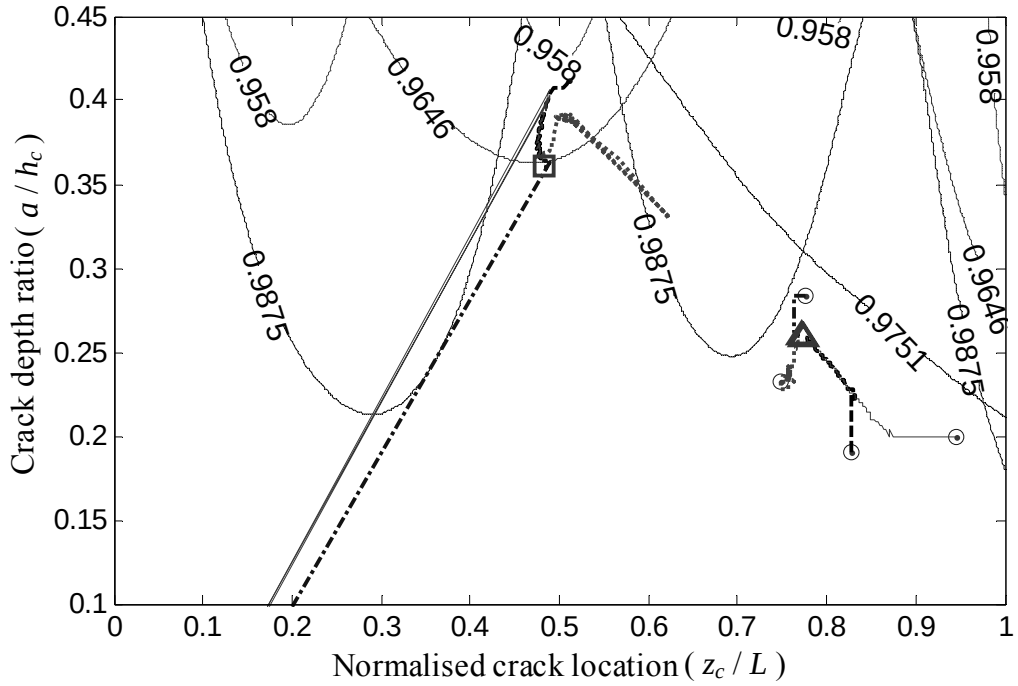

Figure 7.12 Results of the algorithm for the beam used in experiment slotted from the normalised locations 0.55 and 0.75 with the depth ratios 0.35 and 0.25 respectively. (o) Initial predictions for the first crack, (—, – –, – · –, ····) paths from predicted points to resulting positions, (Δ) resulting first crack position, (□) resulting second crack position. Input frequency ratios: First mode 0.9751, second mode 0.9646, third mode 0.9875, fourth mode 0.9580.

7.5 Conclusion

In this chapter, an algorithm that uses the map of the natural frequency ratios is presented for detecting double cracks in beams. Sensitivity of the measured natural frequencies are increased by means of a statistical approach called 'Recursively scaled zoomed frequencies (RSZF)' that uses an interpolation method called 'Derivative aided spline interpolation (DASI)' for obtaining increased resolution.

Success of the algorithm highly depends on the correctness of both the frequency table and the measured natural frequencies. The frequency table is prepared by the theory presented for single cracked beam. In the method, nine termed approximation gives satisfactory results for obtaining natural frequency prediction table. The numerical method allows forming a prediction table in a short time. It is convenient for non-uniform beams. Success of the algorithm and the theoretical frequency table are verified by double cracked beam's frequency ratios obtained by the commercial finite element program and used as inputs for the algorithm. The relation between the frequency ratios of the single cracked and double cracked beams is simply settled by using local flexibility model. The crack interaction effects can be negligible unless the cracks are advanced and are too close to each other.

Measurement errors due to insufficient sensitivity and resolution are successfully minimised by RSZF using DASI. Success of the processes is quite significant for detecting cracks in the algorithm especially when the cracks cause low frequency falls. The methods are verified experimentally on cantilever beams which are considered to have single crack and double cracks. It is shown that RSZF supplies higher sensitivity using lower data length. Thus, it prevents the user from the additional process time, memory and disc capacity. DASI, which increases the success of RSZF, interpolates the frequency data by considering the derivatives that includes the effects of peak characterisation. The processes will especially be helpful in detection of the higher modal frequencies obtained by low sensitivities and in detection of the lower modal frequencies obtained by insufficient resolution in measurement.

Robustness of the algorithm is represented in the examples using the input frequencies obtained by the commercial finite element program and the experiment. Although, the algorithm is started from different positions of the maps, cracks are satisfactorily positioned unless the first prediction is too far from the accurate position.

The methods presented in this chapter contribute to the automated crack detection systems. However, in many cases, there can be differences between the theoretical and the measured natural frequencies of the un-cracked beams mainly for higher modal vibrations. Therefore, un-cracked beam's data are used as references for zero setting procedure in application. This procedure prevents complication in the automated crack detection systems.

CHAPTER EIGHT
CONCLUSIONS

8.1 General Contributions of the Thesis

This doctorate study presents the flexural vibration analyses of multiple cracked beams at first, to use in detection of the cracks. The work does not only consist of the presentation of classical vibration theory, but also contains theoretical developments. Vibrations of the multiple cracked non-uniform Euler–Bernoulli and Rayleigh beams are analysed by the energy based numerical method. Vibration behaviours are modelled for several types of multiple cracks in rectangular cross-sectioned beams. In addition to the transverse edge cracks considered frequently in the literature, the unusual cracks on the height-edge of the beams and the double-edge cracks with asymmetric depths are also considered. Open and breathing cracks are modelled by the rotational springs. Amount of the energy consumed due to the cracks and its distribution along the beam are described for all types of cracks. Interactions of the cracks in multiple cracked beams are also presented for different crack types.

In inverse problems, the method based on the frequency contour lines is employed for detecting only one crack on the beams. As a contribution to current literature addressing the inverse problems, a frequency based algorithm is developed for detection of the double cracks on the beams. An automated single and double crack detection system is settled by using the theoretical natural frequencies as references and the measured frequencies as inputs. Another contribution is presented for more reliable natural frequencies by supporting it with a statistical approach and an interpolation technique. Measured frequencies are modified by the process that results in more stable natural frequencies, which have minor changes in each experiment, as the sensitivity and resolution of the data are increased. The process results in the adequacy of the data having much less samples than the collected data. Consequently, it prevents the user from the additional process time, memory and disc capacity to use.

8.2 Overview of the Conclusions

Chapter 2 reviews current literature including the studies presented for cracked beam vibration analyses and detection of the cracks. It is seen that a few study are presented for continuous vibration analyses of cracked non-uniform beams considered with the special forms. Furthermore, there is no work including general formulations for the analyses of the multiple cracked non-uniform beams having different boundaries and different crack models except for the papers extracted from this thesis. In the most study, the transverse crack models are considered. However, a good method used in the analysis should be adaptable for different conditions of cracks and beams.

In measurement, frequency parameter is obtained easier to use in crack detection when compared with determination of the other modal parameters. In addition, measuring flexural vibration is much easier than measurements of the torsional and the longitudinal vibrations that come into exist in higher frequency bands. Therefore, the methods employing the natural frequencies of flexural vibration are generally proposed in literature for detection of the cracks. However, a method for multiple crack detection using only natural frequency drops has not been presented yet. These lacks in current literature determine the scope of this doctorate study.

Chapter 3 introduces with the vibration analysis of the un-cracked beams and presents continuous methods for the beams with multiple cracks and additional masses. Results show that, analytical method with local flexibility model can only be convenient for the analyses of uniform beams with a few numbers of cracks. Furthermore, it requires defining local flexibility for each different discontinuity like additional masses or steps. It also requires explaining solution form for each different non-uniformity. On the contrary, the energy method can be successfully used in different conditions of beam shaped structures. Therefore, energy used numerical solution is proposed in this thesis and it is employed in following chapters for non-uniform beams with different types of cracks.

Chapter 4 presents the modified energy method to obtain the vibration of multiple cracked non-uniform Euler–Bernoulli beams. It is shown that, both the effects of the stress field caused by the angular displacement of the beam and the strain energy change caused by the crack should be taken into account for calculating the energy consumed. Instead of the analytical methods, usage of the energy distributions in numerical approaches simplifies the solution of non-uniform beams. However, these approaches suffer from the interaction of crack effects in multiple cracked beams. Proposal for the solution of this problem is presented in this chapter. It is observed that double cracked beam behaves like a single cracked beam when both cracks come closer to each other, as one would expect. Effects of truncation factors are evaluated with respect to variation of the natural frequency ratios. It is clear that, the truncation factor of beam's height is much more effective than the truncation factor of beam's width.

In chapter 5, fracture mechanics theory is adapted to the height-edge open cracks via a proposed model for the vibration behaviour of crack. The energy consumed is determined by forming the opening of the crack and distributing the strain disturbance along the beam's length. If the beam has multiple cracks, it is shown that the strain disturbance caused by one of the cracks is damped as much as the depth ratio of the other cracks at their locations. Thus, interaction of the multiple crack effects, which is the problem for the methods based on a variational principle, is defined by the strain disturbance model presented for the height-edge cracks. Unique plane vibrations obtained by the present method can be critical in measuring and crack identification. Determination of the vibration characteristics in two planes results in adequacy of lower frequency modes especially if the cross-section of the beam is not square. It is observed that even if the beam has multiple cracks, the solution time of the method does not rise as much as the solution time of the finite element program.

In chapter 6, a method is presented to obtain the vibration of non-uniform Rayleigh beams having symmetric and asymmetric double-edge breathing cracks. The open crack model is modified by taking into account the effects of crack closing

and compressive stress in addition to crack opening and tensile stress for modelling the breathing cracks. It is shown that, extra cross-section decrease, neutral axis yawing due to the difference between the opening and closing amounts, and neutral axis shift due to the depth difference of the cracks are all influential for modelling the vibration of symmetric and asymmetric double-edge breathing cracks. The model is valid also for single-edge cracks. When the results are compared with the results of the finite element program, we see that the results of the breathing crack model are more accurate than that of the open crack model. The differences between the results of open and breathing crack models become negligible for the single-edge cracks. Results show that higher modes of vibration frequencies require larger number of terms to use in the deflection function. It is also observed that an extended number of terms are required for analysing the vibration of double-edge cracked beams. This means vibration analysis of the double-edge cracked beams needs more time than that of the single-edge cracked beams.

In the chapters covering the methods presented for vibration analysis of cracked beams, coupling effects are neglected. Bending-torsion, which is probably the most coupling type, can have considerable influence if the cracks become deep enough. However, admissible sized cracks do not have clear influence of coupling on the lower modes of bending vibrations as obtained from the results. Advantages of the numerical method can be its speed and its convenience for non-uniform beams. Thus, natural frequencies required for the frequency based inverse methods like prediction schemes or contour graphs can be easily obtained for each different beam. In practise, it is not impossible to obtain exact natural frequency ratios represented in figures. Sensitivity and resolution of the measurement system should be satisfactory. Restriction caused by the sampling can be kept to a minimum by the acquisition of long data with sufficient sampling frequency. Furthermore, sensitivity in the frequency domain can be improved by several statistical methods.

In chapter 7, an algorithm that uses the map of the natural frequency ratios is presented for detecting double cracks in beams. Sensitivity of the measured natural frequencies are increased by means of a statistical approach called ‘Recursively

scaled zoomed frequencies (RSZF)' that uses an interpolation method called 'Derivative aided spline interpolation (DASI)' for obtaining increased resolution. Success of the algorithm highly depends on the correctness of both the frequency table and the measured natural frequencies. Frequency table is prepared by the theory presented for a single cracked beam. Success of the RSZF and DASI processes is quite significant for detecting cracks in the algorithm especially when the cracks cause low frequency falls. The methods are verified experimentally on cantilever beam which is considered with single crack and double cracks. It is shown that RSZF supplies higher sensitivity using lower data length. Thus, it prevents the user from the additional process time, memory and disc capacity. DASI, which increases the success of RSZF, interpolates the frequency data by considering the derivatives that includes the effects of peak characterisation. The processes will especially be helpful in detection of the higher modal frequencies obtained by low sensitivities and in detection of the lower modal frequencies obtained by insufficient resolution in measurement. The algorithm proposed for detection of double cracks is found robust. Although, the algorithm is started form different positions of the maps, cracks are satisfactorily positioned unless the first prediction is too far from the accurate position. The methods presented in this chapter contribute to the automated crack detection systems. However, in many cases, there can be differences between the theoretical and the measured natural frequencies of the un-cracked beams especially for higher modal vibrations. Therefore, uncracked beam's data are used as references for zero setting procedure in application. This procedure prevents complication in the automated crack detection systems.

8.3 Scopes for the Future Works

Following research and development studies can be performed for vibration analyses of the cracked beams and detection of the cracks:

Continuous vibration theories can be studied for different structures having cracks such as stepped beams, frames, and plates. First of all, the cracked beam vibration

theory presented in this thesis can be adapted to multi-cracked stepped beams having additional masses in near future.

The types of the cracks can be identified by using the experimental natural frequencies measured in two vibration planes of bending. In addition, natural frequency based inverse method used can be improved for detecting three or more cracks in beams.

Spatial analysis methods can be developed for detection of cracks by using spatial data taken from rarely located points. Advanced spatial data can be shaped by proposed interpolation methods. In addition to spatial analysis by finding the global values of considered parameters, the data set can be analysed in spatial–time domain by investigating instant parameters such as frequency, damping and several statistical values.

A theoretical crack model can be developed for the cracks in profile beam elements called for example: U shaped, I shaped and T shaped profiles. Vibration effects of cracks in different cross-sectioned beams like an airplane wings can also be investigated in future works.

REFERENCES

Al-Said, S.M., Naji, M., & Al-Shukry, A.A. (2006). Flexural vibration of rotating cracked Timoshenko beam. *Journal of Vibration and Control*, 12, 1271-1287.

Al-Said, S.M. (2007). Crack identification in a stepped beam carrying a rigid disk. *Journal of Sound and Vibration*, 300, 863-876.

Angelo, G., & Arcangelo, M. (2003). On the continuous wavelet transforms applied to discrete vibrational data for detecting open cracks in damaged beams. *International Journal of Solids and Structures*, 40, 295-315.

Bamnios, Y., Douka, E., & Trochidis, A. (2002). Crack identification in beam structures using mechanical impedance. *Journal of Sound and Vibration*, 256, 287-297.

Carden, E.P., & Fanning, P. (2004). Vibration based condition monitoring: A review. *Structural Health Monitoring*, 3, 355-377.

Carneiro, S.H.S., & Inman, D.J. (2001). Comments on the free vibrations of beams with a single-edge crack. *Journal of Sound and Vibration*, 244, 729-737.

Chang, C.-C., Chen, L.-W. (2005). Detection of location and size of cracks in the multiple cracked beam by spatial wavelet based approach. *Mechanical Systems and Signal Processing*, 19, 139-155.

Chang, C.C., Chang, T.Y.P., Xu, Y.G., & Wang, M.L. (2000). Structural damage detection using an iterative neural network. *Journal of Intelligent Material Systems and Structures*, 11, 32-42.

Chasalevris, A.C., Papadopoulos, C.A. (2006). Identification of multiple cracks in beams under bending. *Mechanical Systems and Signal Processing*, 20, 1631-1673.

Chaudhari, T.D., & Maiti, S.K. (1999). Modelling of transverse vibration of beam of linearly variable depth with edge crack. *Engineering Fracture Mechanics*, 63, 425-445.

Chaudhari, T.D., & Maiti, S.K. (2000). A study of vibration of geometrically segmented beams with and without crack. *International Journal of Solids and Structures*, 37, 761-779.

Chen, X.F., He, Z.J., & Xiang, J.W. (2005). Experiments on crack identification in cantilever beams. *Society for Experimental Mechanics*, 45, 295-300.

Chen, X.F., Zi, Y.Y., Li, B., & He, Z.J. (2006). Identification of multiple cracks using a dynamic mesh-refinement method. *The Journal of Strain Analysis for Engineering Design*, 41, 31-39.

Cheng, S.M., Wu, X.J., Wallace, W., & Swamidas, A.S.J. (1999). Vibrational response of a beam with a breathing crack. *Journal of Sound and Vibration* 225, 201-208.

Chinchalkar, S. (2001). Determination of crack location in beams using natural frequencies. *Journal of Sound and Vibration*, 247, 417-429.

Chondros, T.G. (2001). The continuous crack flexibility model for crack identification. *Fatigue & Fracture of Engineering Materials & Structures*, 24, 643-650.

Chondros, T.G., Dimarogonas, A.D., & Yao, J. (1998). A continuous cracked beam vibration theory. *Journal of Sound and Vibration*, 215, 17-34.

Chondros, T.G., Dimarogonas, A.D., & Yao, J. (2001). Vibration of a beam with a breathing crack. *Journal of Sound and Vibration*, 239, 57-67.

Christides, S., & Barr, A.D.S. (1984). One dimensional theory of cracked Bernoulli-Euler beams. *International Journal Mechanics Science*, 26, 639-648.

Dado, M.H. (1997). A comprehensive crack identification algorithm for beams under different end conditions. *Applied Acoustics*, 51, 381-398.

Dharmaraju, N., & Sinha, J.K. (2005). Some comments on use of antiresonance for crack identification in beams. *Journal of Sound and Vibration*, 286, 669-671.

Dharmaraju, N, Tiwari, R, & Talukdar, S. (2004). Identification of an open crack model in a beam based on force–response measurements. *Computers and Structures*, 82, 167-179.

Dilena, M., & Morassi, A. (2004). The use of antiresonances for crack detection in beams. *Journal of Sound and Vibration*, 276, 195-214.

Dilena, M., & Morassi, A. (2005). Damage detection in discrete vibrating systems. *Journal of Sound and Vibration*, 289, 830-850.

Dimarogonas, A.D. (1996). Vibration of cracked structures: a state of the art review. *Engineering Fracture Mechanics*, 55, 831-857.

Doebling, S.W., Farrar, C.R., & Prime, M.B. (1998). A summary review of vibration-based damage identification methods. *Shock and Vibration Digest*, 30(2), 91-105.

Douka, E., Bamnios, G., & Trochidis, A. (2004). A method for determining the location and depth of cracks in double-cracked beams. *Applied Acoustics*, 65, 997-1008.

Douka, E., & Hadjileontiadis, L.J. (2005). Time–frequency analysis of the free vibration response of a beam with a breathing crack. *NDT&E International,* 38, 3-10.

Douka, E., Loutridis, S., & Trochidis, A. (2003). Crack identification in beams using wavelet analysis. *International Journal of Solids and Structures,* 40, 3557-3569.

El Bikri, K., Benamar, R., & Bennouna, M.M. (2006). Geometrically nonlinear free vibrations of clamped-clamped beams with an edge crack. *Computers and Structures,* 84, 485-502.

Farrar, C.R., & Jauregui, D.A. (1998). Comparative study of damage identification algorithms applied to a bridge: I. Experiment. *Smart Mater. Struct.,* 7, 704-719.

Fernandez-Saez, J., & Navarro, C. (2002). Fundamental frequency of cracked beams in bending vibrations: an analytical approach. *Journal of Sound and Vibration,* 256, 17-31.

Fernandez-Saez, J., & Rubio, L., & Navarro, C. (1999). Approximate calculation of the fundamental frequency for bending vibrations of cracked beams. *Journal of Sound and Vibration,* 225, 345-352.

Friswell, M.I., & Penny, J.E.T. (2002). Crack modelling for structural health monitoring. *Structural Health Monitoring,* 1, 139-148.

Gounaris, G., & Dimarogonas, A.D. (1988). A finite element of a cracked prismatic beam for structural analysis. *Computers and Structures,* 28, 309–313.

Hadjileontiadis, L.J., Douka, E., & Trochidis, A. (2005a). Fractal dimension analysis for crack identification in beam structures. *Mechanical Systems and Signal Processing,* 19, 659-674.

Hadjileontiadis, L.J., Douka, E., & Trochidis, A. (2005b). Crack detection in beams using kurtosis. *Computers and Structures*, 83, 909-919.

He, Y., Guo, D., & Chu, F. (2001). Using genetic algorithm and finite element methods to detect shaft crack for rotor-bearing system. *Mathematics and Computers in Simulation*, 57, 95-108.

Hu, J., & Liang, R.Y. (1993). An integrated approach to detection of cracks using vibration characteristics. *Journal of Franklin Institute*, 330, 841-853.

Khiem, N.T., & Lien, T.V. (2001). A simplified method for natural frequency analysis of a multiple cracked beam. *Journal of Sound and Vibration*, 245, 737-751.

Khiem, N.T., & Lien, T.V. (2002). The dynamic stiffness matrix method in forced vibration analysis of multiple-cracked beam. *Journal of Sound and Vibration*, 254, 541-555.

Khiem, N.T., & Lien, T.V. (2004). Multi-crack detection for beam by the natural frequencies. *Journal of Sound and Vibration*, 273, 175-184.

Kim, J.-T., Ryu, Y.-S., Cho, H.-M., & Stubbs, N. (2003). Damage identification in beam-type structures: frequency-based method vs mode-shape-based method. *Engineering Structures*, 25, 57-67.

Kim, J.-T., & Stubbs, N. (2003). Crack detection in beam-type structures using frequency data. *Journal of Sound and Vibration*, 259, 145-160.

Kisa, M., & Gurel, M.A. (2006). Modal analysis of multi-cracked beams with circular cross section. *Engineering Fracture Mechanics*, 73, 963-977.

Kisa, M., & Gurel, M.A. (2007). Free vibration analysis of uniform and stepped cracked beams with circular cross sections. *International Journal of Engineering Science*, 45, 364-380.

Krawczuk, M. (2002). Application of spectral beam finite element with a crack and iterative search technique for damage detection. *Finite Elements Analysis and Design*, 38, 537-548.

Lam, H.F., Lee, Y.Y., Sun, H.Y., Cheng, G.F., & Guo, X. (2005). Application of the spatial wavelet transform and Bayesian approach to the crack detection of a partially obstructed beam. *Thin-Walled Structures*, 43, 1-21.

Lee, J. (2009a). Identification of multiple cracks in a beam using natural frequencies. *Journal of Sound and Vibration*, 320, 482-490.

Lee, J. (2009b). Identification of multiple cracks in a beam using vibration amplitudes. *Journal of Sound and Vibration*, 326, 205-212.

Leonard, F. (2007). Phase spectrogram and frequency spectrogram as new diagnostic tools. *Mechanical Systems and Signal Processing*, 21, 125-137.

Liang, L.Y., Choy, F.K., & Hu, J. (1991). Detection of cracks in beam structures using measurements of natural frequencies. *Journal of the Franklin Institute*, 328, 505-518.

Li, Q.S. (2001). Dynamic behaviour of multistep cracked beams with varying cross section. *Acoustical Society of America*, 109, 3072-3075.

Li, Q.S. (2002). Free vibration analysis of non-uniform beams with an arbitrary number of cracks and concentrated masses. *Journal of Sound and Vibration*, 252, 509-525.

Liew, K.M., Wang, Q. (1998). Application of wavelet theory for crack identification in structures. *Journal of Engineering Mechanics*, 124, 152-157.

Lin, H.P. (2004). Direct and inverse methods on free vibration analysis of simply supported beams with a crack. *Engineering Structures*, 26, 427-436.

Lin, H.P., Chang, S.C., & Wu, J.D. (2002). Beam vibrations with an arbitrary number of cracks. *Journal of Sound and Vibration*, 258, 987-999.

Loutridis, S., Douka, E., & Hadjileontiadis, L.J. (2005). Forced vibration behaviour and crack detection of cracked beams using instantaneous frequency. *NDT&E International*, 38, 411-419.

Luzzatto, E. (2003). Approximate computation of non-linear effects in a vibrating cracked beam. *Journal of Sound and Vibration*, 265, 745-763.

Mahmoud, M.A., & Kiefa, M.A.A. (1999). Neural network solution of the inverse vibration problem. *NDT&E International*, 32, 91-99.

Mares, C., & Surace, C. (1996). An application of genetic algorithms to identify damage in elastic structures. *Journal of Sound and Vibration*, 195, 195-215.

Matveev, V.V., & Bovsunovsky, A.P. (2002). Vibration-based diagnostics of fatigue damage of beam-like structures. *Journal of Sound and Vibration*, 249, 23-40.

Mazanoglu, K., & Sabuncu, M. (2010a). Vibration analysis of non-uniform beams having multiple edge cracks along the beam's height. *International Journal of Mechanical Sciences*, 52, 515-522.

Mazanoglu, K., & Sabuncu, M. (2010b). Flexural vibration of non-uniform beams having double edge breathing cracks. *Journal of Sound and Vibration*, 329, 4181-4191.

Mazanoglu, K., Yesilyurt, I., & Sabuncu, M. (2009). Vibration analysis of multiple cracked non-uniform beams. *Journal of Sound and Vibration*, 320, 977-989.

Mei, C., Karpenko, Y., Moody, S., & Allen, D. (2006). Analytical approach to free and forced vibrations of axially loaded cracked Timoshenko beams. *Journal of Sound and Vibration*, 291, 1041-1060.

Mohiuddin, M.A., & Khulief, Y.A. (1998). Modal characteristics of cracked rotors using a conical shaft finite element. *Computer Methods in Applied Mechanics and Engineering*, 162, 223-247.

Morassi, A., & Rollo, M. (2001). Identification of two cracks in a simply supported beam from minimal frequency measurements. *Journal of Vibration and Control*, 7, 729-739.

Morgan, B.J., & Osterle, R.G. (1985). On-site modal analysis – a new powerful inspection technique. *Second International Bridge Conference*, 108-114.

Nandwana, B.P., & Maiti, S.K. (1997a). Modelling of vibration of beam in presence of inclined edge or internal crack for its possible detection based on frequency measurements. *Engineering Fracture Mechanics*, 58, 193-205.

Nandwana, B.P., & Maiti, S.K. (1997b). Detection of the location and size of a crack in stepped cantilever beams based on measurements of natural frequencies. *Journal of Sound and Vibration*, 203, 435-446.

Narayana, K.L., & Jeberaj, C. (1999). Sensitivity analysis of local/global modal parameters for identification of a crack in a beam. *Journal of Sound and Vibration*, 228, 977-994.

Orhan, S. (2007). Analysis of free and forced vibration of a cracked cantilever beam. *NDT&E International*, 40, 443-450.

Ostachowicz, W.M., & Krawczuk, M. (1991). Analysis of the effect of cracks on the natural frequencies of a cantilever beam. *Journal of Sound and Vibration*, 150, 191-201.

Owolabi, G.M., Swamidas, A.S.J., & Seshadri, R. (2003). Crack detection in beams using changes in frequencies and amplitudes of frequency response functions. *Journal of Sound and Vibration*, 265, 1-22.

Ozturk, H., Karaagac, C., & Sabuncu, M. (2009). Free vibration and lateral buckling of a cantilever slender beam with an edge crack: Experimental and numerical studies. *Journal of Sound and Vibration*, 326, 235-250.

Pandey, A.K., Biswas, M., & Samman, M.M. (1991). Damage detection from changes in curvature mode shapes. *Journal of Sound and Vibration*, 145, 321-332.

Panteliou, S.D., Chondros, T.G., Argyrakis, V.C., & Dimarogonas, A.D. (2001). Damping factor as an indicator of crack severity. *Journal of Sound and Vibration*, 241, 235-245.

Papadopoulos, C.A. (2008). The strain energy release approach for modelling cracks in rotors: A state of the art review. *Mechanical Systems and Signal Processing*, 22, 763-789.

Papaeconomou, N., & Dimarogonas A. (1989). Vibration of cracked beams. *Computational Mechanics*, 5, 88-94.

Patil, D.P., & Maiti, S.K. (2003). Detection of multiple cracks using frequency measurements. *Engineering Fracture Mechanics*, 70, 1553-1572.

Prabhakar, S., Sekhar, A.S., & Mohanty, A.R. (2001). Detection and monitoring of cracks using mechanical impedance of rotor-bearing system. *Journal of Acoustical Society of America*, 110, 2351-2359.

Pugno, N., Surace, C., & Ruotolo, R. (2000). Evaluation of the non-linear dynamic response to harmonic excitation of a beam with several breathing cracks. 235, 749-762.

Qian, G.-L., Gu, S.-N, & Jiang, J.-S. (1990). The dynamic behaviour and crack detection of a beam with a crack. *Journal of Sound and Vibration*, 138, 233-243.

Quek, S.-T., Wang, Q., Zhang, L., & Ang, K.-K. (2001). Sensitivity analysis of crack detection in beams by wavelet technique. *International Journal of Mechanical Sciences*, 43, 2899-2910.

Ratcliffe, C.P. (1997). Damage detection using a modified Laplacian operator on mode shape data. *Journal of Sound and Vibration*, 204, 505-517.

Rizos, P.F., Aspragathos, N., & Dimarogonas, A.D. (1990). Identification of crack location and magnitude in a cantilever beam from the vibration modes. *Journal of Sound and Vibration*, 138, 381-388.

Rucka, M, & Wilde, K. (2006). Crack identification using wavelets on experimental static deflection profiles. *Engineering Structures*, 28, 279-288.

Ruotolo, R., & Surace, C. (1997). Damage assessment of multiple cracked beams: numerical results and experimental validation. *Journal of Sound and Vibration*, 206, 567-588.

Saavedra, P.N., & Cuitino, L.A. (2002). Vibration analysis of rotor for crack identification. *Journal of Vibration and Control*, 8, 51-67.

Sabnavis, G., Kirk, R.G., Kasarda, M., & Quinn, D. (2004). Cracked shaft detection and diagnostics: A literature review. *The Shock and Vibration Digest*, 36, 287-296.

Salawu, O.S. (1997). Detection of structural damage through change in frequency: a review. *Engineering structures*. 19, 718-723.

Sekhar, A.S. (2003). Identification of a crack in a rotor system using a model-based wavelet approach. *Structural Health Monitoring*, 2, 293-308.

Sekhar, A.S. (2008). Multiple cracks effects and identification. *Mechanical Systems and Signal Processing*, 22, 845-878

Shen, M.H.H., & Pierre, C. (1994). Free vibration of beams with a single-edge crack. *Journal of Sound and Vibration*, 170, 237-259.

Shifrin, E.I., & Ruotolo, R. (1999). Natural frequencies of a beam with an arbitrary number of cracks. *Journal of Sound and Vibration*, 222, 409-423.

Sih, G.C. (1973). Some basic problems in fracture mechanics and new concepts. *Engineering Fracture Mechanics*, 5, 365-377.

Suresh, S., Omkar, S.N., Ganguli, R., & Mani, V. (2004). Identification of crack location and depth in a cantilever beam using a modular neural network approach. *Smart Materials and Structures*, 13, 907-915.

Tabarraei, A., & Sukumar, N. (2008). Extended finite element method on polygonal and quadtree meshes. *Computer Methods in Applied Mechanics and Engineering*, 197,425-438.

Tada, H., Paris, P.C., & Irwin, G.R. (Eds.). (1973). *The Stress Analysis of Cracks Handbook*. Hellertown Pennsylvania: Del Research Corporation.

Tsai, T.C., & Wang, Y.Z. (1997). The vibration of a multi-crack rotor. *International Journal of Mechanical Sciences*, 39, 1037-1053.

Vakil-Baghmisheh, M., Peimani, M., Sadeghi, M.H., & Ettefagh, M.M. (2008). Crack detection in beam-like structures using genetic algorithms. *Applied Soft Computing*, 8, 1150-1160.

Wang, B.S., & He, Z.C. (2007). Crack detection of arch dam using statistical neural network based on the reductions of natural frequencies. *Journal of Sound and Vibration*, 302, 1037-1047.

West, W.M. (1984). Illustration of the use of modal assurance criterion to detect structural changes in an orbiter test specimen. *Air Force Conference on Aircraft Structural Integrity*, 1-6.

Yan, Y.J., Cheng, L., Wu, Z.Y., & Yam, L.H. (2007). Development in vibration-based structural damage detection technique. *Mechanical Systems and Signal Processing*, 21, 2198-2211.

Yang, J., Chen, Y., Xiang, Y., & Jia, X.L. (2008). Free and forced vibration of cracked inhomogeneous beams under an axial force and a moving load. *Journal of Sound and Vibration*, 312, 166-181.

Yang, X.F., Swamidas, A.S.J., & Seshadri, R. (2001). Crack identification in vibrating beams using the energy method. *Journal of Sound and Vibration*, 244, 339-357.

Yokoyama, T., & Chen, M.-C. (1998). Vibration analysis of edge-cracked beams using a line spring-model. *Engineering Fracture Mechanics*, 59, 403-409.

Yuen, M.M.F. (1985). A numerical study of the eigen parameters of a damaged cantilever. *Journal of Sound and Vibration*, 103, 301-310.

Zhang, W., Wang, Z., Ma, H. (2009). Crack identification in stepped cantilever beam combining wavelet analysis with transform matrix. *Acta Mechanica Solida Sinica*, 22, 360-368.

Zheng, D.Y., & Fan, S.C. (2001). Natural frequencies of a non-uniform beam with multiple cracks via modified Fourier series. *Journal of Sound and Vibration*, 242, 701-717.

Zheng, D.Y., & Kessissoglou, N.J. (2004). Free vibration analysis of a cracked beam by finite element method. *Journal of Sound and Vibration*, 273, 457-475.

Zhu, X.Q., & Law, S.S. (2006). Wavelet-based crack identification of bridge beam from operational deflection time history. *International Journal of Solids and Structures*, 43, 2299-2317.

APPENDICES

APPENDIX A
NOMENCLATURE

a	crack depth
A	area of cross-section
b	width of a beam
BE	energy balance equation.
C	coefficients of harmonic and hyperbolic terms
CE	the energy consumed
E	modulus of elasticity
f	natural frequency in the unit Hertz
f_s	sampling frequency
G	strain energy release rate
G_N	normalised Gaussian function
h	height of a beam
I	second moment of inertia
J	polar mass moment of inertia
k	(1) stiffness, (2) frequency data index
K_1	stress intensity factor for the first mode crack
KE	maximum kinetic energy
L	length of the beam
m	(1) total number of terms of polynomial mode shape function, (2) lumped mass
M	bending moment
n	(1) total number of discontinuities like cracks or additional masses, (2) time data index
N	number of the data samples
PE	maximum potential energy
r_c	crack depth ratio, (a / h_c)

r_f	ratio between the frequencies of the cracked and un-cracked beams
s	time data
S	frequency data
w	coordinate axis along the beams height
W	transverse vibration mode shape of the beam.
X	(1) deviation of the neutral axis, (2) decreasing amount of the data length
y	coordinate axis along the beams width
z	coordinate axis along the beams length
α	(1) truncation (taper) factor of beam's height or width, (2) displacement–slope compatibility coefficient for crack location
β	(1) additional effects of the closed crack on negative strain and compressive stress, (2) frequency parameter
γ	(1) influence ratio of the energy consumed, (2) additional effects of the open crack on strain and tensile stress
Γ	distribution of the energy
δf	spacing between consecutive samples in frequency data
Δu	linear displacement at the opened side of crack
ΔU	change in strain energy
Δv	linear displacement at the crack tip with the effect of material stress
ΔV	change in stress energy
$\Delta\theta$	angular displacement corresponding to the crack opening
$\Delta\phi$	angular displacement of the beam due to the positive strain at the crack location
$\Delta\psi$	angular displacement corresponding to the crack closing
$\Delta\varphi$	angular displacement of the beam due to the negative strain at the crack location
ε	a coefficient caused by the opening form of the edge crack
κ	coefficient of the term of polynomial mode shape function.
λ	slope–bending moment compatibility coefficient for lumped mass location
μ	displacement–shear force compatibility coefficient for lumped mass location
ν	poisson ratio

ρ	mass density
χ	term of polynomial mode shape function.
ω	circular frequency
ω_0	natural frequency of un-cracked beam
c, dc	subscript for the words “crack” and “double-edge crack”
d	subscript for defining the direct effects of cross-section decreases
i	crack and part numerator
j	numerator of the mode shape terms
p	abbreviation for the word “part”
s	subscript for defining the effects of neutral axis shift
y	subscript for defining the effects of neutral axis yawing
δ	difference between the numerators of crack and part

APPENDIX B

SOME OF CRACKED BEAMS MODELLED IN ANSYS

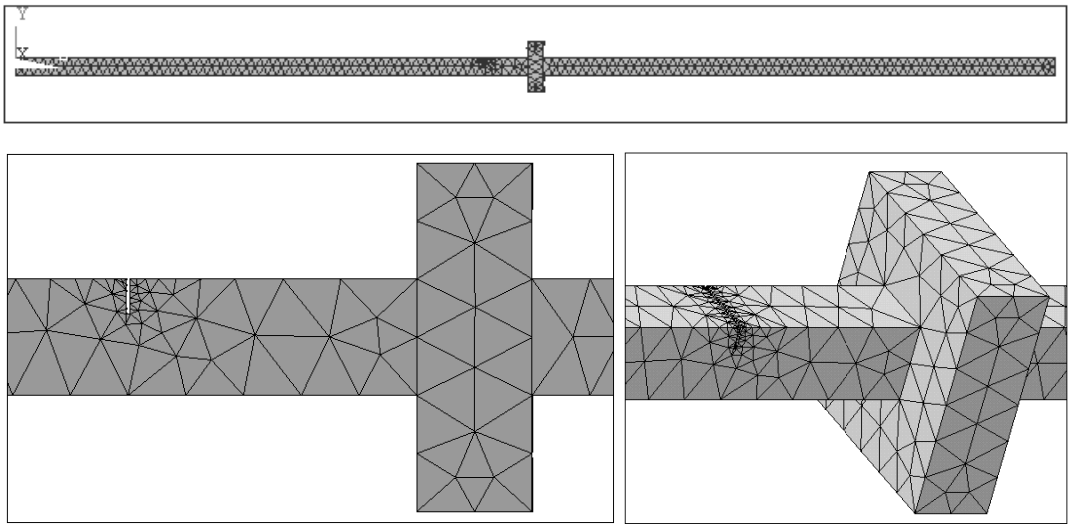

Figure B.1 Transverse crack on the beam with an additional mass.

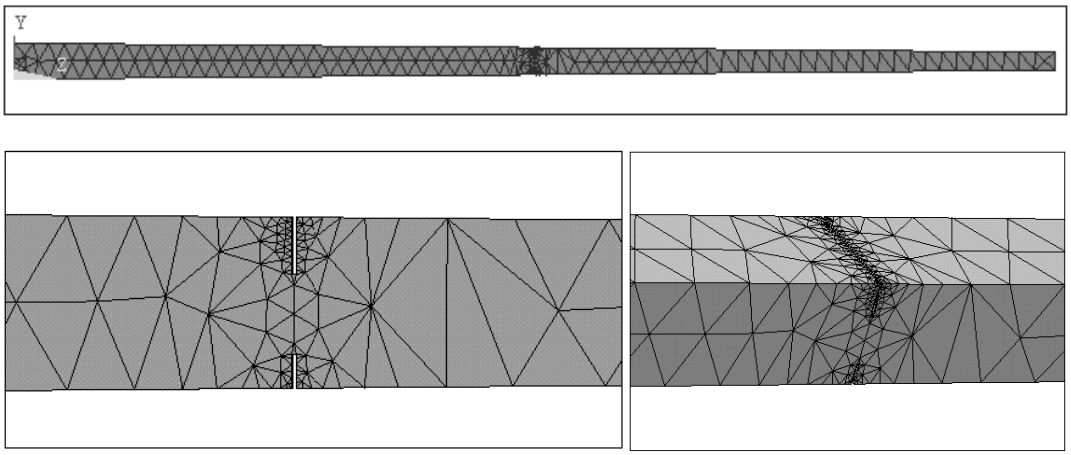

Figure B.2 Double-edge crack on tapered beam.

APPENDIX C
PHOTOS OF TEST STRUCTURE AND MEASUREMENT DEVICES

Figure C.1 Cantilever beam used in experiment.

Figure C.2 Impact hammer and miniature accelerometer.

Figure C.3 Data acquisition and monitoring system.